AD-A061 537 AIR FORCE INST OF TECH WRIGHT-PATTERSON AFB OHIO F/G 6/18
THE SYNERGISTIC EFFECT OF ULTRASOUND AND IONIZING RADIATION ON --ETC(U)
1978 J G BURR
UNCLASSIFIED AFIT-CI-79-71D NL

1 OF 3
AD
A061537

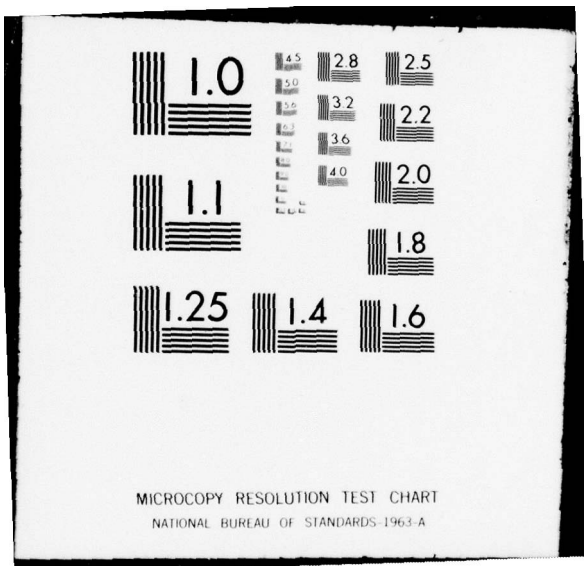
1.0
1.1
1.25
1.4
1.6
1.8
2.0
2.2
2.5
2.8
3.2
3.6
4.0
4.5
5.0
5.6
MICROCOPY RESOLUTION TEST CHART
NATIONAL BUREAU OF STANDARDS-1963-A

UNCLASSIFIED
SECURITY CLASSIFICATION OF THIS PAGE *(When Data Entered)*

AD A061537

REPORT DOCUMENTATION PAGE

READ INSTRUCTIONS BEFORE COMPLETING FORM

1. REPORT NUMBER: CI-79-71D
2. GOVT ACCESSION NO.:
3. RECIPIENT'S CATALOG NUMBER:
4. TITLE *(and Subtitle)*: The Synergistic Effect of Ultrasound and Ionizing Radiation on Human Lymphocytes
5. TYPE OF REPORT & PERIOD COVERED: Dissertation
6. PERFORMING ORG. REPORT NUMBER:
7. AUTHOR(s): John G. Burr, Captain, USAF
8. CONTRACT OR GRANT NUMBER(s): Doctoral Thesis
9. PERFORMING ORGANIZATION NAME AND ADDRESS: AFIT Student at the University of Pittsburgh
10. PROGRAM ELEMENT, PROJECT, TASK AREA & WORK UNIT NUMBERS: 216p.
11. CONTROLLING OFFICE NAME AND ADDRESS: AFIT/CI, WPAFB OH 45433
12. REPORT DATE: 1978
13. NUMBER OF PAGES: 201
14. MONITORING AGENCY NAME & ADDRESS *(if different from Controlling Office)*: AFIT-CI-79-71D
15. SECURITY CLASS. *(of this report)*: UNCLASSIFIED
15a. DECLASSIFICATION/DOWNGRADING SCHEDULE:
16. DISTRIBUTION STATEMENT *(of this Report)*: Approved for Public Release, Distribution Unlimited
17. DISTRIBUTION STATEMENT *(of the abstract entered in Block 20, if different from Report)*:
18. SUPPLEMENTARY NOTES: APPROVED FOR PUBLIC RELEASE AFR 190-17.
JOSEPH P. HIPPS, Major, USAF
Director of Information, AFIT
NOV 9 1978
19. KEY WORDS *(Continue on reverse side if necessary and identify by block number)*:
20. ABSTRACT *(Continue on reverse side if necessary and identify by block number)*:

[redacted]

012 200

DD FORM 1 JAN 73 1473 EDITION OF 1 NOV 65 IS OBSOLETE

UNCLASSIFIED
SECURITY CLASSIFICATION OF THIS PAGE *(When Data Entered)*

THE SYNERGISTIC EFFECT OF ULTRASOUND AND IONIZING RADIATION ON HUMAN LYMPHOCYTES

John G. Burr, Capt., USAF, BSC
021364103FR

Doctor of Science in Hygiene (Sc.D.)

University of Pittsburgh, Pittsburgh, PA
1978

201 pages

Lymphocytes in human peripheral blood were exposed to various combinations and sequences of heat, ultrasound and/or ionizing radiation and their chromosomes analyzed for gross chromosomal aberrations.

The combined use of ultrasound and ionizing radiation showed a statistically significant increase in exchange aberrations for the simultaneous ultrasound (3.0 W/cm^2, CW, 1.1 MHz) and ionizing radiation (300 and 100 rads, Co-60, 120 rads/min) exposures. Ultrasound used before or after irradiation caused no aberrations and extending the time of ultrasound exposure after irradiation had no effect over that of the ultrasound only during the radiation exposure.

The combined use of 43°C heat (same temperature as that induced by 3.0 W/cm^2, CW, 1.1 MHz ultrasound) and ionizing radiation showed basically the same significant results as the combined ultrasound and ionizing radiation exposures. In addition, the combined use of heat at various temperatures (24°C thru 43°C) and ionizing radiation showed that all chromosome aberration types and the number of aberrant metaphase figures increased with increasing temperature.

A statistical comparison of the heat plus ionizing radiation and the ultrasound plus ionizing radiation exposures showed no

statistically significant difference between heat or ultrasound for any type aberration.

79-71D

THE SYNERGISTIC EFFECT OF ULTRASOUND AND IONIZING RADIATION ON HUMAN LYMPHOCYTES

By

John G. Burr

B.S.M.E., Lowell Technological Institute, 1968

M.S.C.E., University of Arizona, 1972

M.S., University of Pittsburgh, 1976

Submitted to the Faculty of the Graduate School
of Public Health in partial fulfillment of
the requirements for the degree of
Doctor of Science

University of Pittsburgh

1978

THE SYNERGISTIC EFFECT OF ULTRASOUND AND IONIZING RADIATION ON HUMAN LYMPHOCYTES

John G. Burr, Sc.D.

University of Pittsburgh, 1978

Lymphocytes in human peripheral blood were exposed to various combinations and sequences of heat, ultrasound and/or ionizing radiation and their chromosomes analyzed for gross chromosomal aberrations. Exposures were made in a specially designed, constructed and tested ultrasound and ionizing radiation exposure system which allowed accurately known exposures of ionizing radiation and ultrasound, continuous monitoring of the temperature and ultrasound exposure in the sample, and carefully controlled environmental temperature.

Ultrasound alone exposures showed no chromosome aberrations for exposures as high as 4.0 W/cm^2, CW, 1.1 MHz for 30 minutes and 3.0 W/cm^2, CW, 1.1 MHz for 60 minutes. Heat used alone (conductive heating) showed no chromosome aberrations for temperatures up to 50°C for 30 minute exposure and 43°C for 60 minutes exposure with lymphocyte cell death occurring in the range of 43-46°C for 30 minute exposure. Ionizing radiation alone (Co-60, 122 rads/min) showed a chromosome aberration dose response which was consistent with the recently published literature.

The combined use of ultrasound and ionizing radiation showed a statistically significant increase in exchange aberrations for the simultaneous ultrasound (3.0 W/cm^2, CW, 1.1 MHz) and ionizing radiation (300 and 100 rads, Co-60, 120 rads/min) exposures. Ultrasound used before or after irradiation caused no aberrations and extending the time of ultrasound exposure after irradiation had no effect over that of the ultrasound only during the radiation exposure.

The combined use of 43°C heat (same temperature as that induced by 3.0 W/cm^2, CW, 1.1 MHz ultrasound) and ionizing radiation showed basically the same significant results as the combined ultrasound and ionizing radiation exposures. In addition, the combined use of heat at various temperatures (24°C → 43°C) and ionizing radiation showed that all chromosome aberration types and the number of aberrant metaphase figures increased with increasing temperature.

A statistical comparison of the heat plus ionizing radiation and the ultrasound plus ionizing radiation exposures showed no statistically significant difference between heat or ultrasound for any type aberration.

The results suggest that heat or ultrasound when used simultaneously with ionizing radiation act in a similar manner by increasing the number of primary chromosome breaks. Heat or ultrasound used after ionizing radiation has a much reduced effect in the form of an increase in exchange aberration frequency.

ACKNOWLEDGEMENTS

Special acknowledgement must go to the United States Air Force for their sponsorship of my education at the University of Pittsburgh under the Air Force Institute of Technology Program.

Individually I would like to thank my advisor and committee members Drs. Wald, Watson, Herron, Pan, Rockette and Yen for their support and guidance during this research.

I thank Janice Austin for the preparation of the manuscript and Maureen O'Farrell and Carol Sherer for their assistance in developing proper chromosome harvesting techniques.

Special thanks are given to Dr. David Gur, a fellow student and now faculty member of the Department of Radiation Health for his technical advise, review of preliminary drafts, and moral support.

The Department of Radiation Health University of Pittsburgh is to be thanked for their financial support and both the departments of Radiation Health and Radiation Oncology, Presbyterian Hospital, University of Pittsburgh are thanked for the use of their facilities.

Lastly and most importantly I thank my family for their patience and encouragement through this long effort.

TABLE OF CONTENTS

TABLE OF CONTENTS - Continued

TABLE OF CONTENTS - Continued

LIST OF FIGURES

LIST OF FIGURES - Continued

LIST OF FIGURES - Continued

Figure

LIST OF TABLES

LIST OF TABLES - Continued

Table

I. INTRODUCTION

A. Importance of this Study

Numerous studies have reported a possible synergistic relationship between ultrasound and ionizing radiation [Lehmanm and Krusen (1955), Woeber (1959), Dharkar (1964), Pydorich (1966), Javish (1966), Kim (1968), Spring (1969), Rapacholi (1970), Spring et al. (1970), Martins (1971), Fujita and Sakuma (1974), Todd and Shroy (1974), Kunze-Muhl (1975), Burr et al. (1977) and Craig and Tyler (1977)] using various plant and animal cell systems.

If one accepts that synergism exists between ultrasound and ionizing radiation then an obvious benefit could result from their combined use in radiation therapy. In addition, since ultrasound can be focused and ionizing radiation collimated, a two port treatment regime (see Figure 1) could be utilized where only the tumor would receive the combined sonation and irradiation. The surrounding tissue would be exposed to ultrasound alone or ionizing radiation alone and would be spared from the synergistic effect.

The potential beneficial effect in tumor therapy relates to the possible increase in cell damage resulting from the synergism. However, a potentially serious negative effect may co-exist when we consider simultaneous uses of ultrasound and ionizing radiation on other portions of the population. A close temporal relationship in the administration of ultrasound and ionizing radiation is becoming more widely significant because of the increased use of ultrasound in medical diagnostic and therapeutic procedures. This is particularly true in obstetrical practice where diagnostic procedures impinge on the fetus. Diagnostic

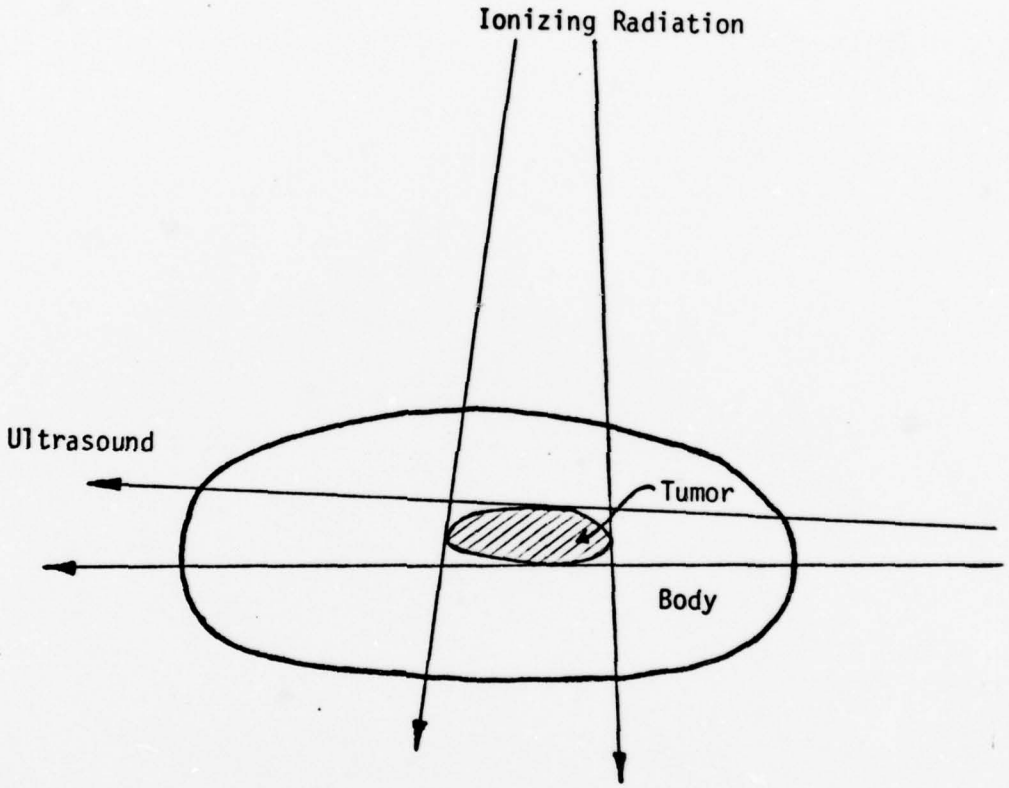

Figure 1. Hypothetical Treatment Regime for the Combined Use of Ultrasound and Ionizing Radiation in Tumor Therapy.

ultrasound has not replaced diagnostic x-ray examinations or nuclear medicine techniques but is often used as an additional diagnostic tool. Thus, it is quite possible that large numbers of fetuses are being subjected to sonation and irradiation administered within a short time period. If synergism occurs under these conditions, a number of possible detrimental consequences, e.g., an increase in teratogenic, mutagenic and/or carcinogenic effects, might occur.

Both the positive and negative aspects of the possible synergism between ultrasound and ionizing radiation are therefore of importance to public health. Additional research is necessary before one can clearly define and quantify this effect and thereby predict the magnitude of the potential benefit or hazard.

The object of this study is to evaluate the possible synergy of ionizing radiation and ultrasound by determining, under stringently controlled conditions, whether damage to the genetic material of human cells is enhanced by their combined use. If so, the study will also try to determine whether the temporal sequence of their application significantly influences the overall magnitude of the effect.

B. Background Information

A detailed study of the synergistic effects of ultrasound and ionizing radiation on the genetic material of the cell requires background information about the effects of each agent when used alone as well as the effect of their combined use. In addition, a review of the physics of ultrasound radiation is included to help clarify concepts and terminology that are not generally as familiar as those of the ionizing radiation field.

1. Physics of Ultrasound and Its Interaction with Materials

The physics of ultrasonic radiation and its interaction in materials is a very complex subject. Only the basic physical principles pertaining to an ideal propagation medium and the resultant general interactions will be considered that will serve as an aid to an understanding of the experiments performed. More detailed discussions of these subjects may be found in Fry and Dunn (1962), Kinsler and Frey (1962), El'piner (1964), Baum (1966), Brown and Gordon (1967), Blitz (1967), Peacocke and Prichard (1968), Interaction of Ultrasound and Biological Tissue (1972) and Hussey (1975).

a. Physics of Ultrasound

(1) Definition of Ultrasound

Sound is a mechanical vibratory transmission of energy through a medium caused by the direct interaction of the particles of that medium. Sound, therefore, requires a transmission medium and cannot be propagated in a vacuum as can electromagnetic waves. Ultrasound is sound propagated at frequencies greater than 18 KHz. The general range of frequencies used in diagnostic and therapeutic ultrasonics is 500 KHz to 20 MHz, with the most common frequencies in the range of 1 to 5 MHz.

(2) Basic Wave Properties

The transmission of ultrasonic energy follows the basic laws of physics which describe the motion of waves traveling through a medium. For simplification, this discussion will be limited to the properties of pure longitudinal sound waves (with single frequency and particle motion in the direction of the flow of energy) propagated sinusoidally in an ideal medium. Figure 2 indicates the basic wave motion with the

1. Physics of Ultrasound and Its Interaction with Materials

The physics of ultrasonic radiation and its interaction in materials is a very complex subject. Only the basic physical principles pertaining to an ideal propagation medium and the resultant general interactions will be considered that will serve as an aid to an understanding of the experiments performed. More detailed discussions of these subjects may be found in Fry and Dunn (1962), Kinsler and Frey (1962), El'piner (1964), Baum (1966), Brown and Gordon (1967), Blitz (1967), Peacocke and Prichard (1968), Interaction of Ultrasound and Biological Tissue (1972) and Hussey (1975).

a. Physics of Ultrasound

(1) Definition of Ultrasound

Sound is a mechanical vibratory transmission of energy through a medium caused by the direct interaction of the particles of that medium. Sound, therefore, requires a transmission medium and cannot be propagated in a vacuum as can electromagnetic waves. Ultrasound is sound propagated at frequencies greater than 18 KHz. The general range of fre uencies used in diagnostic and therapeutic ultrasonics is 500 KHz to 20 MHz, with the most common frequencies in the range of 1 to 5 MHz.

(2) Basic Wave Properties

The transmission of ultrasonic energy follows the basic laws of physics which describe the motion of waves traveling through a medium. For simplification, this discussion will be limited to the properties of pure longitudinal sound waves (with single frequency and particle motion in the direction of the flow of energy) propagated sinusoidally in an ideal medium. Figure 2 indicates the basic wave motion with the

basic parameters noted below:

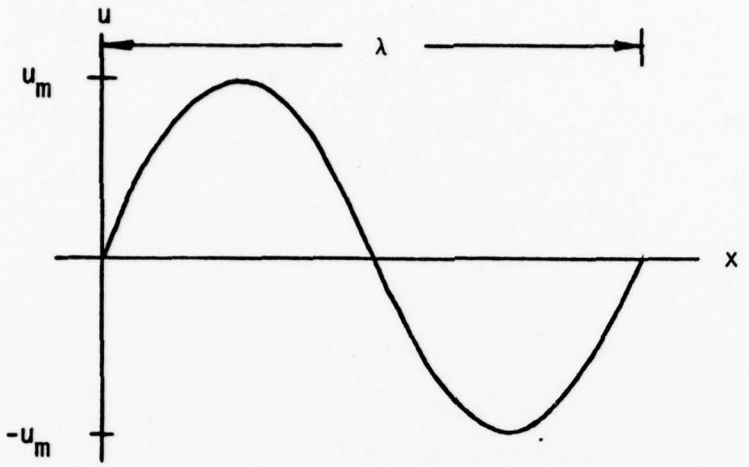

Figure 2. Typical Sinusoidal Wave Motion

(a) Frequency (f)

The number of vibrations completed in one second. The unit of frequency is the Hertz (Hz) and is defined as one cycle per second.

(b) Wavelength (λ)

The distance between two consecutive troughs or crests is the wavelength and has units of cm.

(c) Wave Number (k)

By definition is $2\pi/\lambda$ with units of cm^{-1}.

(d) Angular Frequency (ω)

The frequency of rotation of the sinuosidal function and defined as $2\pi f$ with units sec^{-1}.

(e) Speed of Sound (c)

The velocity of the wave traveling through the medium (often referred to as the phase velocity). This speed is related to the frequency and wavelength through the relationship $c = \lambda f$ and has the units cm/sec. The speed of sound in a medium is related to the thermodynamic and physical properties of the medium by

$$c = \frac{\gamma P_o}{\rho_o}$$

where γ = ratio of the specific heat at constant pressure to that at constant volume

P_o = equilibrium pressure in the medium

ρ_o = density in the medium

(f) Particle Displacement (u)

The displacement of a particle in the medium from its rest position due to passage of the wave can be described by $u = u_m \sin(\omega t - kx)$ where the maximum displacement is u_m with units of cm.

(g) Particle Velocity (v)

The velocity of the displaced particle is defined as the time rate of change of the displacement or $v = \frac{du}{dt} = \omega u_m \cos(\omega t - kx)$ where the maximum velocity is $v_m = \omega u_m$ with units of cm/sec.

(h) Particle Acceleration (a)

The acceleration of the displaced particle is defined as the time rate of change of the particle velocity or $a = \frac{dv}{dt} = -\omega^2 u_m \sin(\omega t - kx)$ with units of cm/sec^2.

(i) Acoustic Pressure (p)

The displacement of the particles in the medium caused by passage of the wave results in compression and rarefraction of the medium. The resulting pressure changes are called the acoustic pressure and can be shown to follow the relationship $p = \rho cv$ for a pure longitudinal wave with units of force per unit area or $dynes/cm^2$.

(j) Characteristic Impedance (Z)

For a plane, progressive longitudinal wave the characteristic impedance is defined as $Z = \rho_o c$ with units of $gram/cm^2\text{-sec}$. It should

be noted that this is only true when the wave is associated with a pure resistance. Spherical waves or standing waves have other than resistive components and consequently the impedance is described in complex notation as $\hat{Z} = Z + jX$ where X is the specific acoustic reactance. Characteristic impedance is a useful tool to be used in the discussion and modeling for acoustic interactions in media.

(k) Acoustic Energy (E) and Intensity (I)

When a sound wave travels through a medium there is no net movement of the medium (particles oscillate about a fixed position) but there is a transfer of energy between particles, which results in a net flow of energy away from the sound source. At any point in time the wave can be described in terms of its potential energy caused by particle displacement and kinetic energy caused by particle velocity with a total instantaneous energy density of $E = \rho v^2$. The time weighted average energy density for a sinusoidal plane wave would be $E = 1/2\ \rho v_m^2$. The units of energy density are g/cm-sec.

A much more commonly used term in acoustics is the acoustic intensity (I) which describes the average power transmitted per unit area in the direction of wave propagation. It can be shown that $I = 1/2\ \rho c v_m^2$ for a sinusoidal plane wave and has units of erg/sec-cm^2 or Watts/cm^2. This can be described as the amount of energy carried by the wave in one second through an area of 1 cm^2 perpendicular to the direction of propagation. Acoustic energy and intensity are related by $I = Ec$.

(l) Radiation Pressure (P_r)

An object having a characteristic impedance different from that of the medium, when placed in an ultrasonic field will be subjected to a net force on its surface parallel to the direction of the wave propagation. This force is not a consequence of the flow of the

fluid medium (as there is no net flow) but is caused by a change in particle momentum at the interface of the dissimilar media. It can be shown that the radiation pressure is equal to the energy density. Since energy density (E) is related to intensity (I) then $P_r = I/c$. This relationship is extremely important because it provides a method of directly determining the intensity of the sound wave if the speed of sound in the medium is known and the force on the object can be measured.

b. Methods of Generating Ultrasound

There are basically four methods currently utilized in the conversion of electrical energy to mechanical energy (ultrasound) in the medical ultrasonics applications field. These include the magnetostrictive transducer, the electrostatic transducer, the electrodynamic transducer and the most common type, the piezoelectric transducer. A brief discussion of each type is presented below with particular emphasis placed on the piezoelectric transducer because of its use in this study as an ultrasonic generator and an ultrasonic detector.

(1) Magnetostrictive Transducer

Various ferromagnetic materials such as iron, nickel, cobalt and a number of alloys exhibit a property known as the magnetostrictive effect or Joule effect which cause a change in their length when subjected to a magnetic field. By varying the magnetic field at very high frequencies the ferromagnetic material can be made to oscillate and generate ultrasonic fields. Generally, the operating frequencies are limited to 150 KHz but the high efficiency and consequently high possible outputs make them useful in certain applications.

(2) Electromagnetic Transducers

A wire carrying an electric current experiences a force when placed in a magnetic field. If the current in the wire is alternating at high frequency then the force developed also alternates. This alternating force can be used to generate ultrasound by oscillation of a plate or diaphram just as is done with loudspeakers and some microphones. Most electromagnetic transducers are limited to approximately 2 MHz.

(3) Electrostatic Transducers

Two adjacent metal plates of opposite charge create a force between them. If the charge on the plates is alternated the forces will change and thus the possible high frequency oscillation needed to produce ultrasound. Frequencies as high as 90 MHz can be generated. Electrostatic transducers are normally used for low power applications.

(4) Piezoelectric Transducers

Certain crystals such as quartz, barium titanate, lead zirconate titanate, and lead metaniobate exhibit a property called the piezoelectric effect. These crystals when mechanically stressed develop electrical charges on their surfaces. Conversely, if an electrical field is applied in the direction of an axis of nonsymmetry the crystal will be mechanically strained. These two principles allow the crystals to be specially cut and fabricated into transducer materials for both the generation of ultrasound and the measurement of ultrasound. The typical construction of a piezoelectric transducer is shown in Figure 3. The transducer material is usually cut to a specific thickness in the shape of a circular disk. The thickness of the disk is chosen as an integral number of one-half wavelengths of the ultrasound to be propagated so that it will resonate at its fundamental

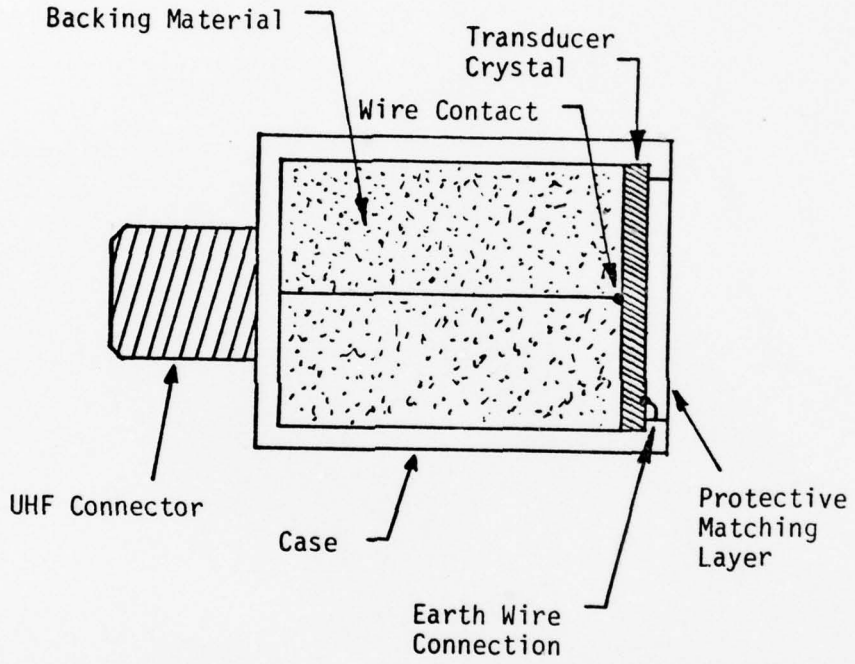

Figure 3. Typical Construction of a Piezoelectric Transducer

frequency. The outer face of the disk is held at ground potential and the inner face is subjected to various alternating voltages. The material directly in back of the crystal significantly affects the output properties of the transducer and very careful design is performed for different applications. For applications where the maximum energy efficiency (50% electric to mechanical) is needed and continuous wave operation is used, a plain air backing is preferable with the crystal allowed to resonate at its fundamental frequency. Where the application requires very short ultrasonic pulses, such as diagnostic procedures, the backing material must be highly damping. The object is to produce a single pulse with very few oscillations thereafter until the next pulse. This damping comes at the price of poor efficiency, generally less than 1% (electric to mechanical).

c. Interaction of Ultrasound with Matter

(1) Ultrasonic Fields

Most ultrasonic applications use a circular transducer transmitting into a medium by direct coupling of the transducer to the medium. The distribution of the ultrasonic energy after leaving the transducer is a complex phenomenon described in Figure 4. It should be noted that two distinct regions of the field exist; the near field and far field. Within the near field the ultrasonic energy remains fairly well confined to a volume bounded by the outer dimensions of the transducer but the intensity is quite variable depending on location in the volume. The intensity varies both vertically and horizontally with respect to the field center line. The far field on the other hand is characterized by the diverging of the beam with distance from the transducer and a more uniform intensity distribution. The separation between the near and far fields is defined as the

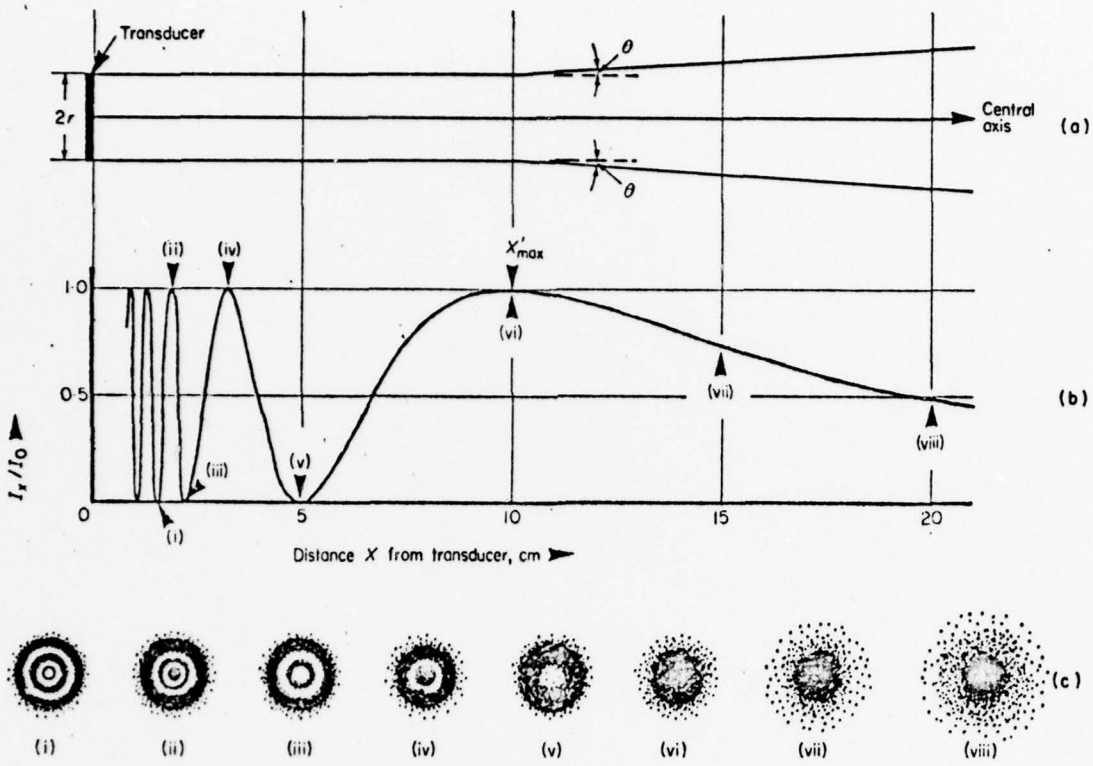

Figure 4. The ultrasonic field. This example shows the distribution for a 1.5 MHz transducer of radius r = 1 cm. (a) Almost all the ultrasonic energy lies within the limits shown in this diagram; (b) Relative intensity distribution along the central axis of the beam; (c) Ring diagrams showing the energy distribution of beam sections at positions indicated in (b) [Wells (1969)].

location of the last intensity maximum on the center line of the field. $X = r^2/\lambda$ where r = radius of the transducer; λ = wavelength of ultrasound; X = distance from transducer to beginning of the far field. Once past the last maximum the intensity then decreases due to absorption and dispersion only.

In addition to the main ultrasound field or beam there are minor fields called side lobes (see Figure 5). These side lobes are of minor importance in most applications because they contain only a small fraction of the total power but must be considered for small transducers and at very low frequencies.

(2) Attenuation of Ultrasound

Attenuation of ultrasonic energy is defined as the loss of energy with distance. It is due to several factors, which include dispersion, diffraction, scattering, and absorption.

(a) Dispersion

Once the ultrasonic energy has entered the far field of the transducer and assuming an infinite transmission medium the field diverges at an angle θ called the beam width. Where $\sin \theta = 1.22 \lambda/2r$ and r = radius of the transducer. Since the cross sectional area of the field is increasing continuously the energy per unit area must decrease continuously. This loss or decrease in energy per unit area is called dispersion loss.

(b) Scattering

When an object of differing characteristic impedance in the ultrasonic field has dimensions that are comparable with or less than the wavelength of the ultrasound, scattering of the ultrasound can occur. Ultrasonic energy is scattered in all directions and the amplitude of the scattered waves is inversely proportional to the

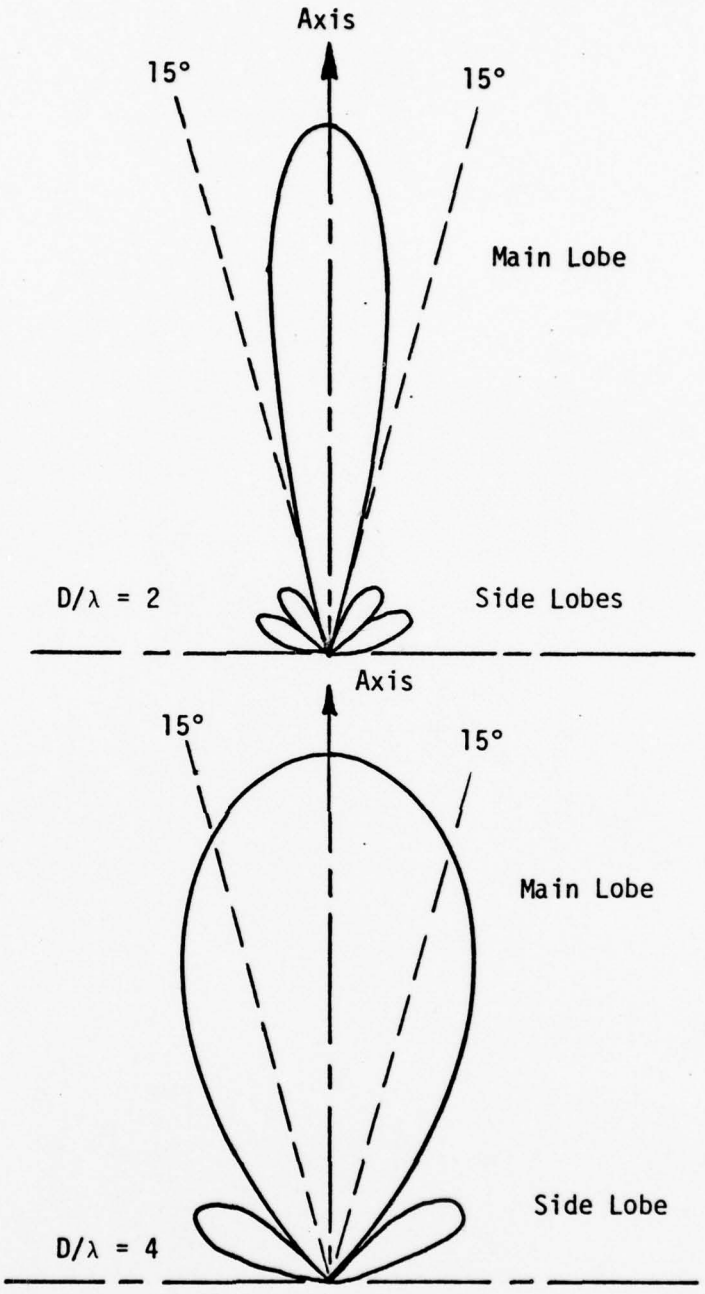

Figure 5. Far Field Intensity Patterns Showing Major and Minor Intensity Lobes.

square of the wavelength. Therefore, at high frequencies scattering from small objects can produce significant attenuation.

(c) Diffraction

When sound waves meet an obstacle which is larger than a wavelength, the sound will spread around the object giving rise to diffraction. The waves are bent and their direction of propagation altered causing a decrease in energy per unit area.

(d) Absorption

Absorption is the loss of ultrasonic energy due to its conversion to other forms of energy, primarily heat. Absorption has been shown to follow a simple exponential function:

$$I = I_o e^{-2\alpha x}$$

where I = intensity at distance - x

I_o = intensity at $x = 0$

α = absorption coefficient

x = distance traveled during absorption.

The absorption coefficient is unique for all media and results from a number of distinct absorption mechanisms. These mechanisms are dependent on the properties of the media (temperature, pressure, density, viscosity, etc.) and the frequency of the ultrasound. The complexity of the absorption processes makes it impossible to calculate the absorption coefficients accurately so empirical data is used.

Most types of absorption mechanisms fall under the category of relaxation mechanisms where relaxation mechanisms involve a loss of energy due to a time lag between the conversion of energy to one form and then back again. This conversion delay can manifest itself in many ways:

1. Conductional Relaxation - losses due to time lag in heat conduction.

2. Thermal Relaxation - thermal excitation of molecules due to rotation and vibration.

3. Viscous Relaxation - dissipation of energy due to small shear flow at the time of compression.

4. Structural Relaxation - Movement of molecules into and out of intermolecular spaces.

(3) Reflection, Refraction and Transmission

Plane waves incident on the surface of an object which has a characteristic impedance (Z) different from that of the medium in which they are propagated will be partially reflected and transmitted. The relative values of each may be expressed as the reflection coefficient $\phi_r = \frac{I_r}{I_i}$ and the transmission coefficient $\phi_t = \frac{I_t}{I_i}$ where I_i is the incident intensity, I_r = reflected intensity and I_t = transmitted intensity. It then follows that $\phi_r + \phi_t = 1$. These values can be better visualized in Figure 6.

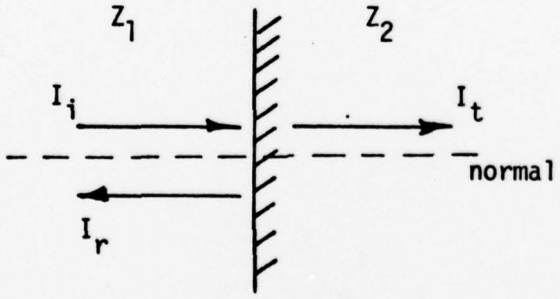

Figure 6. Plane Waves Normally Incident to a Single Interface

For a plane wave of normal incidence it can be shown that

$$\phi_t = \frac{4Z_1Z_2}{(Z_2 + Z_1)^2}$$

For a plane wave at other than normal incidence it can be shown that

$$\phi_t = \frac{4Z_1Z_2\cos\theta_i \cos\theta_t}{(Z_2\cos\theta_i + Z_1\cos\theta_t)^2}$$

where the angles θ are defined in Figure 7.

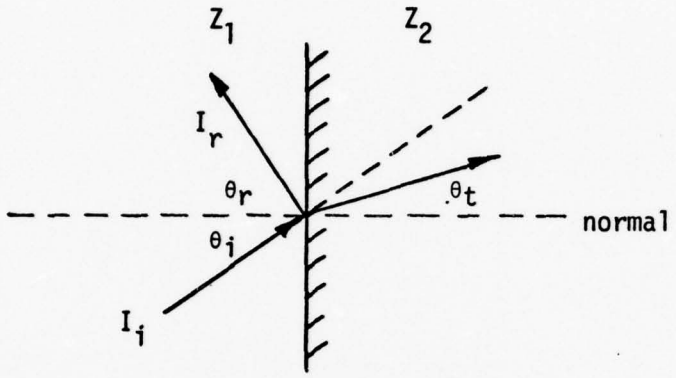

Figure 7. Plane Waves at Other than Normal Incidence to a Single Interface

The angles θ may be calculated from the simple law of refraction

$$\frac{\sin\theta_i}{\sin\theta_t} = \frac{c_1}{c_2}$$

where c_1 = speed of sound of medium 1

c_2 = speed of sound of medium 2

Special cases of these general equations are of interest

1. When $Z_1 = Z_2$ $\phi_t = 1$
2. When $Z_1 >> Z_2$ or $Z_2 >> Z_1$ then $\phi_t \longrightarrow 0$
3. Even if $Z_1 \neq Z_2$ but $Z_2\cos\theta_i = Z_1\cos\theta_t$, then $\phi_i = 1$, where angle, θ_i, is the angle of intromission.
4. When $\sin\theta_1 = \frac{c_1}{c_2}$, for $c_1 < c_2$, then $\phi_t \rightarrow 0$, where angle, θ_1, is the critical angle.

The above equations and analysis only apply to simple single interface problems and cannot be used to analyze complex multi-interface problems. There are complex methods available, however, which can be used to analyze multiple interface problems but they will not be discussed here [Beranek and Work (1949)]. It is beneficial, however, to briefly discuss a simple two interface analysis because it points out several important facts that are necessary for the understanding of multi-interface problems and the design of biological sample holders. Consider the configuration of Figure 8.

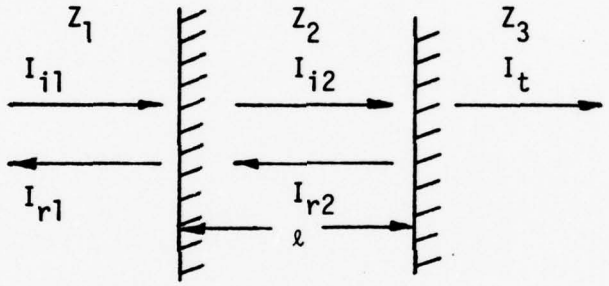

Figure 8. Plane Waves Normally Incident to a Two Interface System

It can be shown that:

$$\phi_t = \frac{4 Z_1 Z_3}{(Z_1 + Z_3)^2 + \sin^2(k_2\ell)\left[\frac{(Z^2_2 - Z^2_3)(Z^2_2 - Z^2_1)}{Z^2_2}\right]}$$

Special cases of this equation are of interest.

1. if $Z_1 = Z_2 = Z_3$ then $\phi_t = 1$ no interface case.
2. if $Z_2 = Z_3$ then $\phi_t = \frac{4 Z_1 Z_3}{(Z_1 + Z_3)^2}$ which is the simple single interface problem.
3. if we make ℓ very small where $k_2\ell \rightarrow 0$, then $\phi_t = 1$

This shows that a very thin interface acts as if there is no interface.

4. if $\sin^2(k_2\ell) \longrightarrow 0$ keeping a finite value for ℓ then $\phi_t = 1$ when $\ell = \frac{n\lambda}{2}$. For interface thicknesses which are equal to integral numbers of half wavelengths we get perfect transmission (assuming no loss due to absorption).

5. if $\sin^2(k_2\ell) \longrightarrow 1$ we can get $\phi_t = 1$ by fixing the values of $\ell = \frac{n\lambda}{4}$ and adjusting the impedances of the medium to $Z_2 = \sqrt{Z_1 Z_3}$. This is called quarter wavelength matching where we select the impedances of the mediums so as to get perfect transmission.

These special cases show that in a multi-interface problem there is an interaction between all interfaces based on not only their impedance but the wavelength and the thickness of that medium.

(4) Standing Waves

Up until this point in the discussion all waves have been considered to be of the progressive type propagated into an infinite environment. In real life situations we must always deal in a bounded medium which means that a portion of all propagated waves must be reflected back upon itself. The interaction of the forward and backward running wave causes superimposition of waves, resulting in constructive and destructive interference. The result is the formation of standing wave patterns in the bounded medium. Depending on the phase of the reflected wave and the reflection coefficient of the boundary, the standing wave will vary in amplitude with maximum values at the anti-nodes and minimum values at the nodes. A simple index used to indicate the relative degree of standing waves is the standing wave ratio (SWR) which is defined as:

$$SWR = \frac{P_{max}}{P_{min}}$$

where P_{max} = acoustic pressure at the anti-mode

P_{min} = acoustic pressure at the node

A SWR = 1 means that there is no reflected wave.

d. Physical Effects of Ultrasound

(1) Cavitation

At higher levels of ultrasonic intensity the alternating compression and rarefraction of the medium causes small cavities of gas to form. These cavities can collapse violently if the intensity is large enough, sending shock waves through the medium. In addition, very high (2000°K) temperatures may occur at the cavitation site. These adverse conditions have been shown to cause chemical reactions including: oxidation, reduction, degradation and synthesis of inorganic and organic substances, polymerization, and intermolecular regrouping.

Another type of cavitation, called stable cavitation, has also been shown to produce chemical interaction. Stable resonance bubbles produced by the rarefraction do not collapse but pulsate at the frequency of the ultrasonic radiation. These bubbles present adverse conditions for chemical systems including high temperatures and pressure extremes, which create changes in structure.

(2) Microstreaming and Eddy Formation

The interaction of the ultrasonic field with objects of differing characteristic impedance cause the formation of microstreaming and eddys. The forces produced by this distortion of the field have been analyzed in detail and are too complex to discuss here. Such forces as Bernoulli forces where particles are attracted to each other by hydrodynamic flow, Oseen Forces caused by distortion of the wave by the media, and Stokes Forces due to particle interactions are among those produced. These forces are responsible for intercellular

movement and shear force which have been shown to result in significant biological effects.

(3) Heating of Medium

The absorption of ultrasonic energy by the medium results in a conversion of ultrasonic energy from mechanical to heat. Two types of heating are known to exist in the medium-average or gross heating of the medium and instantaneous or excess heating. The instantaneous heating of the medium caused by the fluctuation in ultrasonic pressure can be shown to follow the relationship:

$$\tau = \frac{(\gamma - 1)pT_o}{\rho c^2}$$

where τ = the instantaneous temperature

γ = ratio of specific heat at constant volume to specific heat at constant pressure

T_o = ambient temperature of medium

p = peak acoustic pressure

Note that at a highly reflective interface the value of τ can be twice as large, due to a possible doubling of the peak pressure at the nterface.

The average temperature increase in the medium caused by the absorption of the ultrasonic energy can be shown to follow the relationship:

$$\frac{dT}{dt} = \frac{\alpha I}{\rho s}$$

where $\frac{dT}{dt}$ = time rate of change of the temperature

s = specific heat of the medium

α = absorption coefficient.

This equation shows the rate at which the temperature would increase in a lossless system. In actuality, the temperature would rise to an equilibrium state where the heat flowing from the medium would equal the heat input due to ultrasound.

e. Ultrasound Dosimetry

Ultrasound dosimetry involves not only the measurement of the average ultrasound intensity but the total characterization of the ultrasound field. Such parameters as peak intensity, pulse rate, pulse width, frequency, intensity distribution in the field, acoustic pressure, standing wave ratio, etc., all combine to characterize the total ultrasound field. A large number of dosimetry systems have been developed to measure various parameters of the ultrasonic field. These systems include: thermal methods such as calorimetry, volumetric expansion, thermocouples and liquid crystals; optical methods such as diffraction, refraction, and Schlieren; mechanical systems such as radiation balances, vane deflection and hanging ball radiometers; and electrical methods such as condenser microphones, piezoelectric transducers, magnetostrictive transducers, and electrostatic transducers. All of these systems are described in detail in the referenced physics of ultrasound texts. Only those systems which were utilized in this research will be discussed, namely the hanging ball radiometer and the piezoelectric transducer.

(1) Hanging Ball Radiometer

Figure 9 shows the basic components of a hanging ball radiometer. Radiation pressure discussed previously causes deflection of the suspended ball and measurement of the deflection distance is an indication of the intensity of the ultrasound through the following equation.

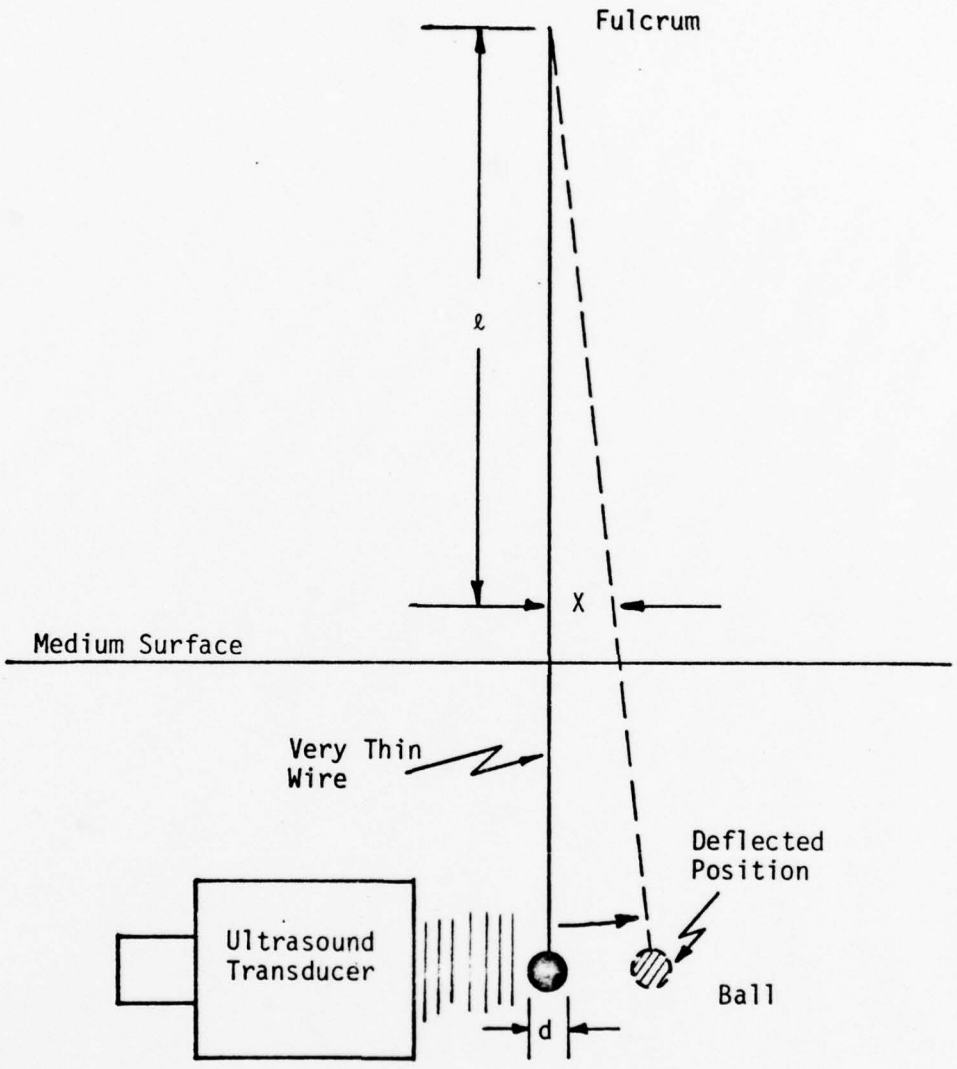

Figure 9. Hanging Ball Radiometer Calibration Method

$$I = \frac{xg\ c\ (m_s - m)}{\pi\ a^2\ \ell}$$

where x = deflection of wire

ℓ = length of wire from fulcrum to x

g = acceleration of gravity

c = speed of sound

m_s = mass of the sphere

m = mass of the water displaced by the sphere

a = radius of the sphere.

Very small spheres may be used in this system with the result that the intensity distribution in the beam may be plotted. Care must be taken to avoid streaming or eddy interference, standing waves or cavitation bubbles. Intensities as low as 2 mW/cm^2 have been measured with $\pm$ 3% accuracy. This is becoming the most accepted method for calibration because of its simplicity and accuracy and is being used as a primary standard in many applications [Dunn and Fry (1971), Stockdale and Hill (1976), and Takaki and Yosioka (1969)].

(2) Piezoelectric Transducer

The piezoelectric transducer, which has been discussed previously, can be used as an ultrasound dosimeter. The piezoelectric crystal responds to acoustic pressure changes and the voltage induced is directly proportional to the pressure and directly proportional to the square root of the intensity. All crystals are frequency sensitive due to their resonance effects and must be calibrated against another standard for each frequency used. In addition, the orientation of the crystal to the direction of propagation of the ultrasound is critical for larger crystals. When the crystal approaches the size

of one wavelength of the ultrasound then this orientation effect is greatly diminished. There are presently very small piezoelectric probes available commercially that satisfy this requirement. The small size of the probe allows detailed mapping of the ultrasound fields.

2. Chromosome Aberrations

a. Chromosomes and the Cell Cycle

Chromosomes are nucleoprotein complexes located within the nucleus of the cell which contain the genetic code for all cell functions. The major chemical components of the chromosome are DNA, RNA, non-histone proteins and histones as supporting structures. The accepted structure of the chromosome is the Watson and Crick model of two helical strands of DNA surrounded by its supporting structure of non-histone and histone proteins. The configuration of the chromosomes in the nucleus depends on the stage of the cell cycle. During G_1, the chromosomes are extended throughout the nucleus in a random fashion and are not recognizable as individual bodies under the light microscope. During synthesis (S), the chromosome is duplicated with the configuration now composed of two sister chromatids connected at a centromere. During G_2, the extended doublet configuration continues with the cell manufacturing those materials necessary for the final stage called mitosis (M). These premitotic stages are collectively called interphase.

During mitosis, a major reorganization of the cell and nucleus take place with the condensation of the chromosomes into more compact structures. This condensation proceeds during prophase and culminates with the chromosomes reaching maximum condensation and alignment at metaphase. During metaphase and late prophase the chromosomes become

compact enough to be visible under the light microscope, if properly stained, and appear as shown in Figure 10 for the human cell.

The individual chromosomes separate from each other by division of the centromere during anaphase producing two daughter chromosomes which go to opposite poles of the cell. Finally the cytoplasm divides at telophase and the chromosomes return to their extended form to begin the cell cycle again at G_1. Detailed discussions of the structure of the chromosome and its functions can be found in Loewy and Siekevitz (1969), Garber (1972) and DeRobertis et al. (1975).

b. Chromosome Aberrations - General

Aberrations or alterations in the normal structure of the chromosome can be caused by many insults on the cell. Structural abnormalities arise due to the breaking of chromosomes at several locations and the cells' attempt to repair the breaks. If the cell can repair the break by reconnecting the two related segments, then there will be no visible aberration present. If, however, there is no repair, or the repair takes place between two unrelated chromosome segments, then the resulting configuration will be aberrant in some way. There is some question as to the exact mechanisms involved with the breaking of the chromosomes (actual fracture of DNA, disruption of histone coat causing DNA separation, or separation during the cells attempt to repair the damage) but indeed they can be shown to break into well defined segments after an insult. These breaks may take the form of single strand breaks where only one strand of DNA is fractured or double strand breaks where both DNA strands are broken.

The cell attempts to repair the breaks through very complex mechanisms of excision of the damage and re-synthesis of broken or missing materials [Fox and Lajtha (1973)] with the majority of repair

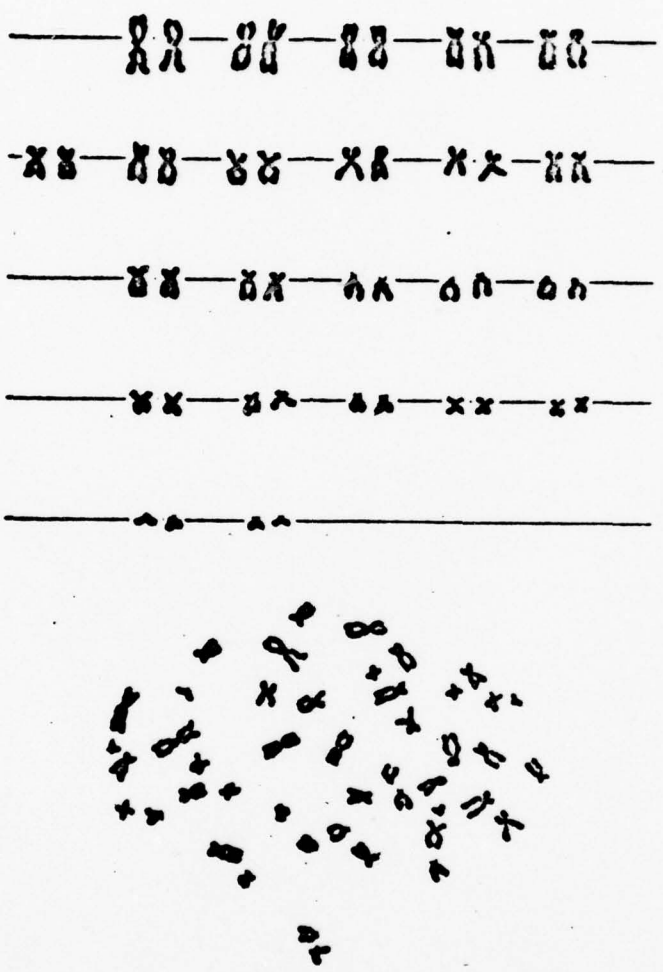

Figure 10. Normal Human Karyotype (female).

occurring within minutes of the insult. Estimates of the mean time to repair radiation-induced chromosome damage range from 12 minutes [Dewey et al. (1971)] to 5 or 6 hours [Evans (1967)] with the most accepted value falling between 1 to 3 hours [Elkind and Sinclair (1965), Prempree et al. (1969)]. The majority of the single strand DNA breaks are properly repaired with no aberrations present but a small percentage of double strand DNA breaks result in aberrations due to improper repair or no repair.

The types of aberrations that are seen in cells are determined by the type of insult and the time during the cell cycle that it occurs. Because our interest in this study is in irradiation of human lymphocytes at G_0, a description of aberrations will be limited to those which may result from irradiation at G_0. At G_0 the cell is resting and not normally dividing, therefore, the chromosome is in its extended configuration. The types of aberrations that could be found when the cell is viewed at metaphase after an insult at G_0 are shown in Figure 11. The major types of aberrations are acentric fragments, minutes, dicentrics and centric rings. Other aberrations occur such as inversions, but these can not be recognized at metaphase unless a banding technique is utilized and a karyotype is performed. These aberration types can be further categorized into exchanges (dicentrics plus centric rings) which represent the misrepaired or improperly repaired chromosomes and the deletions (acentric fragment plus minutes) which represent the non-repaired chromosomes. It should be noted that deletions are only those acentric fragments and minutes which are not associated with an acentric ring or dicentric.

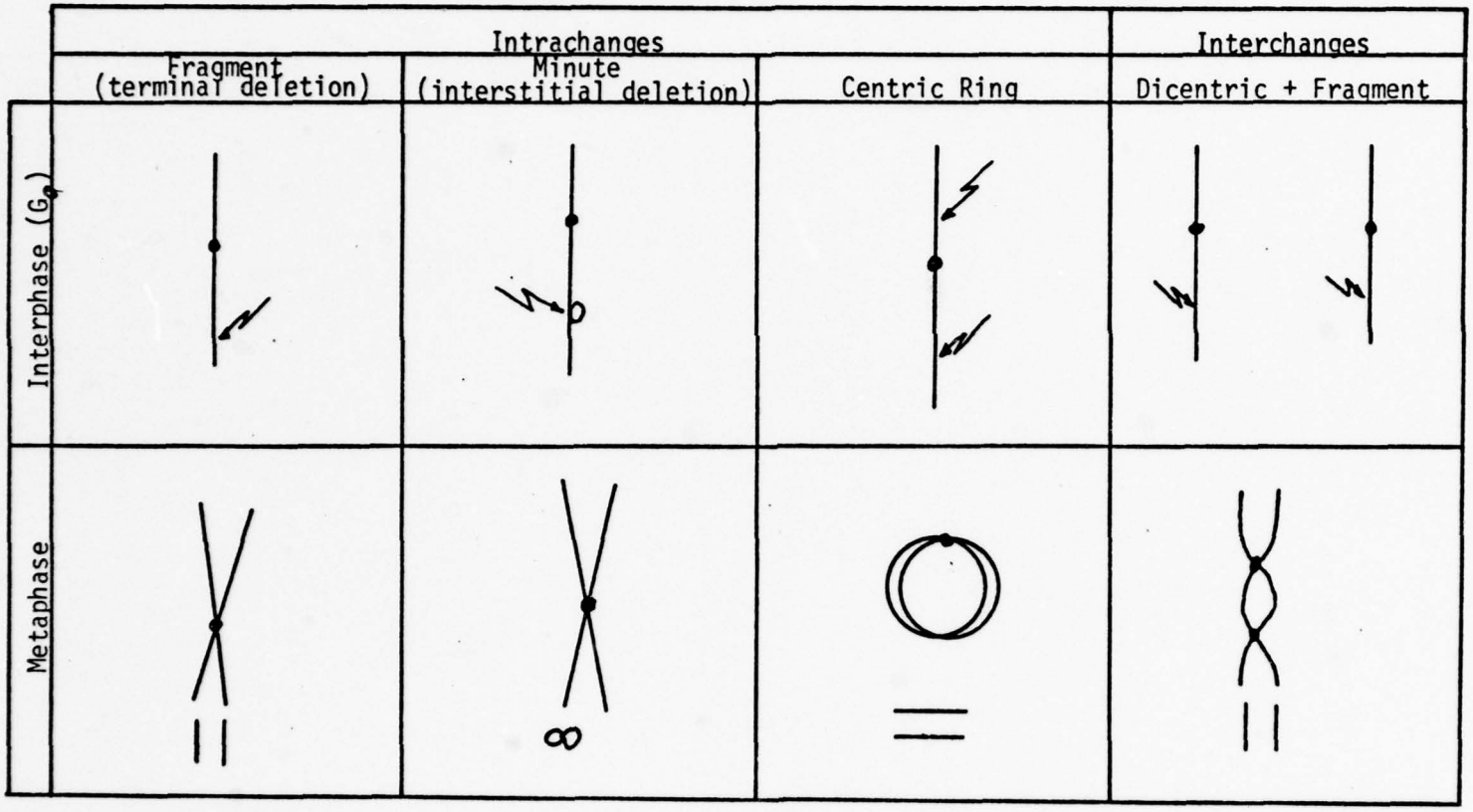

Figure 11. Diagram illustrating the four easily distinguishable chromosome-type aberrations.

c. Chromosome Aberrations from Exposure to Ionizing Radiation

It has been known for many years that ionizing radiation causes chromosome aberrations. Many detailed studies have been conducted using human lymphocytes to determine the types of aberrations and the effects of such variables as dose rate and quality of radiation [Evans (1967), Brewen et al. (1972), Lloyd et al. (1975), and Purrott and Reeder (1976)]. These studies have shown that when cells in G_0 or G_1 are exposed to low LET radiation, the resulting aberration yields follow the mathematical relationship of $Y = C + \alpha D + \beta D^2$ where Y = aberration yield (aberration/100 cells), D = dose in rads, C = background level of aberrations, and α and β are constants. This relationship has been found to hold true for both one hit and two hit aberrations as well as deletions. It has also been shown that the dose rate and LET affect the β constant more than the α constant, resulting in larger numbers of dicentrics and centric rings for higher dose rates and LET.

The referenced studies, also, point out that specific precautions should be taken when performing chromosome analysis on human lymphocytes <u>in vitro</u>. The following items must be considered:

(1) All exposures must be accomplished at 37°C to avoid inconsistent aberration yields. Exposure temperature and the temperature during the chromosome damage repair time are critical. [Bajerska and Liniecki (1969) and Bora and Soper (1971)].

(2) The degree of blood oxygenation has an effect on the aberration frequencies. Freshly drawn venous blood yields lower aberrations than oxygen saturated blood (Liniecki et al. (1973)).

(3) Irradiation in the whole blood state yields more consistent results than exposure in culture medium especially if the medium contains the mitogenic agent Phytohemaglutinin (PHA)

[Lloyd et al (1975)].

(4) The total incubation time for cultures is critical because incubation periods of longer than 54 hours results in some cells passing through their first mitosis. A significant change in aberration yield has been noted because of the loss of certain cells and chromosome fragments during the passage through mitosis (Buckton and Evans (1973)).

d. Chromosome Aberrations from Exposure to Ultrasound

(1) Early Studies

The investigation of chromosome aberrations in sonated cells was stimulated by the experiments of Yamaha and Ueda (1939) when they discovered chromosome aberrations in the root tips of Vicia faba sonated with ultrasound from physical therapy equipment. Subsequent investigations on various plant species at intensities used in physical therapy (.5-5 W/cm^2) by Wallace and Bushnell (1948), Wallace et al. (1948), Newcomer and Wallace (1949), Asche (1951), Spencer (1952), Selman (1952), Lehmann et al. (1954), and Newcomer (1954) showed similar results. Damage to the reported species included chromosome and chromatid breaks, chromosome fusions, coagulations, uncoiling, nuclear dislocation and necrosis. A damage threshold of between 1 W/cm^2 and 10 W/cm^2 was noted. No relationship between total energy delivered to the cells or frequency of irradiation was seen. Possible causes of this damage which were considered included heating, cavitation and mitotic interference and various studies were undertaken to evaluate these etiologic theories.

Selman (1952) found that increasing the external pressure on the sonated sample, reduced the cavitation effect and reduced the chromosome damage. Lehmann et al. (1955) and Spencer et al. (1952),

however, showed that there was no difference in chromosome damage when cavitation was suppressed by imbedding root tips in an agar gel. Dyer (1965) used a 80 KHz vibratory needle to irradiate selectively the nucleus of the cells of a special strain of moss and found that there was a breakage of the mitotic spindle leading to chromatid aberrations. Slotova et al. (1967) continued the work with Vicia faba root tips and found a decrease in mitotic activity with more breaks in small chromosomes than in large chromosomes. They also noted that the numbers of aberrations decreased with time after exposure, suggesting a repair mechanism. Angulio-Carpio and Orellans (1951) and Dubrow (1949) also noted chromosome rearrangement after a suitable recovery time.

During this time of intensive research using plant tissue, several investigators performed studies on amphibians [Bessler (1952)] and on mammals [Woeber (1951) and Pourhardi et al. (1965)] at physical therapy doses. These studies confirmed that doses similar to those which cause chromosome damage in plant tissue are capable of producing chromosome damage in other species.

(2) Recent Studies

Beginning in the late 1960's, considerable interest was generated concerning the biological effects from ultrasound exposure because of its increasingly wide spread use for medical diagnostic purposes. Hill (1968) reviewed the literature concerning the potential for ultrasound damage at that time and suggested increased study on the area of human exposures, in particular, exposure to the fetus during diagnostic procedures. From 1967 onward, numerous studies have been performed to determine the presence of chromosome damage in human tissues from exposure to ultrasound. A listing of a number of these studies is presented in Table 1 with pertinent exposure

Table 1

Summary of Chromosome Damage from Exposure to Ultrasound

Authors	Cell System	Frequency of Ultrasound-MHz	Power Levels of Ultrasound	Chromosome Aberrations	Remarks
Fisher et al. 1967	Leukocytes from human umbilical cord	810 KHz	3 W/cm^2	None	
Bernstine 1969	Human leukocytes	6 MHz	20-30 mW/cm^2	None	15 min and 18 hr exposure time.
Serr et al. 1970	Fetal Cells in Amniocentesis	6 MHz	22.5 mW/cm^2 10 hrs Exposed in vivo	Yes	2 cases out of 10 had 6% abnormalities.
Macintosh and Davey 1970	Human leukocytes	2.25 MHz	Focused Beam 8-17 mW/cm^2	Yes	High standing wave ratio in sample.
Coakley et al. 1971	Human leukocytes	1 MHz	3-45 W/cm^2 5 min	Yes	Positive result attributed to chemical toxin not ultrasound.
Boyd et al. 1971	Human lymphocytes	1.5-2.0 MHz	25-30 mW/cm^2 13 hrs	None	Used polystyrene sample holder.
Bobrow et al. 1971	Human lymphocytes	1.5 MHz	0.014-2.77 W/cm^2	None	Polyethylene holder but different type holder.
Abdulla et al. 1971	Blood cultures of fetuses sonated in utero	1.5 and 2.0 MHz	0.8-22 W/cm^2 1 hr and 10 hrs	None	Pulsed and continuous.
Watts et al. 1972	Human lymphocytes	1.0 and 2.5 MHz	8 W/cm^2 20 hrs	None	High standing wave ratio to maximize cavitation
Lucas et al. 1972	Fetus in utero fetal heart monitor	2 MHz	5 mW/cm^2 at surface	None	

Table 1 (Continued)

Hill et al. 1972	Chinese hamster cells	1 MHz	150 W/cm^2 2 hrs	None	Pulsed 1 KHz 50 μs pulse.
Fischmann et al. 1972	Human leukocytes	1.3 MHz	5-40 W/cm^2 2 min	Yes at 22 W/cm^2 to 40 W/cm^2	Threshold at 22 W/cm^2.
Coakley et al. 1972	Human lymphocytes	1 MHz 2.5 MHz	0.18-350 W/cm^2	None	Large comprehensive study pulsed + continuous.
Buckton and Baker 1972	Whole blood cultured leukocytes	1 MHz	30 mW/cm^2 300 mW/cm^2 3 W/cm^2 one hour	None	
Abdulla et al. 1972	Human lymphocytes	2 MHz	23 mW-3.5 W/cm^2 2 to 8 hours	Yes at high intensity	No standing waves far field exposure.
Brock et al. 1972	Wallaby lymphocytes	2.25 MHz	0.4-425 W/cm^2 1-100 min	Minor gaps noted at high intensity	
Rott and Soldner 1973	Human lymphocytes at first mitosis	2 MHz 870 KHz	0.2-35 W/cm^2	None	Pulsed 2000 Hz, 1 μsec at 870 KHz.
Mermut et al. 1973	Lymphocytes of fetal umbilical cord blood	2.25 MHz	3 mW/cm^2 72-90 hrs	None	Pulsed - 3 μsec at 1 KHz.
Ikeuchi et al. 1973	Fetus in vivo cultured fibroblast of embryonic tissue	2 MHz	40 mW/cm^2	None	
Galperin-Lemaitre et al 1973	Golden hamster bone marrow cells	.87 MHz	1.5 W/cm^2 2-5 min	None	

Table 1 (Continued)

Levi et al. 1974	Bone marrow cells of golden hamster *in vivo*	.87 MHz	1-1.5 W/cm^2	None	Refinement of previous study of Galperin-Lematire.
Braeman et al. 1974	Human lymphocytes	2.25 MHz	50 mW/cm^2	None	Use system of Macintosh and Davey 1970 but induced cavitation.
Macintosh et al. 1975	Human leukocytes	1 MHz	30 W/cm^2	None	Repeat of previous Macintosh and Davey 1970 study with other extensions.
Khokhar and Oliver 1975	*Vicia faba* root tips	1.5 MHz	5 W/cm^2 30 min CW	None	
Kunze-Muhl 1972	Human lymphocytes	810 KHz	3 W/cm^2 Cw 10 min	None	
		2 MHz	20 mW/cm^2 1 hr-pulsed	None	Small gaps only.

data and results.

Of the 26 referenced studies only six showed significant chromosome aberrations. Of these six, three were at exposure levels where cavitation effects predominate (greater than 1 W/cm^2) and have been shown to cause chromosome damage in other species [Coakely et al. (1971), Fischmann et al. (1972), and Abdulla et al. (1972)]. Of the three studies showing chromosome damage at lower exposure levels, one has questionable findings due to lack of control data [Serr et al. (1970)], and the other two have been criticized for the dosimetric methods utilized in the study [Macintosh and Davey (1970) and Macintosh and Davey (1972)]. This leaves no conclusive evidence about the occurrence of chromosome damage at low intensity.

(3) Conclusions

This large volume of data appears to support the conclusion that high levels of ultrasound (> 10 W/cm^2) can cause chromosome aberrations in some cell systems. Between 1.0 and 10 W/cm^2 there is an area of uncertainty where the effects are not as clear and below 1.0 W/cm^2 there are few reports of chromosome damage at all. No mechanism has been proven to be responsible for the damage, but cavitation which appears to coincide with the onset of effects has been suggested as a possible mechanism.

3. Synergism of Ultrasound and Ionizing Radiation

From the previous discussion it can be seen that the literature suggests that ultrasound used alone at lower intensities (< 1 W/cm^2) probably causes no chromosome aberrations and ionizing radiation used alone at any level produces predictable quantities and types of chromosome aberrations. What then is the effect on chromosomes if both

ultrasound and ionizing radiation are used simultaneously, as they may be in medical diagnostic problems involving the fetus in particular, as well as older members of the population?

The answer to this question is not clear because to date very few studies have shown that a synergistic effect between ultrasound and ionizing radiation exists at the chromosome level. Numerous studies have shown, however, that synergism does exist at the cellular level and these studies have suggested that the genetic material of the cell is affected. It is beneficial, therefore, to review the literature concerning the synergism of ultrasound and ionizing radiation to determine what is presently known concerning the effects on chromosomes.

a. General Effects

The possibility of a synergistic effect between ultrasound and ionizing radiation was suggested initially by Conger (1948) who observed an increase in the number of chromosome aberrations in Tradescantia buds when x-irradiation was followed immediately by exposure to high intensity sound waves. Since that time, interest in the possible use of ultrasound and ionizing radiation in tumor therapy stimulated studies on mammalian tumor systems by Lehmann and Krusen (1955), Woeber (1959), Pydorich (1966), and Clark et al. (1970). All studies, with the exception of that of Clark et al. (1970), show a definite synergism between ultrasound and ionizing radiation. Significantly less ionizing radiation was required to achieve the same biological end point when used simultaneously with ultrasound. Additional studies conducted using other plant, animal and human cell systems [Dharkar (1964), Javish (1966), Kim (1968), Spring (1969), Rapacholi (1970), Martins (1971), Spring et al. (1970), Fujita and Sakuma (1974), Todd and Shroy (1974), Kunze-Muhl (1975), Hering and

Shepstone (1976), Burr et al. (1977), and Craig and Tyler (1977), Harkanyi et al. (1978)] all showed some degree of synergistic effect with the exception of that of Hering and Shepstone (1976) and Harkanyi et al. (1978). A summary of these studies is presented in Table 2.

These studies suggest that some type of synergistic effect between ultrasound and ionizing radiation exists but the mechanism(s) responsible for this effect are as yet not known. The results of these studies do, however, indicate several important facts:

1. The cell membrane appears to be a possible site of damage enhancement [Martins (1971), Rapachoti (1970)].

2. The genetic material of the cell, i.e., chromosomes and DNA, may be the site of damage enhancement [Conger (1948), Martins (1971), Kim (1968), Burr et al. (1977), Kunze-Muhl (1975)].

3. The synergistic effect is evident even in situations where ultrasound alone causes no detectable effect [Spring (1969), Todd and Schroy (1974), Martins (1971), Conger (1948), Kim (1968), Kunze-Muhl (1975), Burr et al. (1977), Craig and Tyler (1977), Fugita and Sakuma (1974)].

4. Synergism has been shown when ionizing radiation exposure is followed by cell vibration or centrifugation, suggesting mechanical disruption of cellular components as a possible mechanism [Conger (1948)].

5. Ultrasound used after ionizing radiation appears to be a more effective radiosensitizer than when used before radiation suggesting an effect on the cellular repair mechanisms [Martins (1971)]. Kim (1968), Kunze-Muhl (1975), Burr et al. (1977), Craig and Tyler (1977), Fugita and Sakuma (1974)].

6. No effect of ultrasound frequency has been noted but a possible ionizing radiation dose rate effect was noted [Spring et al

Table 2

Summary of Studies on Synergism of Ultrasound and Ionizing Radiation

Author	Object of Study	Ionizing Radiation	Ultrasound Irradiation	Significant Results (over either one used alone)
Conger (1948)	Tradescantia Buds	78 r/min	9.1 KHz Power Unknown U.S. after x-rays for 5 min	Increase in chromosome aberrations
Lehmann and Krusen (1955)	Tumor in Rat Tail	135 kVp 165 r/min	1 MHz 1 W/cm ^{2} 15 min before x-rays	Reduced dose need for same biologic effect by 50%. Suggested heating as cause.
Woeber (1959)	Tumor in Rat	60 kVp 350 R	1 MHz 1 W/cm ^{2} simultaneous	Reduced dose need for same biologic effect by 40%. Suggested heating as cause.
Dharhar (1964)	Microorganism (Bacteria)	^{60}Co	Unknown	Marked increase in bacterial death.
Javish (1966) (Abstract)	Hamster Cells	Unknown x-rays	960 KHz Power Unknown	Marked reduction in cells left intact.
Pydorich (1966)	Eyelid Epithelioma	40-50 kVp 3,470-4,950 rad	0.8 MHz 0.8 W/cm ^{2}	Reduced dose of x-ray for cure by 40-42%.
Spring (1969)	Grass Seed	^{60}Co 2500-15,000 rad	2 MHz 1 mW/cm ^{2} simultaneous	2.6 times increase in radiosensitivity for germinative grass seed.
Clark et al. (1970)	Rat leg tumor and L5178Y Lymphoma Cells	250 kVp 100-2000 rad	1 MHz 1-5 W/cm ^{2}	No detectable change in radiosensitivity.

Table 2 (Continued)

Spring et al. (1970)	HeLa Cells	^{60}Co 50-400 rads	2 MHz 1 mW/cm^{-2}	1.7 at 50 rad 1.0 at 200 rad radiosensitivity 0.7 at 400 rad
Rapachoti (1970)	Tumor cells	220 kVp 55 rad/min	pulsed 1 MHz-5 min 10 W/cm^2	Reduced electrophoretic mobility of cells (membrane effect).
Martins (1971)	Male adult hamster M3-1 cells	150 kVp 600 rad/min	1 MHz 0.125 W/cm^2 1 min	Cell survival curves showed synergistic effect from U.S. More effect when U.S. used after irradiation with x-ray than when used before x-ray.
Todd and Schroy (1974)	Hamster Cells	50 kVp 395 rad/min 200-1000 rads	920 KHz 10 min 0.14 W cm^2 after x-rays	Increase in cell death. Also showed that just heating cells did not cause effect.
Kim (1968)	Human Peripheral Blood	200 kVp 45 rad/min 50,100,200 rads	810 KHz 10-20 min 3 W/cm^2	Significant increase in chromosome aberrations for x-ray before U.S.
Kunze-Muhl (1975)	Human Peripheral Blood	200 kVp 45 rad/min	2 MHz 0.02 W/cm^2 pulsed 10 min + 1 hr	Significant increase in chromosome aberration frequency when x-ray after U.S.
Burr (1977)	Human Peripheral Blood	^{60}Co 45 rad/min 200 rads	2 W/cm^2 30 min 1 MHz	Significant increase in chromosome aberration when x-ray before U.S.
Craig and Tyler (1977)	E. Coli	^{60}Co 1.95 Krads/min	13 K 30 min	Increase in cell death.
Hering and Shepstone (1976)	Roots of Zea mays	250 kVp 775 rads	1 MHz 962 W/cm^2 2 min pulsed + CW	No effect

Table 2 (Continued)

Fujita and Sakuma (1974)	Conchae	^{60}Co	1 MHz_2 3 W/cm^2 60 min	Destroyed tissue when Co-60 followed by U.S. or simultaneous.
Harkanyi et al. (1978)	Chromosomes of CBA/H-T_6J Mice	190 kVp 20.7 R/min 50 R whole body	0.1 and $_2$ 1.0 W/cm^2 800 KHz,CW	Ultrasound given 2 hours before radiation showed no effect in bone marrow cells <u>in vivo</u>.

(1970)].

b. Synergism for Chromosome Aberrations

Literature concerning the synergistic effects of ultrasound and ionizing radiation on chromosomes is very limited with only five studies available [Conger (1948), Kim (1948), Kunze-Muhl (1975), Burr et al. (1977) and Harkanyi et al. (1978)]. All of these studies have shown a synergistic effect when ultrasound and ionizing radiation are combined except Harkanyi et al. (1978). Details of each study are presented below.

Conger (1948) found 1.27 times as many two hit aberrations and 1.26 times as many one hit aberrations in Tradescantia paludosa when high intensity sound (9100 Hz-CW) was used simultaneously with 250 kVp x-rays at 78 rads/min. Sonation was started with the irradiation and continued for 5 minutes after completion of the 250 rad dose. Exposures were made at 18°C in a sonic cup and the sound power level was not measured but reported as 30 V on the transducer. The sonic treatment alone caused no chromosome aberrations. Conger suggests that the increase in aberrations may be due to the mechanical movement of the chromosome fragments resulting in a decrease in the amount of restitution and an increase in the amount of detectable new reunions (exchanges). He hypothesized that the synergistic effect might be increased with the use of ultrasonic waves (much higher frequency).

Kim (1968) went several steps farther in investigating the synergistic effect on chromosomes by exposing human whole blood to 3 W/cm^2, CW, 80 KHz ultrasound at various doses of 200 kVp x-rays at 44.67 rads/min. He exposed the blood in glass ampules which were rotated and moved up and down in front of the ultrasonic transducer resulting in a true average intensity in the blood of much less than 3 W/cm^2. Blood was cultured for 72 hours, harvested and scored for

aberration yields. Specific experiments showed a significantly greater number of one hit and two hit type aberrations when 10 minutes of ultrasound was applied immediately after 50, 100, and 200 rads of x-rays. There appeared to be no effect of ionizing radiation dose rate over that of the x-ray alone. Increasing the ultrasound exposure time to 20 minutes did not significantly affect the results, nor did delaying the application of the ultrasound by 2 hours and keeping the x-ray exposed blood at 5°C. Since most repair processes are known to be inhibited, if not completely stopped at 5°C, it was suggested by Kim that the ultrasound interferred with the radiation repair process.

Kunze-Muhl (1975) reported the results of Kim (1968) and several additional experiments. Using the ultrasound and ionizing radiation exposure system of Kim (1968) she found no significant increase in chromosome aberrations when ultrasound precedes the x-rays. In addition, she reports results from one hour exposures using a 2 MHz, pulsed, diagnostic ultrasound unit of 0.02 W/cm^2 average output combined with 200 rads of x-ray. The results show a significant reduction in the aberration yields for all types of aberrations when ultrasound is given after x-rays and a significant increase in aberration frequency when ultrasound is given immediately before x-rays. This is exactly the reverse of the effects of higher intensity CW application of ultrasound. No explanation of this apparent inconsistency was given. Methods of controlling the environmental conditions during, before and after the experiments were not reported.

Burr et al. (1977) have reported results which confirm those reported by Kim (1968) and Kunze-Muhl (1975) and go several steps further. Combined exposures (2 W/cm^2, CW, 1.0 MHz ultrasound for 30 min and Co-60 radiation at 45.3 rads/min for 200 rads) of human

peripheral blood were made using various exposure sequences. All blood was cultured for 48 hours and all exposures were at room temperature (23°C). The results showed that there is no significant increase in chromosome aberration frequency when ultrasound precedes γ-rays by 6 hours or immediately. There is, likewise, no increase if ultrasound follows the γ-ray by 2 or 6 hours. There is, however, a significant increase in the total aberration frequency when ultrasound is given simultaneous with γ-rays (2.3 times) and when given immediately after γ-rays (1.77 times). One hit aberrations were increased significantly in both simultaneous and immediately after sequences but two hit aberrations were increased significantly only in the simultaneous sequence.

Harkanyi et al. (1978) reported no apparent synergistic effect on chromosomes of the CBA/H-T_6J mouse exposed <u>in vivo</u> to 0.1 and 1.0 W/cm^2, 800 KHz, CW, ultrasound and 190 kVp, x-rays, 20.7 rads/min, for 50 rads. Ultrasound exposure preceded the radiation exposure by two hours with the result that there was no statistically significant change in chromosome aberration frequencies over that of the radiation alone (ultrasound alone caused no aberrations). The authors note that their result is consistent with the findings of Kunze-Muhl (1975).

C. Statement of the Problem

The previously referenced studies concerning the possible synergistic effect of ultrasound and ionizing radiation on the chromosomes of human and plant cells have shown that there is some type of synergistic effect or interaction but the mechanisms for the interaction have not been determined. In addition, each study had

particular shortcomings which made it difficult if not impossible to compare the results. Problems found in these studies include:

1. The temperature was not properly controlled or measured in almost all of the studies. It has been shown previously that temperature has an effect on the chromosome aberration yield.

2. The dosimetry of the ultrasound exposures was poor. In all cases the ultrasound intensity was measured at the location of the sample holder but not inside the sample holder. The potential variation in intensity between studies and between samples in each study make it impossible to compare results.

3. Several experiments utilized culture times of 72 hours for the human peripheral blood lymphocytes. Culture times of greater than 54 hours have recently been criticized because of the procession of some cells into their second mitosis.

The objective of this study is to evaluate the possible synergy of ionizing radiation and ultrasound by determining, under stringently controlled conditions, whether the damage to the genetic material of human cells is enhanced by their combined use. In addition, the study will attempt to determine whether the temporal sequence of their application significantly influences the overall magnitude of the effect. Specifically, these studies will involve two separate areas of technical work:

1. An ultrasound and ionizing radiation exposure and dosimetry system will be designed, constructed and tested which will deliver accurately known and controlled doses of ultrasound and ionizing radiation to blood samples under controlled environmental conditions. The intensity of the ultrasound and the temperature within the sample will be monitored at all times. A temperature simulation system will be

included to simulate the heat exposures generated by the ultrasound.

2. Various sequences of ultrasound and ionizing radiation will be applied to human peripheral blood using the above system. Chromosome analysis using 48 hour incubation will be conducted on all blood samples to determine the effect of each exposure sequence. Sequences such as ultrasound alone, ionizing radiation alone, heat alone, heat and ionizing radiation, and ultrasound plus ionizing radiation will be performed in an attempt to determine if there is a synergistic effect between ultrasound and ionizing radiation and what the possible mechanism for this effect might be. Ultrasound and ionizing radiation exposure parameters for these experiments will be chosen so as to as closely as possible reproduce actual exposure conditions which occur in vivo, i.e., 37°C exposure temperature, Co-60 irradiation from a radiation therapy source, 1.0 MHz, CW, ultrasound, etc.

II. DEVELOPMENT OF THE ULTRASOUND AND IONIZING RADIATION EXPOSURE SYSTEM

A. Materials and Methods

The purpose of these experiments is to conduct specific exposures of human peripheral blood to ultrasound, heat and ionizing radiation under controlled conditions. The exposure system used for these experiments is shown schematically in Figure 12A. A photograph of the apparatus is shown in Figure 12B. It consists of the following basic components; a sonation tank with temperature control system, an ultrasound generation system, biological sample holder, ultrasound dosimetry system, ionizing radiation exposure system, and a temperature detection system. Each of these basic components are discussed in detail below with the criteria used for their designand the actual design.

1. Ultrasound Dosimetry System

a. Criteria for Design

(1) The ultrasound dosimetry system must be capable of accurately and simply determining the ultrasound intensity.

(2) The method must not be affected by fluctuating temperatures.

(3) It should be able to measure intensity distribution in sample holder and sonation tank.

(4) It should be able to monitor intensity during exposures.

Figure 12A. Ultrasound and Ionizing Radiation Exposure System

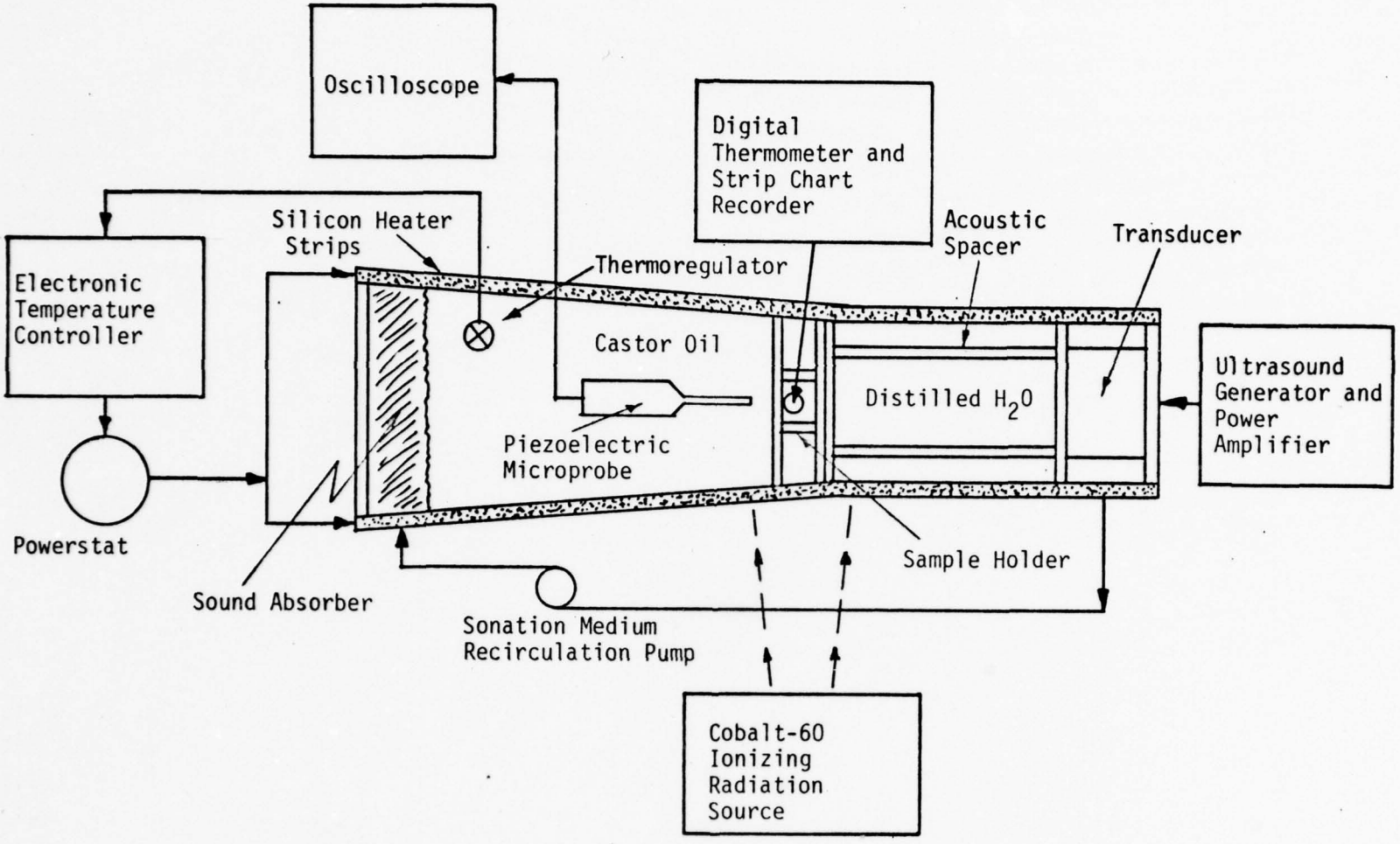

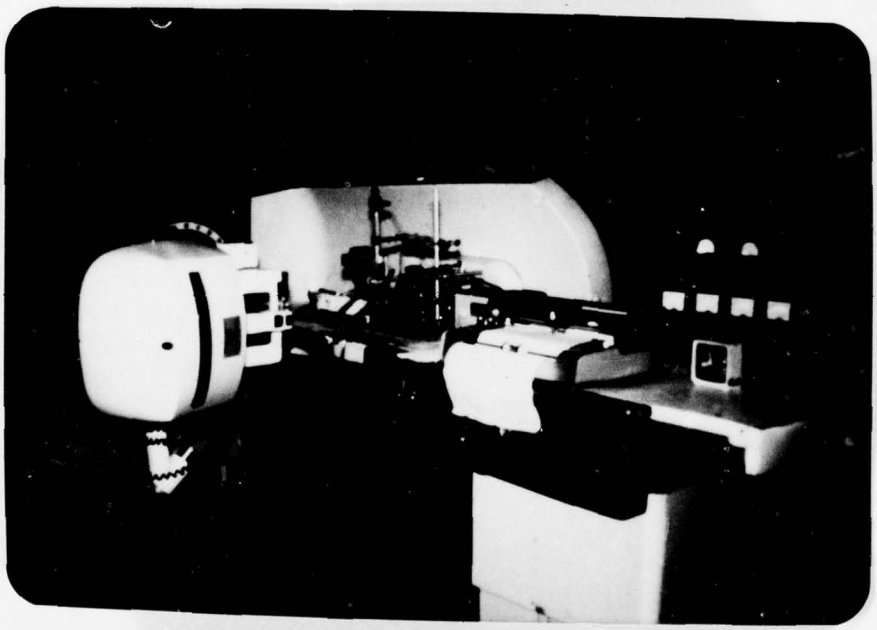

Figure 12B: Ultrasound and Ionizing Radiation Exposure System

b. Design

(1) The ultrasound dosimetry system consisted of both a primary standard (hanging ball radiometer) and a secondary standard (peizoelectric microprobe). The hanging ball radiometer was used to calibrate the piezoelectric microprobe and the probe was used to monitor all ultrasound exposures and map the ultrasound intensity distribution in the tank and biological sample holder. The specifications of the hanging ball radiometer are given in Table 3. (Refer to Figure 9 and Introduction for a discussion of the theory). The ultrasonic microprobe, serial no. 116, manufactured by Mediscan, Inc., East Hartford, Connecticut, was composed of a 0.8 mm diameter, Lead Zirconate Titanate piezoelectric ceramic disk, mounted in the tip of a modified #18 gauge hypodermic needle. The microprobe was mounted on a modified microscope stage in the vertical position so that rectilinear intensity scanning could be performed at any location in the sonation tank. The voltage produced by this probe is proportional to the square root of the acoustic intensity. Because of the probes small size it is very insensitive to errors in alignment to the ultrasound beam. The probe output was measured using a Tektronix, Model T 932, serial no. B010565, 35 MHz bandwidth oscilloscope with a 1 MΩ, 30 pf input.

(2) The sensitivity of the ultrasonic microprobe was determined as follows:

(a) The uncalibrated microprobe was used to measure the ultrasound field distribution at 1 cm from the face of the acoustic spacer in castor oil at 22°C. The field map produced was in terms of the output voltage of the microprobe at 1.1 MHz frequency.

(b) The hanging ball radiometer was then used to measure the ultrasound intensity at the center of the field. This

Table 3

Specifications for Hanging Ball Radiometer

Length of Wire from Fulcrum to X	48 cm
Diameter of Wire	0.005 cm (stainless steel)
Acceleration of Gravity	980.6 cm/sec^2
Mass of Sphere	2.9969 gm
Material of Sphere	Yellow brass
Diameter of Sphere	0.89 cm
Mass of Water Displaced by Sphere	0.369 gm
Speed of Sound in Castor Oil	1.54×10^5 cm/sec
Resulting Intensity Relationship	$I = 1.329 X$
	Where I = Intensity in W/cm^2
	and X = deflection of wire in cm

intensity is the average intensity for the cross-section of the sphere.

(c) Since the microprobe cross-sectional area is very much smaller than the sphere a correction factor had to be determined to make the intensity values comparable. The microprobe, in effect, measures the peak intensity, whereas the sphere measure the average intensity for its cross-sectional area. Assuming a parabolic distribution of energy in the ultrasound field (Figure 22 supports this assumption) it can be shown that

$$I_B = \frac{I_m + I_a}{2}$$

where I_B = average intensity on the ball

I_m = maximum intensity on ball

I_a = minimum intensity on ball.

Assuming that $I_p = I_m$ where I_p = intensity on probe, the correction factor will be

$$C_f = \frac{I_B}{I_p} = 1/2 \left(1 + \frac{I_a}{I_m}\right)$$

Since the ultrasound intensity is directly proportional to the output of the microprobe squared it can be shown that

$$C_f = 1/2 \left(1 + \left(\frac{mV_a}{mV_m}\right)^2\right)$$

where mV_a = minimum millivolt output of the probe (measured at edge of sphere).

mV_m = maximum millivolt output of probe (measured at center of sphere).

(d) The sensitivity of the microprobe is defined as the ratio of the voltage output of the probe to the acoustic pressure that produced the voltage. Usual units are $\mu V/dyne/cm^2$. This sensitivity allows the use of the microprobe in any medium if the acoustic impedance of the medium is known. For this case the sensitivity (s) is defined as:

$$s = mV_m/P_p$$

where P_p = true acoustic pressure on the probe.

The true acoustic pressure is found from

$$P_p = \sqrt{I_B/C_f \cdot Z}$$

where Z = characteristic impedance of medium.

(e) This sensitivity was then used for converting all ultrasound field maps from millivolts to intensity (W/cm^2).

2. Ultrasound Generating System

a. Criteria for Design

(1) System should be capable of continuous wave (CW) operation at typical diagnostic and therapeutic frequencies with as high an efficiency as possible.

(2) System should be stable and provide reproduceable ultrasonic intensity outputs.

(3) The output of the system should be capable of being monitored at all times during exposure.

b. Design

(1) A schematic of the ultrasound generation system is shown in Figure 13 with the basic components and parameters noted. The design of the piezoelectric transducer is shown in Figure 14 and the physical and electrical properties of the transducer crystal are given in Table 4.

(2) The normal operating frequency of the ultrasound transducer was determined by measuring the intensity at 10.5 cm from the transducer for different frequencies near the natural frequency of the crystal using the hanging ball radiometer. The intensity output was then mathematically weighted due to the differences in the input voltage of the transducer so that a normalized output could be used as a comparison of the intensity values. The normalized intensity was:

$$I_n = a^2 I_a$$

where I_n = normalized intensity - W/cm^2

I_a = measured intensity - W/cm^2

a = ratio of actual voltage on the transducer to a reference voltage.

(3) The efficiency of the ultrasound transducer was estimated by measuring the electrical power into the transducer and comparing it to the measured power output. This procedure required the determination of the electrical impedance of the transducer, and the resultant intensity output of the transducer. The electrical impedance, voltage and power into the transducer were estimated using the electrical circuit described in Figure 15 and the equations below.

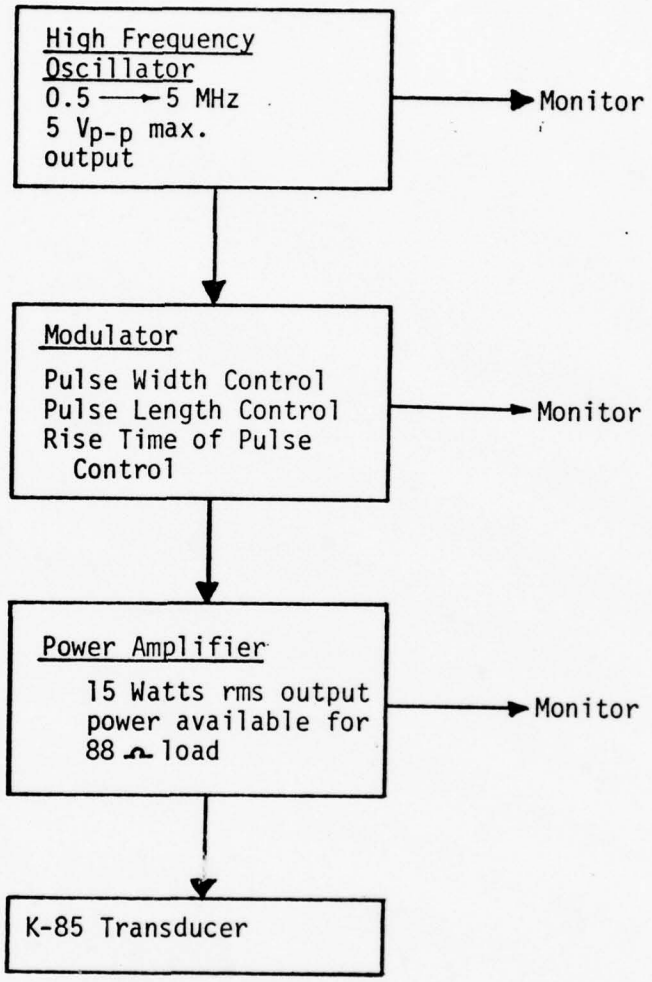

Figure 13. Schematic of the Ultrasound Generation System

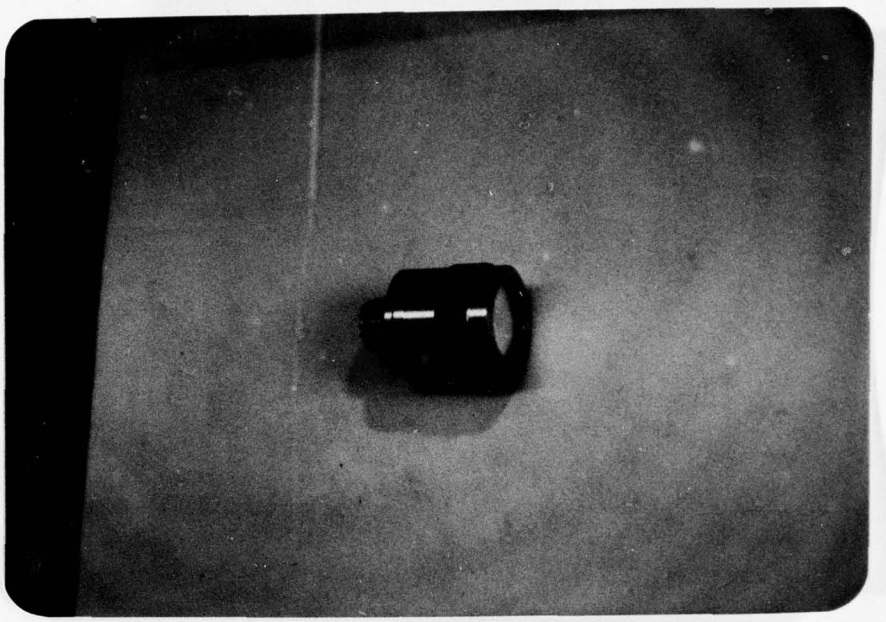

(a)

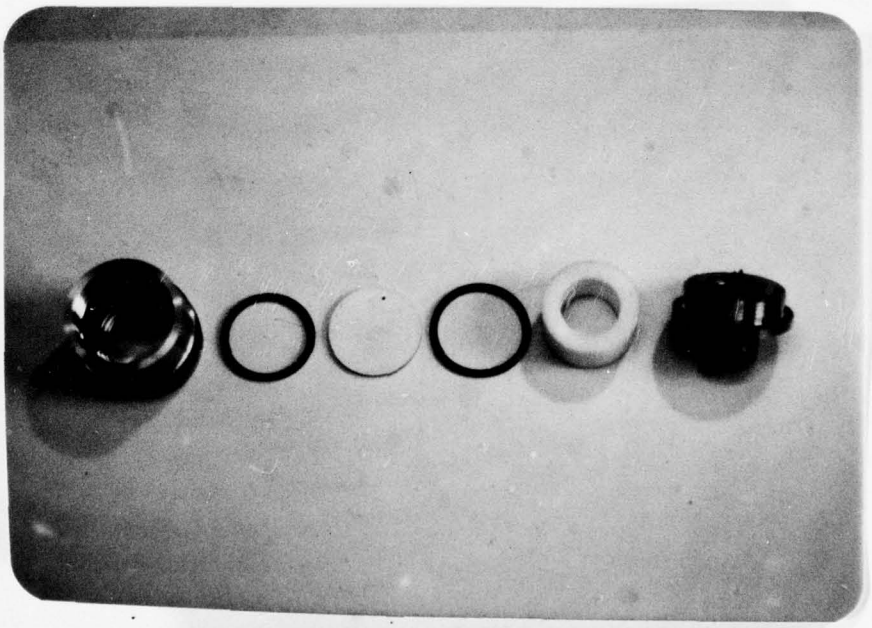

(b)

Figure 14. Ultrasound Transducer. (a) Completed Assembly; (b) Exploded View of Transducer

Table 4

Physical and Electrical Properties of Transducer
as Supplied by Manufacturer

Manufacturer	Keramos, Inc. 104 North Church Road Lizton, ID 46149
Crystal Material	KEZITE Modified Lead Metaniobate
Model No.	K-85
Relative Dielectric Constant-K_3	800
Piezoelectric Strain Constant-d_{33}	160×10^{-12} Coul/Newton
Piezoelectric Voltage Constant-g_{33}	22×10^{-3} Voltmeter/Newton
Mechanical Q (Thickness)-Q_m	15
Frequency Constant (Thickness)	66 KC in./sec.
Density	5.5 gm/cm^3
Longitudinal Coupling Coefficient-K_{33E} Y_{33}	.43 6.8×10^{10} Newton/m^2
Planar Coupling Coefficient-K_p	.35
Diameter	2.54 cm
Frequency	1.0 MH_z
Thickness	0.174 cm

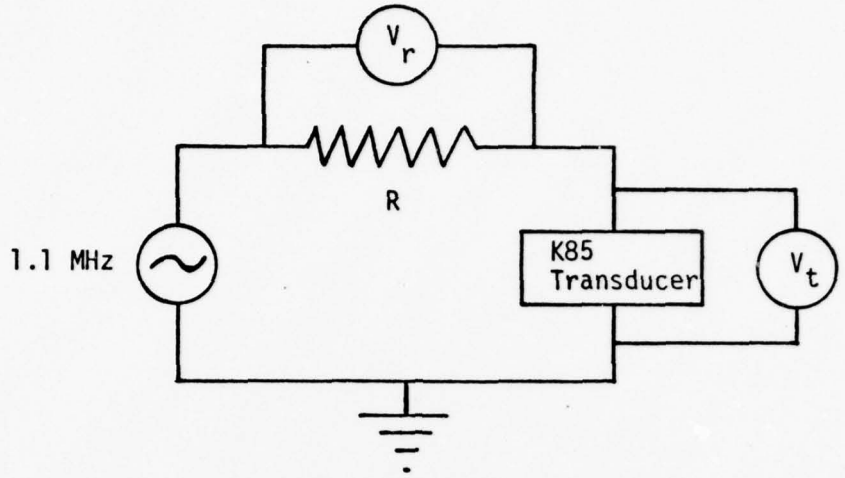

Figure 15. Electrical Circuit for the Determination of the Transducer Impedance

$$Z_T = \frac{V_T R}{V_R} \quad \text{and} \quad P_w = \frac{V_T^2}{Z_T}$$

where Z_T = Impedance of transducer

V_T = voltage across transducer

V_R = voltage across resistor

R = resistance of resistor

P_w = rms power into transducer

The intensity output of the transducer was measured using the piezoelectric microprobe.

3. Sonation Tank and Temperature Control System

a. Criteria for Design

(1) Small total size so that the tank could be placed in front of almost any radiation source and be portable.

(2) Minimize standing waves in the tank as much as possible.

(3) Provide exposures in the far field of the transducer.

(4) Provide a constant uniform tank temperature adjustable from room temperature to 50°C.

(5) Provide a fixed geometry for locating the biological sample holder so that reproduceable ultrasound and ionizing radiation exposures could be made.

b. Actual Design

The sonation tank and temperature control system are shown in Figure 16 (photo of top and bottom view). The basic components are the lucite tank, castor oil sonation medium, sound absorber at end of tank, ultrasound transducer, rectilinear scanner, acoustic spacer, sonation medium, recirculation pump and associated plumbing, temperature sensor, temperature controller and tank heater strips.

(1) Tank - The sonation tank was constructed of 0.635 cm commercial lucite in a very specific shape. The shape was dictated by three requirements: small size, provision for exposures in the far field of the transducer, and fixed geometry of exposures. It should be noted that the flaring of the tank takes place at the approximate location of the start of the far field (10 cm from transducer) and the divergence angle of the tank walls follow the approximate beam width (4.13°) of the transducer.

(2) Castor Oil Sonation Medium - Castor oil was selected due to its high absorption coefficient (0.95 dB/cm for castor oil as compared to water of 0.002 dB/cm) and characteristic impedance (1.48×10^5 g/cm^2-sec) close to blood (1.61×10^5 g/cm^2-sec) and water (1.43×10^5 g/cm^2-sec). Ultrasound energy leaving the acoustic spacer and biological sample holder would be absorbed in the castor oil

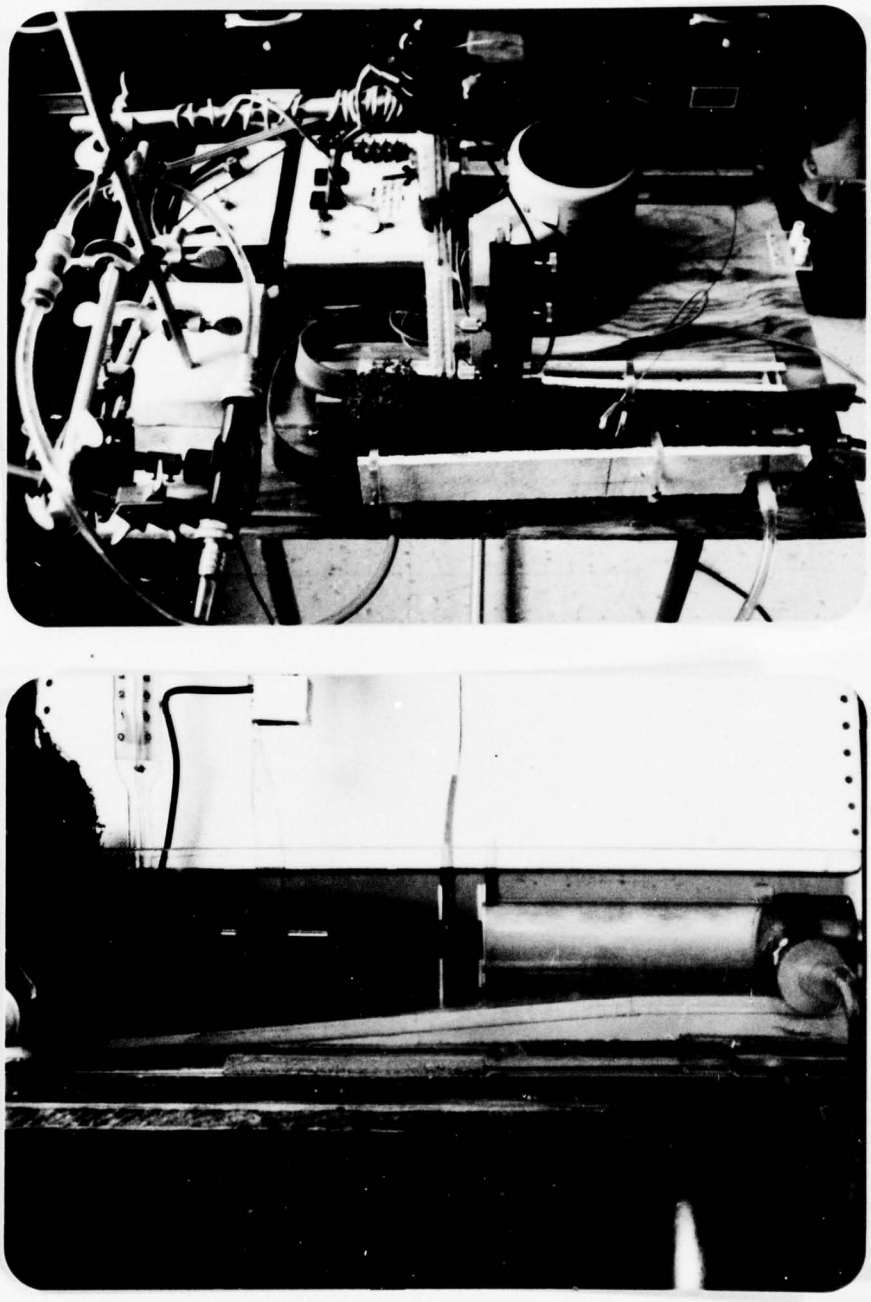

Figure 16. Photographs of Sonation Tank and Temperature Control System

and would not be available to be reflected from the rear wall of the tank. This would make it possible to build a smaller tank with less need for sound absorbing materials on the walls of the tank.

(3) Sound Absorber - The sound absorber was composed of a 5 cm thick piece of rubberized wool packaging material that was found to be very effective at absorbing ultrasound in the frequency range that would be used (Burr (1976)).

(4) Acoustic Spacer - The design of the acoustic spacer is shown in Figure 17. This spacer was utilized to provide a fixed geometry for exposures of the biological sample in the far field of the transducer. The spacer was filled with distilled water to provide a low absorption path for the ultrasound and the ends of the spacer were covered with 0.00127 cm thick mylar to provide a non-reflecting interface.

(5) Sonation Medium Recirculation System - The high viscosity of the castor oil medium provided poor heat transfer characteristics between the tank walls and medium so some type of mixing of the tank contents was necessary to provide uniform temperature distributions. This mixing was accomplished with a centrifugal pump and motor combination which delivered approximately 100 ml/min. The mean replacement time of the sonation medium was approximately 10 minutes.

(6) Temperature Control System - Temperature control consisted of a Versatherm Electric Temperature Control Relay, Model 2149 and a Precision Mercury Thermoregulator, Model 2150, sensitivity 0.005°C, (Scientific Instruments, Inc., P.O. Box 705, Skokie, Ill.) connected to two (one on each side of the tank) 300 watt each silicon strip heaters. The maximum power (peak temperature) to the heater

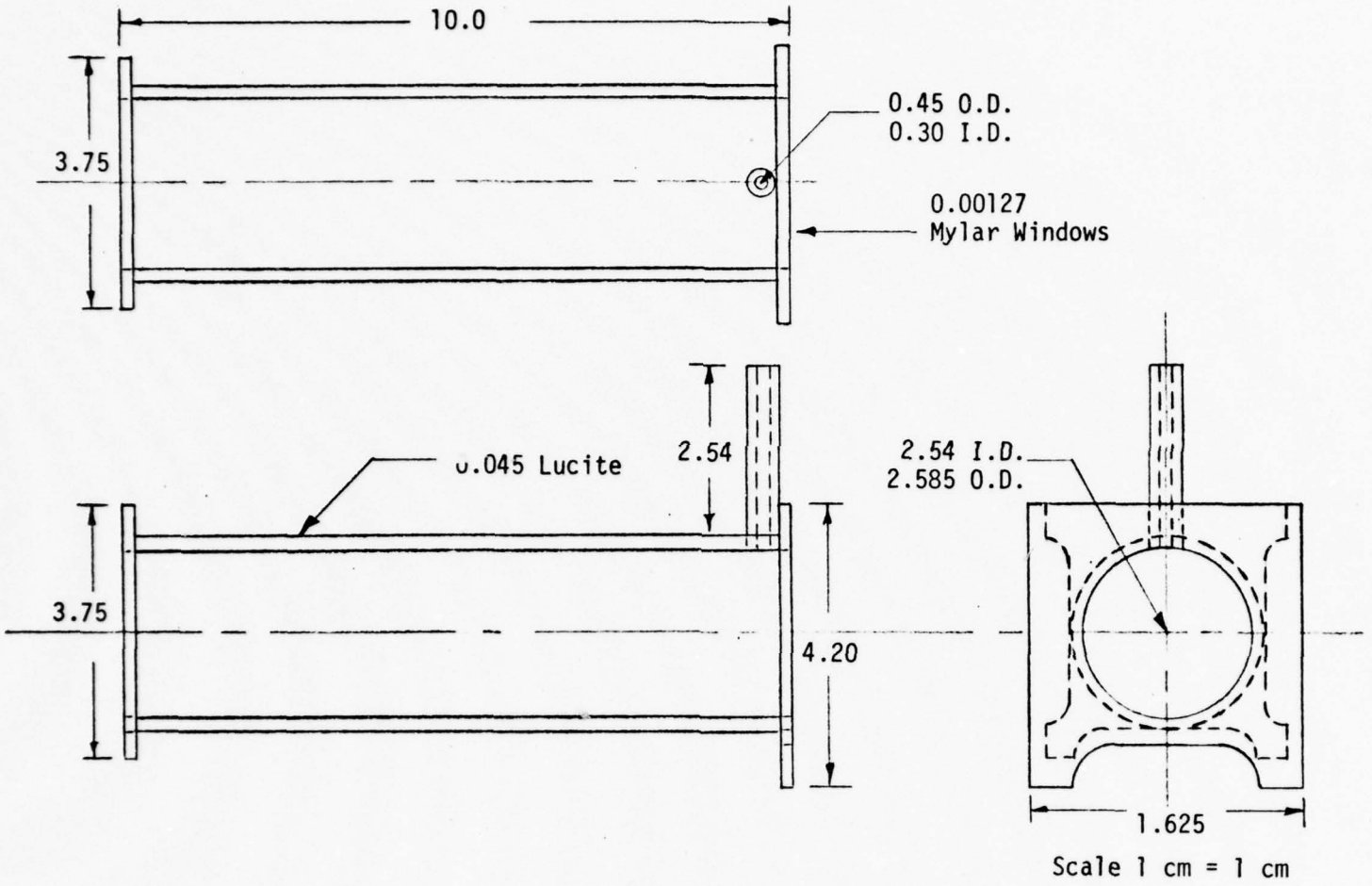

Figure 17. Acoustic Spacer (Critical Dimensions Only)

Figure 17 Continued: Acoustic Spacer

strips was controlled with a Superior Electric Co., Powerstat.

4. Biological Sample Holder

a. Criteria

(1) Sample holder must be made of non-toxic materials.

(2) Must be sterilizable and reuseable.

(3) Must provide reproduceable exposure for the same sample holder and between all sample holders in a set.

(4) The ultrasound field intensity must be as uniform as possible inside the sample holder with minimum standing waves.

(5) The ionizing radiation dose must be as uniform as possible inside the sample holder.

(6) The ultrasound exposure and ionizing radiation exposure must be measureable inside the sample holder.

(7) The temperature distribution inside the sample holder must be as uniform as possible. Continuous monitoring of the temperature must be feasible with minor perturbation of the ultrasound field.

b. Design

(1) The sample holder used in these experiments is shown in Figure 18. The lucite walls and mylar windows are both non-toxic materials and can be sterilized in a gas autoclave. The dimensions of the holder were a trade off between volume of sample needed (1 cm^3), uniformity of radiation dose and uniformity of ultrasound intensity. The filling tube provided an access point for the insertion of the temperature detection probe (discussed later under Temperature Detection System).

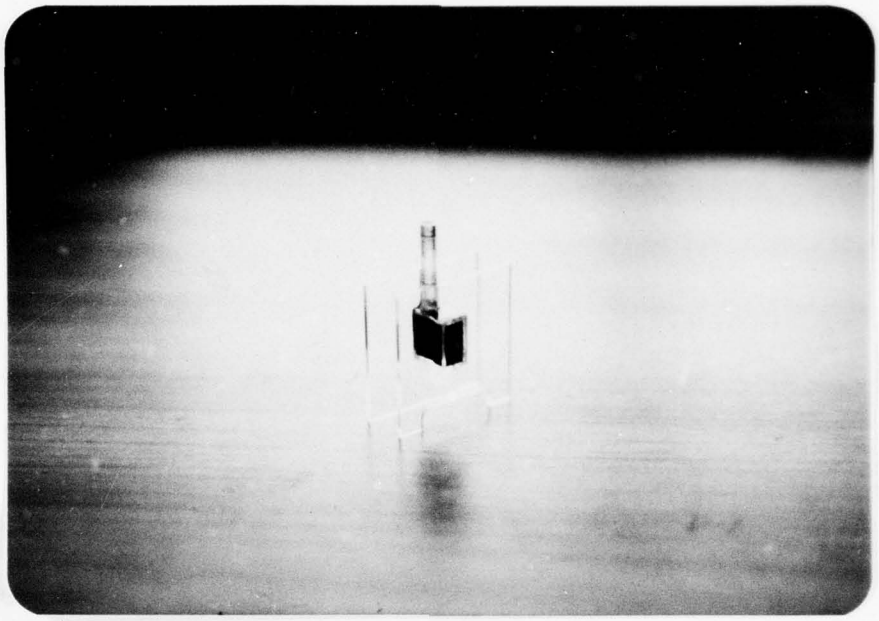

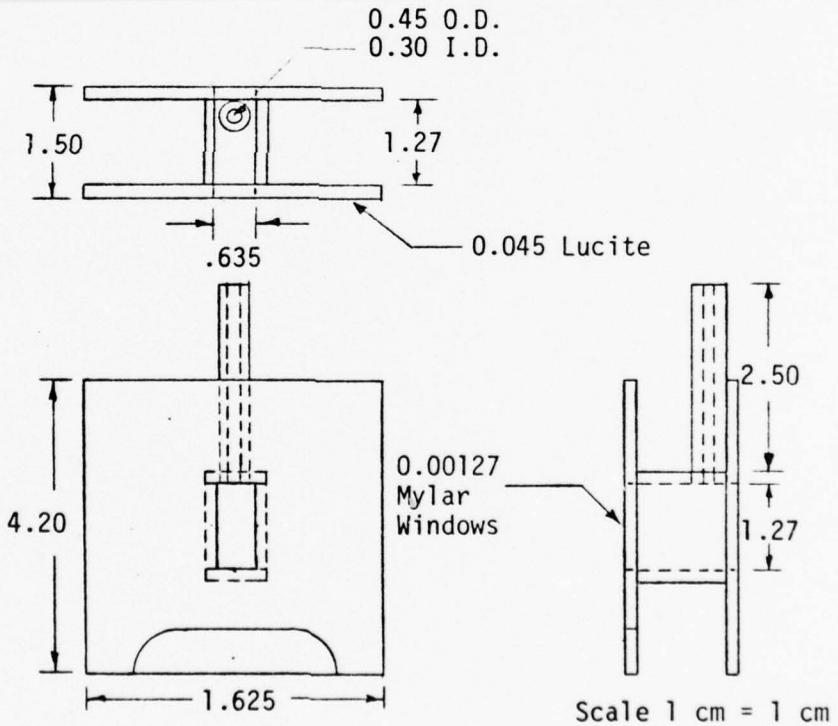

Figure 18. Biological Sample Holder (Only Critical Dimensions are Included)

(2) The sample holder design was analyzed theoretically to insure that small changes in the frequency of the ultrasound or changes in the dimensions of the holders from one sample to another did not result in significant changes in ultrasound intensity transmission. This computer analysis was accomplished using the method of Beranek and Work (1949) (see Appendix I for a copy of the computer program).

(3) The intensity distribution along the center line of the sample holder parallel to the direction of ultrasound propagation was measured using the piezoelectric microprobe by filling the sample holder with blood and piercing a small entrance hole for insertion of the probe through the mylar window. The ultrasound intensity was measured both inside and outside the sample holder to determine the relationship between the routinely measured intensity (outside holder during all experiments) and the maximum, minimum and geometric average intensities inside the holder.

(4) The intensity distribution across the face of the sample holder was also measured using the piezoelectric microprobe with the resultant iso-intensity profiles plotted using the computer.

5. Ionizing Radiation Exposure System

a. Criteria for Design

(1) Capable of delivering a reproduceable total radiation dose to the biological sample holder.

(2) Provide a method of measuring the radiation dose in the biological sample holder.

(3) Provide as uniform a radiation dose as possible to the biological sample holder.

b. Design

(1) The ionizing radiation dose was delivered to the blood samples using a 6707 Ci (as of March 1977) Cobalt-60, (1.33 and 1.17 MeV photons) radiation therapy source located in the Radiation Oncology Department of Presbyterian-University Hospital, Pittsburgh, PA. The specific exposure conditions were - 74.5 cm source to surface distance with a 4 x 4 cm field size on the surface of the tank resulting in dose rates between 130 and 120 rads/min. The actual dose rate was calculated at the time of each experiment by correcting for the decay of the radiation source with time.

(2) Calibration of the dose delivered to the blood sample for the exposure geometry was determined as follows:

(a) A biological sample holder was modified for the calibration procedure by drilling a hole in the top surface center and placing a precision ionization chamber into the center of the sample holder. The hole was sealed with very thin surgical rubber sheet, the sample holder filled with blood, and inserted into the sonation tank. Exposures were made under the described geometry conditions and the dose recorded.

(b) The precision ionization chamber used for this calibration was the Model 30-340, serial no. 2H136, long micro chamber, of 0.05 cm^3 volume, flat response from 30 keV through Co-60, ion collection efficiency of 100% up to 2000 R/sec, calibration accuracy of $\pm$ 2%, manufactured by Nuclear Associates, Inc., Westbury, NH 11590. The output of the ion chamber was measured on a Solid State Electrometer, Model 610C, serial no. 32402A, Keithley Instruments, Cleveland, OH.

6. Temperature Detection System

a. Criteria for Design

(1) Accurate to 0.1°C.

(2) Must not perturb the ultrasound field.

(3) Must provide representative temperature reading from the biological sample holder.

(4) Must provide a continuous recording of the temperature with time.

b. Design

The temperature detection system was composed of a 0.0254 cm diameter copper-constantan thermocouple connected to a Model BAT-8, Digital Thermometer, serial no. 8510, Bailey Instruments, Inc., Saddle Brook, NJ 07662, which in turn was connected to a Fischer Recordall Model A5113-5I, serial no. 5/6209-115, strip chart recorder for continuous recording of temperature. The thermocouple was inserted a fixed distance into the sample holder file tube during all ultrasound, heat, and/or ionizing radiation exposure and the temperature profile recorded. The temperature detection system was calibrated against an expanded scale mercury thermometer that was accurate to 0.05°C.

B. Results

1. Ultrasound Dosimetry System

The sensitivity of the microprobe for 1.1 MHz continuous wave ultrasound was determined to be 0.0477 $\mu V/dyne/cm^2$.

2. Ultrasound Generation System

a. The results of the experiment to determine the operating frequency of the transducer are shown in Figure 19. It shows that the peak efficiency of the transducer occurs at approximately 1.1 MHz. This is slightly higher than the manufacturers claimed crystal natural frequency of 1.0 MHz and is probably due to the transducer case construction and the impedance match of the medium used.

b. The resistance of the transducer was found to be 88Ω and the voltage across the transducer was 40 volts rms for a measured ultrasound peak output of 1.0 W/cm^2. Assuming a gaussian distributed ultrasound intensity the efficiency of the transducer was calculated as 37.5%.

3. Sonation Tank and Temperature Control System

a. Temperature variations with time in the sonation tank were measured at the location where the biological sample holder would be placed. It was found that the temperature control system would maintain the tank within $\pm$ 0.5°C of the desired temperature with the temperature variations taking on a periodic function with a period of approximately 30 minutes. This variation in temperature was due to the conductive lag caused by the high viscosity of the castor oil and the thick lucite tank walls.

b. The acoustic properties of the sonation tank were tested using the Piezoelectric microprobe. With no acoustic spacer in the tank measurements of the ultrasound intensity distribution were made along the center line of the transducer (Figure 20) and perpendicular to the direction of propagation at 12.5 cm from the transducer

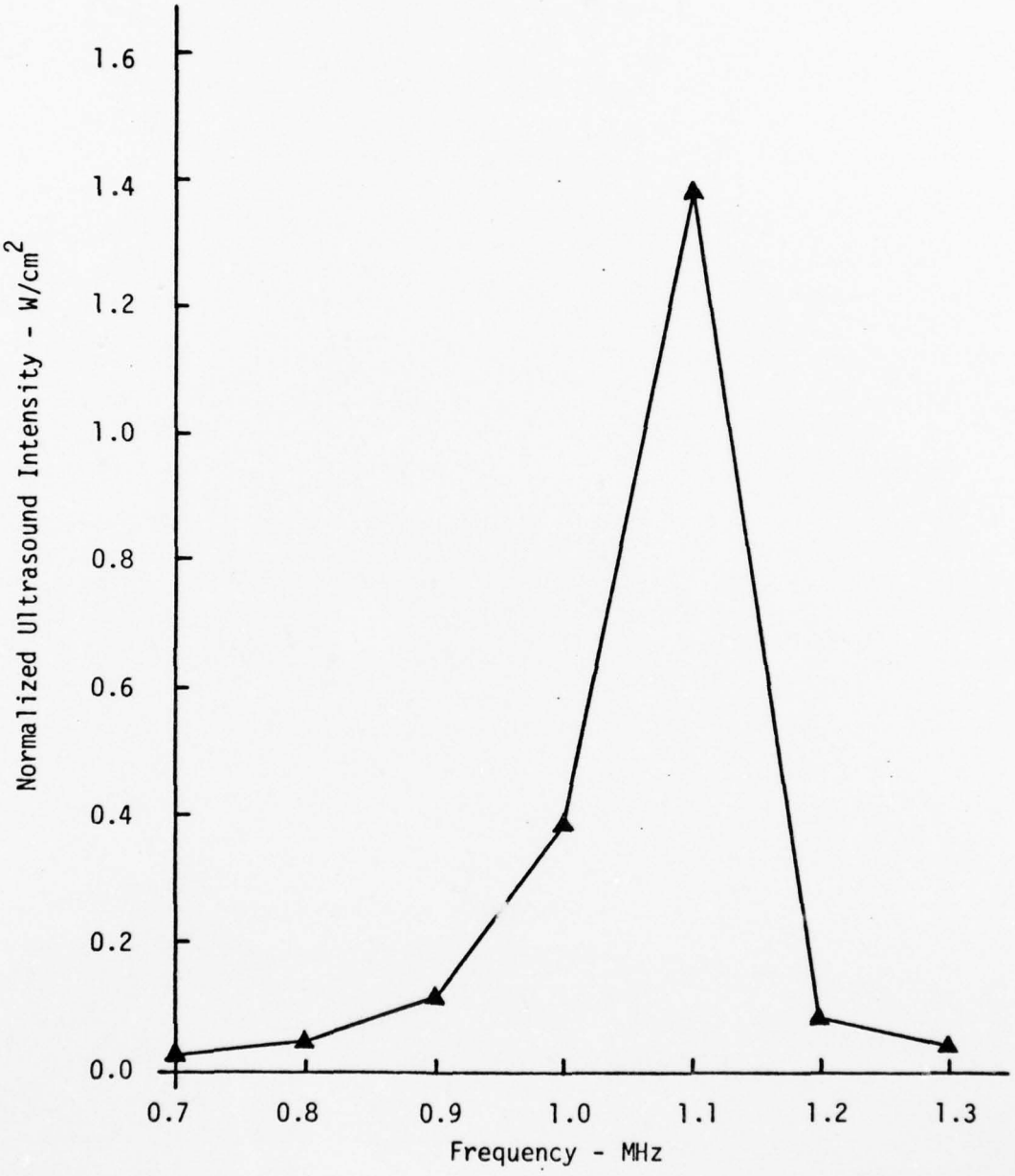

Figure 19. Determination of the Operating Frequency of the Ultrasound Transducer (K-85 Keramos, Inc.)

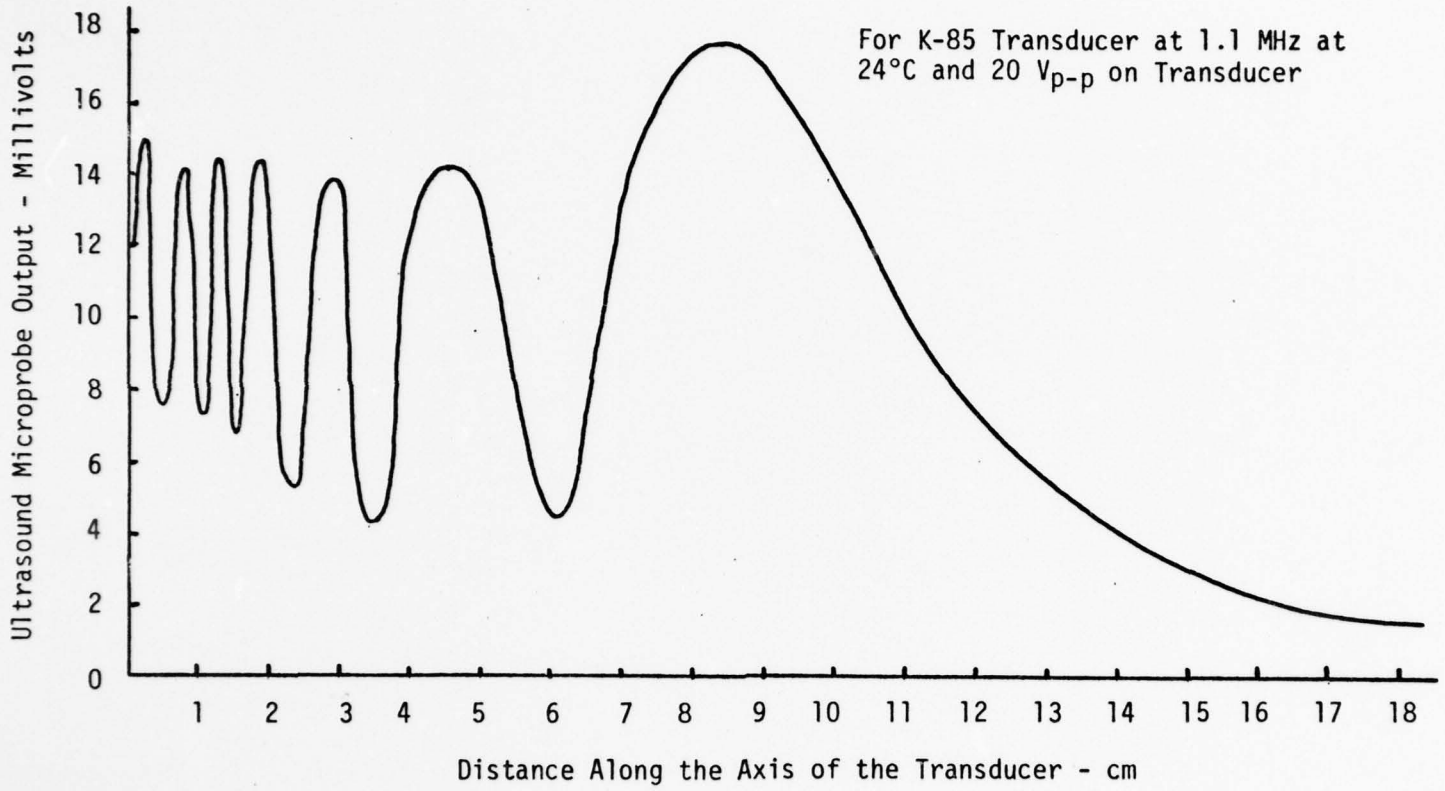

Figure 20. Ultrasound Pressure Distribution Along the Axis of the Ultrasound Transducer (K-85) with nothing in Sonation Tank. Relative Pressure Reported in Terms of Millivolt Output of Microprobe.

(Figure 21). (Note: all ultrasound intensity maps were generated using a computer isodose plotting program). Figure 20 shows the expected periodic nature of the nearfield intensity and the location of the last intensity maximum (start of far field). The start of the far field coincides closely with the calculated value of 10 cm. The standing wave ratio (SWR) in the far field was measured as 1.026 indicating very little reflection of energy from the tank walls. Figure 21 shows the distribution of ultrasound intensity to be somewhat irregular and slightly displaced from the geometrical center line of the transducer and tank. This is due to several causes; the shape of the tank with its upper flat surface causes rechanneling of energy into the upper part of the beam and the transducer crystal may not be properly aligned in the transducer case.

c. With the acoustic spacer in position in the tank the ultrasound field intensity was measured at 12.5 cm from the transducer (Figure 22). The ultrasound field is shown to be more uniform and follows the axis of the acoustic spacer.

d. The standing wave ratio (SWR) in the far field with the acoustic spacer in position was measured as 1.026. This again shows the effectiveness of the castor oil and sound absorber material in reducing the reflections within the tank.

4. Biological Sample Holder

a. The results of the analysis for the sample holder design are shown in Figures 23, 24 and 25. Figure 23 shows the effect of varying the ultrasound frequency on the transmission coefficient. Slight changes in frequency appear to cause little change in the

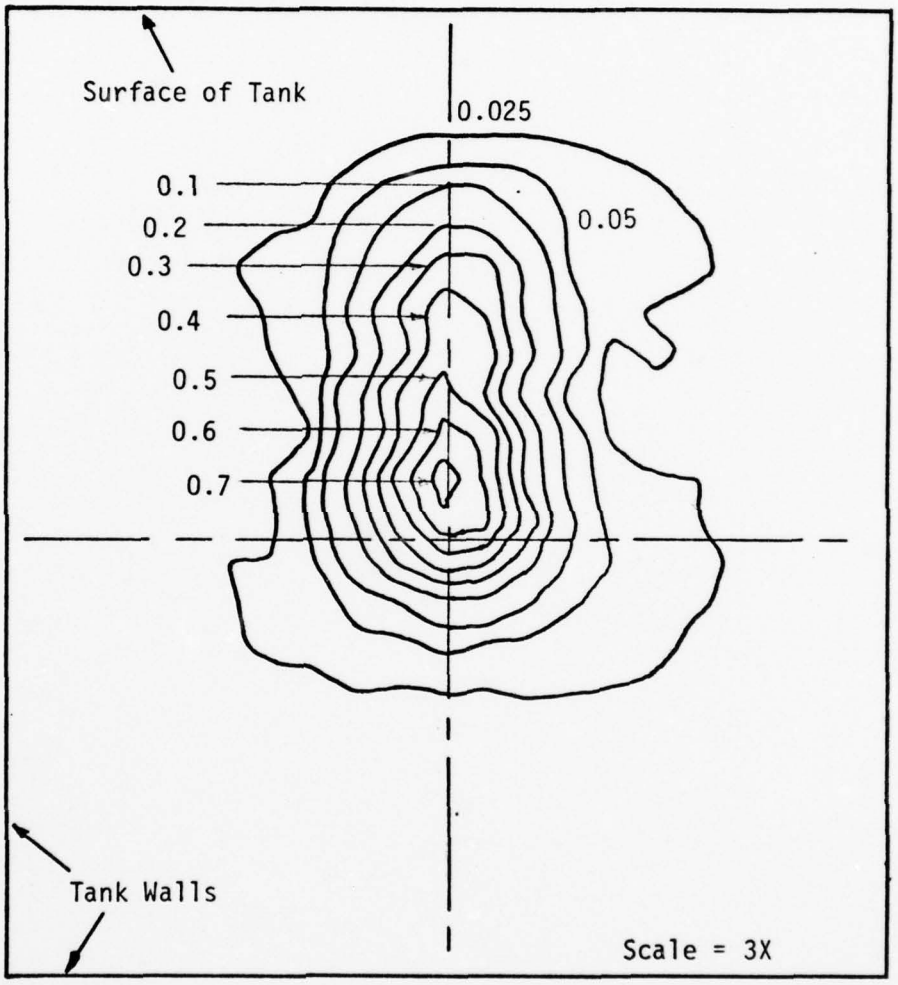

Figure 21. Ultrasound Intensity (W/cm^2) Distribution at 12.5 cm from the Ultrasound Transducer with Nothing in the Field

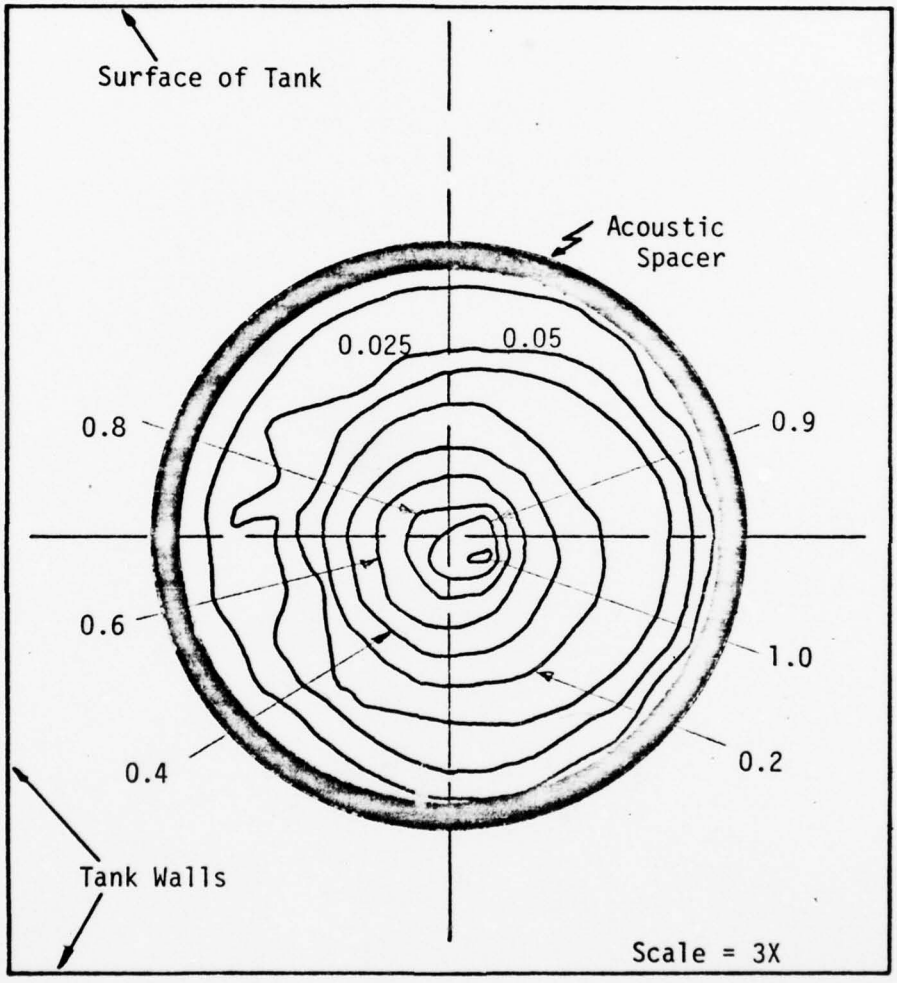

Figure 22. Ultrasound Intensity (W/cm^2) Distribution at 12.5 cm from Ultrasound Transducer with Acoustic Spacer in the Field

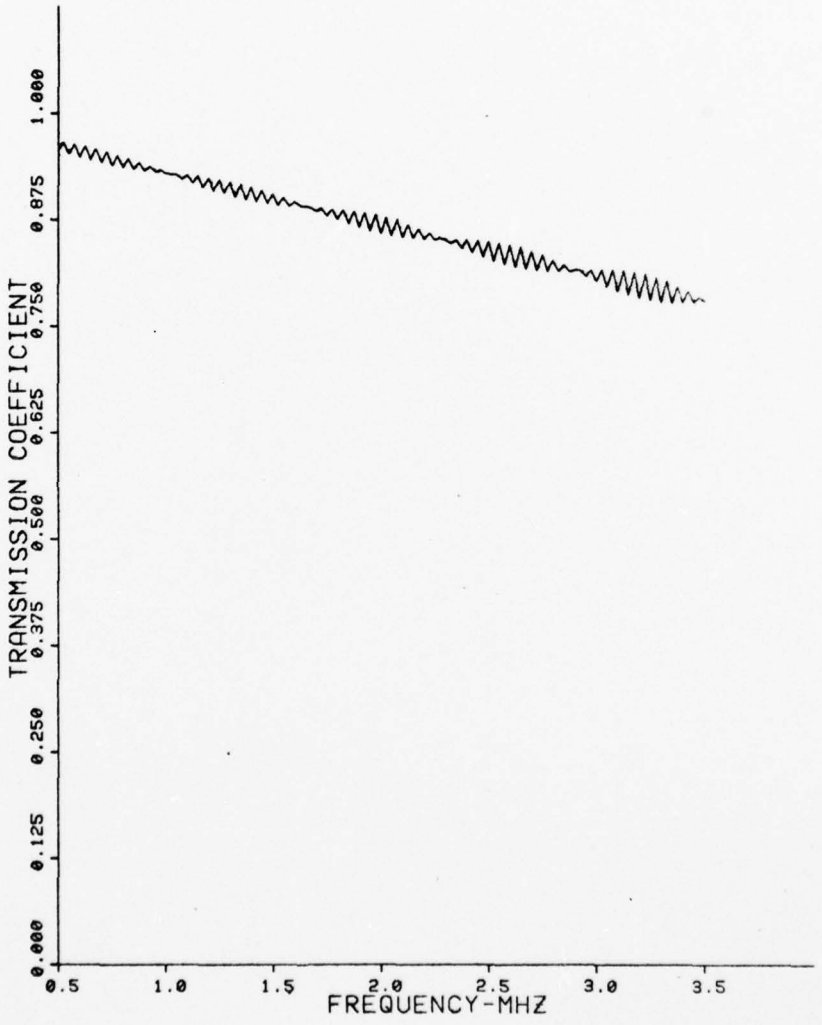

Figure 23. Effect of Varying the Ultrasonic Frequency on the Intensity Transmission of the Biological Sample Holder Design of Figure 18. Analysis for Sample Holder Filled with Blood and Emersed in Castor Oil Sonation Medium

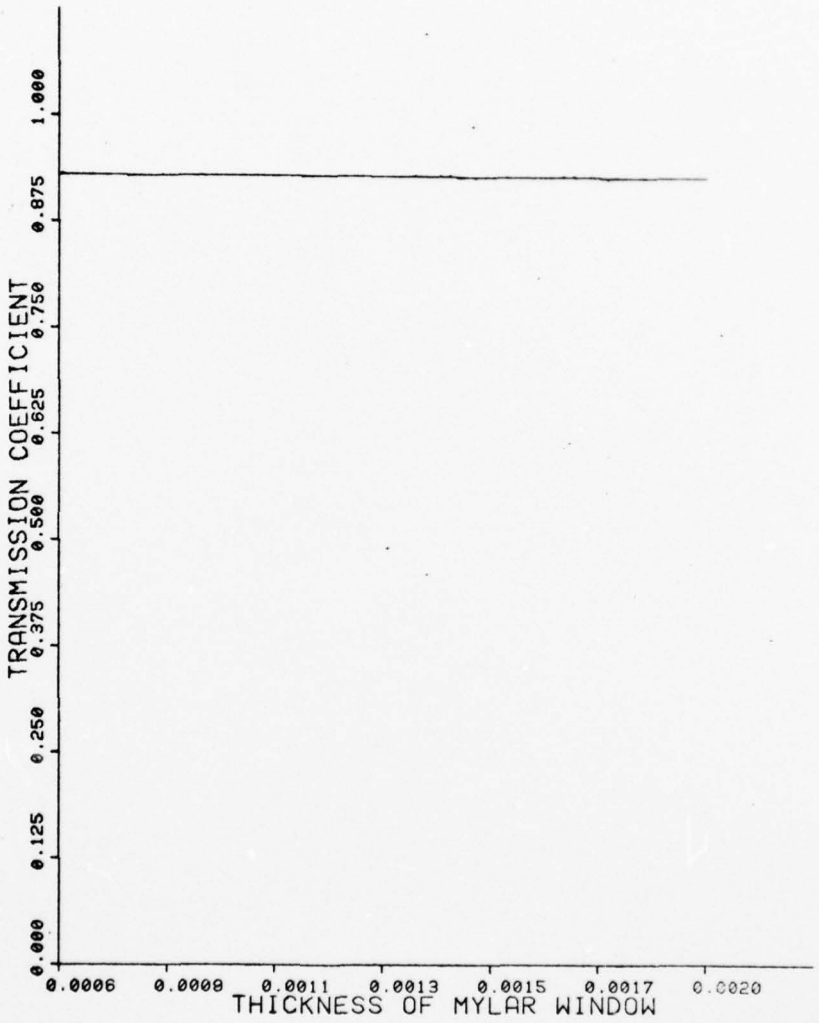

Figure 24. Effect of Varying the Thickness of the Mylar Windows in the Biological Sample Holder Design of Figure 18 on the Intensity Transmission. Sample Holder Filled with Blood and Emersed in Castor Oil Sonation Medium

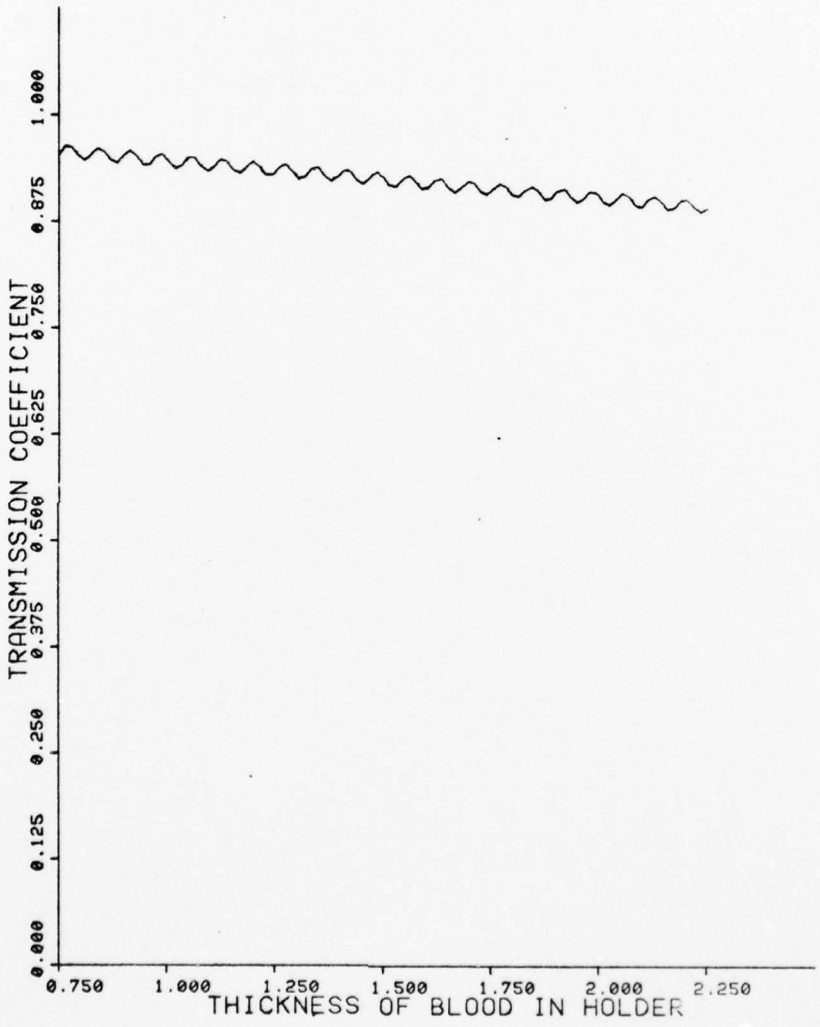

Figure 25. Effect of Varying the Thickness of the Blood in the Biological Sample Holder of Figure 18 on the Intensity Transmission. Sample Holder Filled with Blood Emersed in Castor Oil Sonation Medium

transmission coefficient (ratio of the ultrasound intensity incident on the sample holder to the ultrasound intensity exiting the sample holder). Figure 24 and 25 show the effect of varying the dimensions of the sample holder on the transmission coefficient. Both figures show that changes in the dimension of the mylar windows or blood have little effect on the transmission coefficient. All three figures show that this sample holder design has low susceptibility to changes in ultrasound frequency and dimensions and consequently should provide uniform ultrasound intensity exposures inside of the sample holder from one sample holder to another and from one experiment to the next. Details of the significance of the transmission coefficient and the susceptibility of sample holder designs to changes in frequency and dimensions are presented in the discussion.

b. The distribution of the ultrasound intensity across the biological sample holder at 12.5 cm from the transducer is shown in Figure 26 and 27 and the intensity inside of the holder is shown in Figure 28. The insertion of the temperature detection probe into the sample holder made no noticeable difference in these intensity profiles. The slight increase in intensity under the fill tube shown in Figure 28 is caused by the difference in pressure due to being open to the atmosphere. The standing wave ratio (SWR) in the sample was calculated to be approximately 1.33. The ratios of the outside intensity to the inside intensities along the centerline (Figure 28) were: maximum value - 0.86, minimum value - 2.77 and geometric average value 1.64. The intensities reported throughout the biological experiments are the exposure values as measured outside of the sample holder but related to the maximum value inside the sample holder.

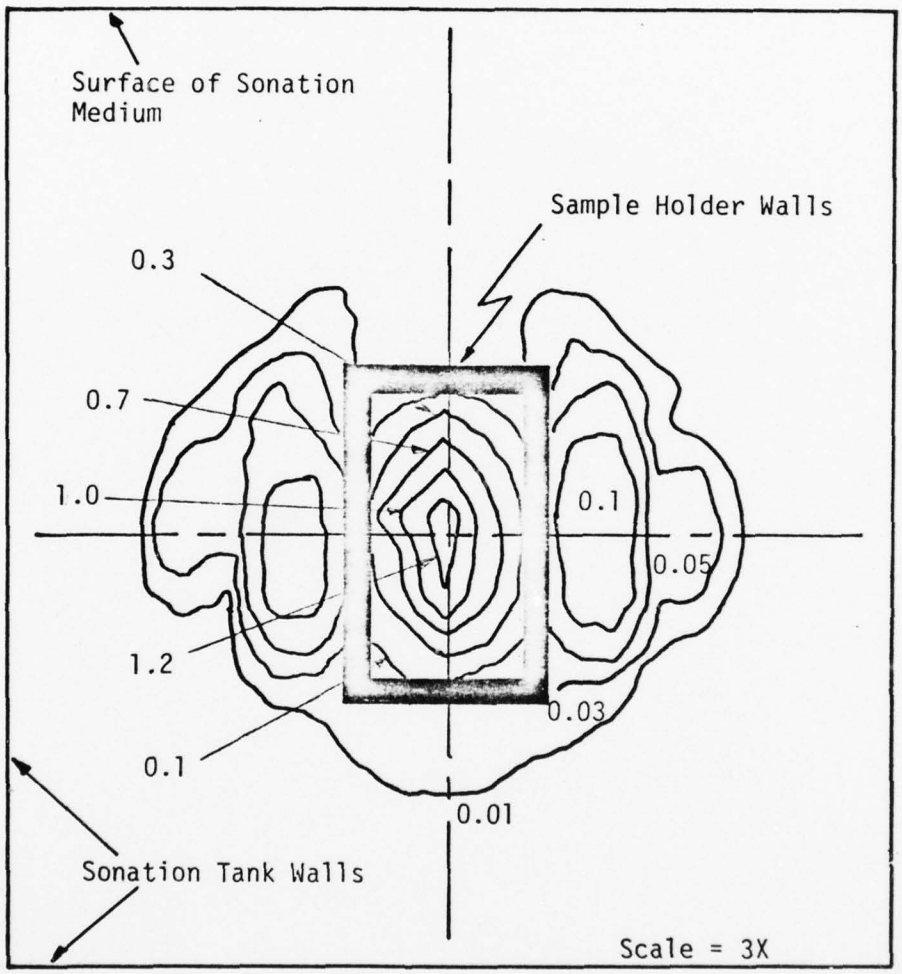

Figure 26. Ultrasound Intensity (W/cm^2) Distribution at 12.5 cm from Transducer with Acoustic Spacer and Sample Holder in the Field

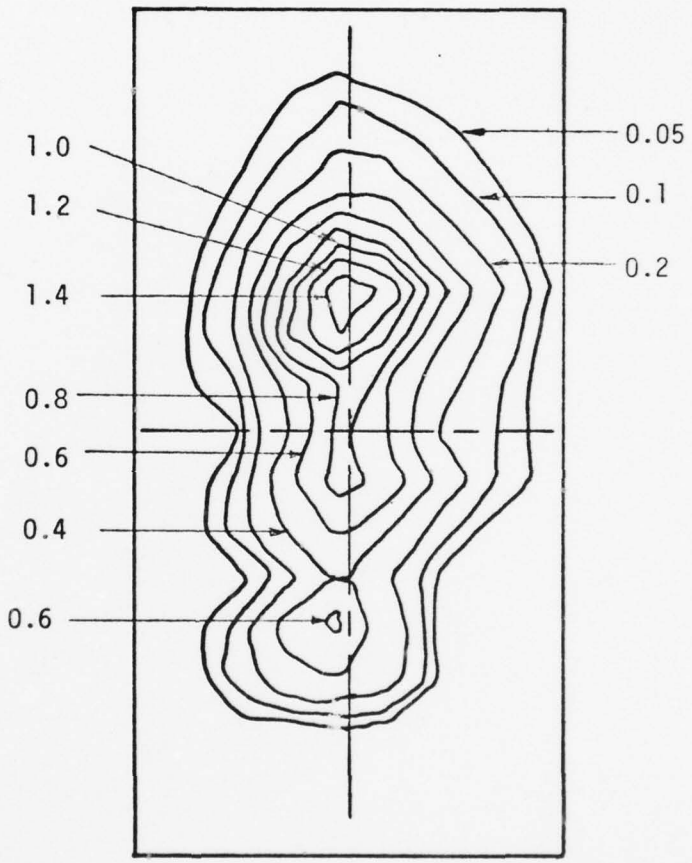

Figure 27. Ultrasound Intensity (W/cm^2) Distribution in the Sample Holder (Expanded View-10X) at 12.5 cm from Transducer.

AD-A061 537 AIR FORCE INST OF TECH WRIGHT-PATTERSON AFB OHIO F/G 6/18
THE SYNERGISTIC EFFECT OF ULTRASOUND AND IONIZING RADIATION ON --ETC(U)
1978 J G BURR
UNCLASSIFIED AFIT-CI-79-71D NL

2 OF 3
AD
A061537

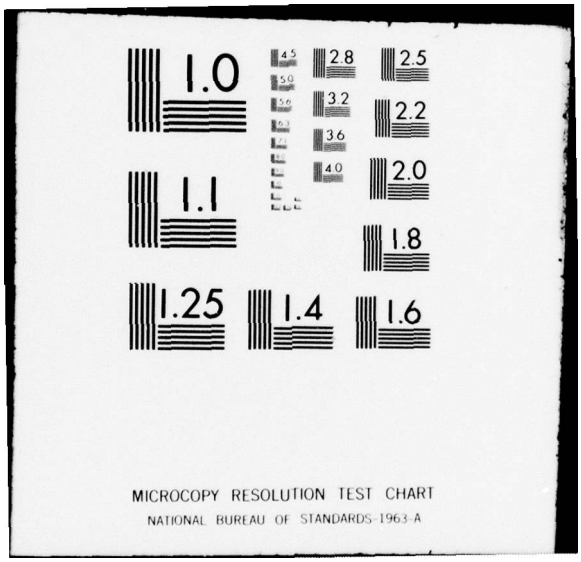
1.0
1.1
1.25
1.4
1.6
1.8
2.0
2.2
2.5
2.8
3.2
3.6
4.0
4.5
5.0
5.6
6.3
MICROCOPY RESOLUTION TEST CHART
NATIONAL BUREAU OF STANDARDS-1963-A

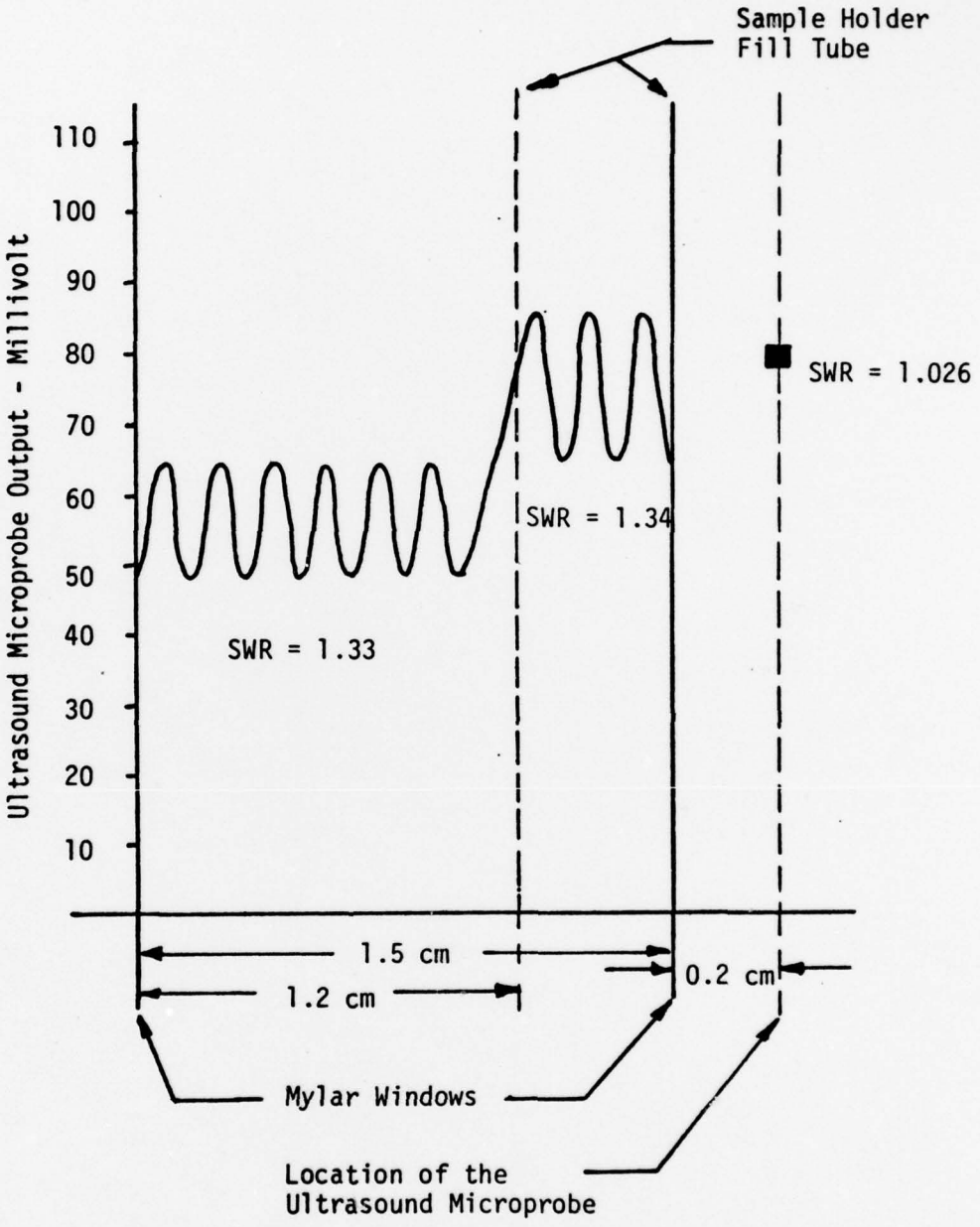

Figure 28. Ultrasound Pressure Distribution Inside of the Sample Holder. Relative Pressure Reported as Millivolt Output of the Microprobe

c. The temperature distribution in the sample was measured using the temperature detection probe under both unsteady (first turn on ultrasound) and steady (equilibrium) state conditions. In the unsteady condition the temperatures in the sample never differed by more than $\pm$ 0.5°C and in the equilibrium condition there was never more than $\pm$ 0.1°C difference in any location in the sample.

d. Fifteen sample holders were constructed for these experiments and each holder was tested for reproduceability of ultrasound exposures. Each holder was tested by filling the holder with blood (all holders filled from same blood source), inserting it into the apparatus, adjusting the input to the ultrasound transducer for 40 V_{p-p} and measuring the field distribution and equilibrium temperature in the sample holder. The equilibrium temperatures for all samples differed by a maximum of only $\pm$ 0.5°C and the intensity distributions were slightly different between exposures but generally were of the same shape and peak intensity shown in Figure 27. There were noticeable differences in the intensity distributions if small air bubbles existed in the sample holder or if the holders were not placed in the proper position in the tank.

e. The maximum ultrasound intensity that could be delivered to the biological sample holder was approximately 4 W/cm^2 at 1.1 MHz, CW.

5. Ionizing Radiation Source

The dose rate delivered to the biological sample holder vs date of exposure is shown in Figure 29. These dose rates are for the geometry noted in the Materials and Methods.

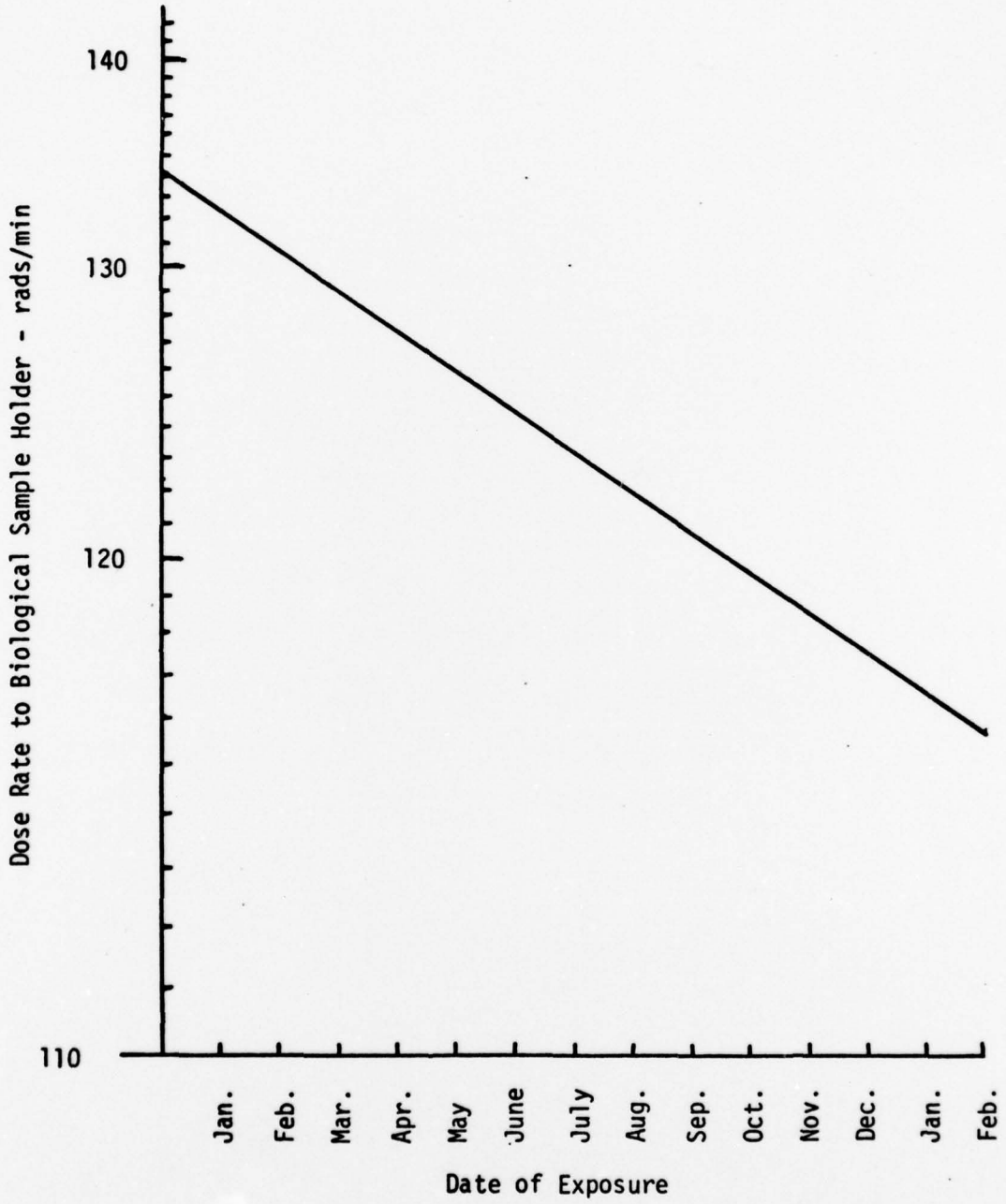

Figure 29. Dose Rate Delivered to Biological Sample Holder from Co-60 Therapy Source

6. Temperature Detection System

The temperature detection system was calibrated using a mercury thermometer and was found to be accurate to within $\pm$ 0.1°C.

C. Discussion

The ultrasound and ionizing radiation system used in the biological experiments was for all practical purposes suitable for these experiments. The system provided known exposure levels which were fairly uniform and allowed monitoring of the exposures and environmental conditions. Experience and knowledge gained during the design, construction, and testing of the exposure system, however, revealed several limitations in the capabilities of the present system which could be corrected if the apparatus is to be used for future scientific investigations. In addition, several important acoustic design principles were defined that have a significant impact on the design of biological sample holders used for ultrasound research. The limitations of the present system, the proposed modification to the system, and the general acoustic design principles for sample holder design are presented below.

1. Limitations

a. The temperature control system for the sonation tank, although acceptable for these studies, may not be acceptable for other biological systems which are more temperature sensitive. The present system is capable of maintaining the sonation tank temperature at a desired level within the range from room temperature (approximately 23°C) to 50°C with an accuracy of $\pm$ 0.5°C. The variation around the desired level is cyclic with a period of 30 minutes. This temperature

variation is due to the high viscosity of the castor oil sonation medium, the slow mixing of the tank contents, and the thick lucite tank walls.

b. The ultrasound generation system does not provide exposures at high ultrasound intensities (> 4 W/cm^2). The transducer that was constructed appears fully capable of providing the high ultrasound intensities but the ultrasound amplifier is not.

c. The reproduceability of the ultrasound exposures is not exact. The intensity distribution within the biological sample holders varies slightly from exposure to exposure even for the same sample holder. Several reasons for this variation exist: sample holders are difficult to construct to identical dimensions, placing the sample holder in the identical geometry in the tank each time is not possible, and small discontinuities inside the sample holder, such as minute air bubbles, affect the distribution.

d. No adequate real time method was available for detecting the presence of ultrasonic cavitation in the biological sample. This deficiency is not unique to this exposure system but is a limitation of all exposure systems. There are presently no acceptable non-invasive real time methods of detecting cavitation at lower levels of ultrasound intensity. Research is being conducted in this field but at present this is a limitation of all ultrasound dosimetry systems.

2. Proposed Improvements

a. The temperature control in the sonation tank can be improved significantly by the use of a less viscous sonation medium (water, culture medium, etc.) and a constant temperature circulator system. Both heat and cooling could be provided with the temperature sensing element attached to the biological sample holder. This would

allow cooling of the sample as the ultrasound intensity rose. A larger sonation tank with anechoic walls (sound absorbing materials) would be needed and degassing of the sonation medium would be required at higher intensities due to the off-gassing and bubble forming capability of high intensity ultrasound.

b. Reproduceability of ultrasound exposures is the primary criterion for the design of an adequate ultrasound exposure system. This criterion, however, is made more restrictive by several other design criteria such as uniformity of the ultrasound field intensity and the need to expose samples in the far field of the transducer. On purely theoretical grounds it appears extremely difficult to design a biological sample holder that can satisfy all three criteria.

A uniform ultrasound field can be achieved by placing the sample holder in the center of a very large ultrasound field to take advantage of the minimum slope of the energy distribution. This can be achieved by using a very large transducer or by using a diverging lens on the face of the transducer. In either method only a small portion of the total field is used, resulting in a very inefficient utilization of the total energy. In addition, to satisfy the criteria of exposure in the far field the sample holder must be mounted at considerable distance from the transducer (far field distance is proportional to the diameter of the transducer squared). This creates alignment problems and makes it difficult to achieve the desired reproduceability.

To achieve the desired reproduceability it is necessary to place the sample holder as close as possible to the transducer in a fixed location. One approach is shown in Figure 30 where the transducer, acoustic spacer and sample holder are constructed as one unit.

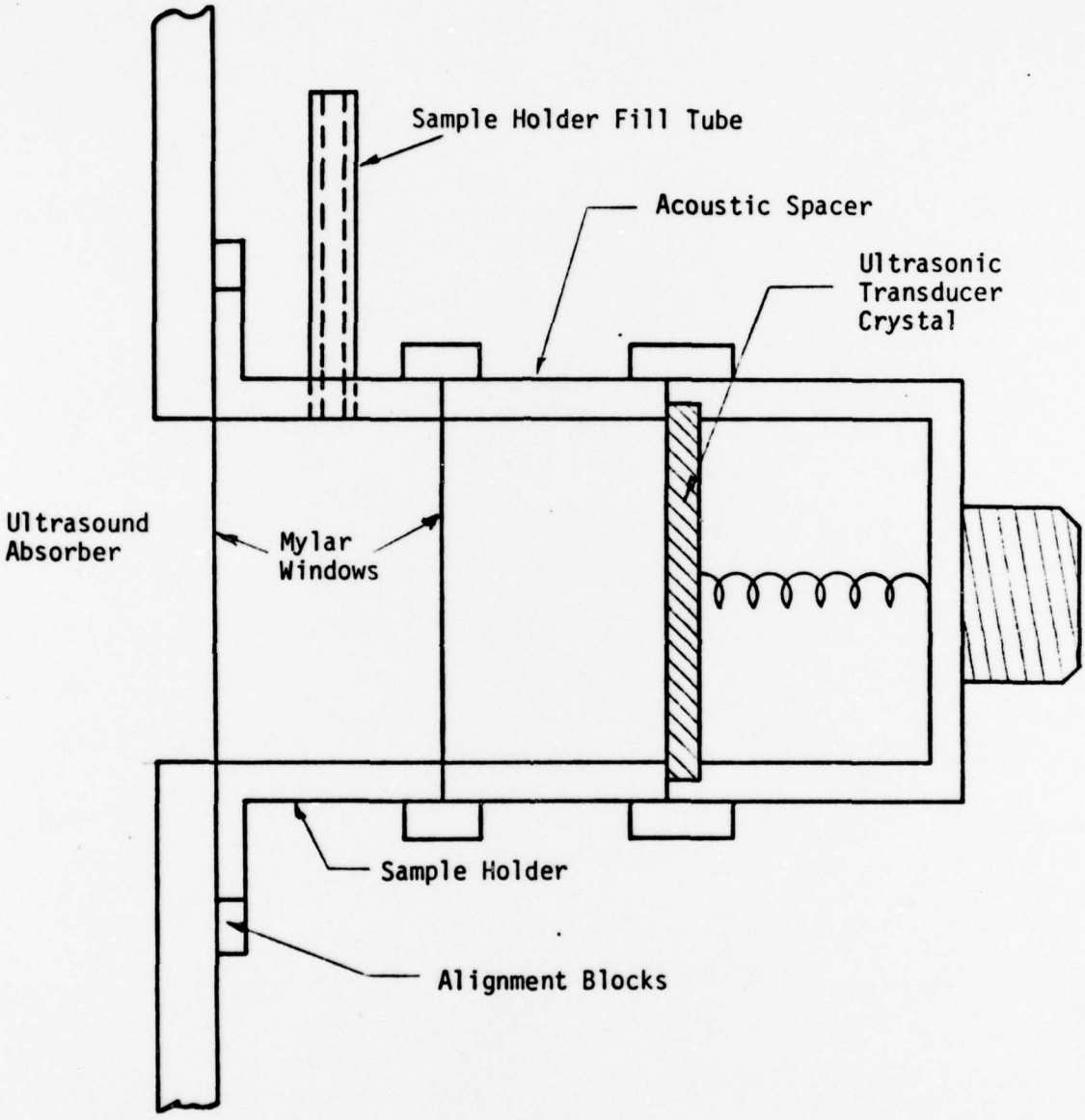

Figure 30. Proposed Biological Sample Holder Design

By making the diameter of the transducer small, the near field distance is reduced and the entire assembly can be made less than 5 cm long while still maintaining a sample volume of approximately 1 cc. By matching transducers for size and frequency it would be possible to construct closely matched sample holders. Mylar windows and sonation and acoustic spacer media with good impedance matching would guarantee low standing waves. Since the acoustic spacer and sample holder act as a wave guide, the energy distribution would tend to be gaussian in shape with maximum value at the center and minimum at the walls. The energy distribution would not be uniform across the face of the holder but it would provide a consistent energy distribution from sample holder to sample holder and exposure to exposure.

c. An automatic rectilinear scanning device for producing automatic ultrasound field plots would be an excellent modification. At present the ultrasound field plots are produced by determining the intensity at individual points in the field and then using the computer to construct isodose lines. This is a very time consuming process and lacks the resolution needed for good ultrasound dosimetry. An automatic system could record the intensity distribution in a short time with excellent resolution and improved accuracy. The energy distribution for each biological exposure could be obtained to guarantee reproduceability of exposures.

d. A real time non-invasive cavitation detection method is needed. Two potential methods of detection of cavitation have been published which might be applicable for this apparatus. Briefly, these methods include using a listening hydrophone (transducer) tuned to the first subharmonic of the propagated ultrasound [Coakley (1971)], and analyzing the changes in the ultrasound transducer driving voltage

(cavitation events change the impedance of the medium causing a change in drive voltage) [Coakley (1971)]. Measuring the changes in transmission through the sample using an interrogating (transmitting) ultrasound transducer and receiving transducer of much higher frequency (> 10 MHz) is another possible method that should be considered. Each method requires very sensitive electronic detection circuitry to limit noise and lower the cavitation detection threshold. These systems or some combination should be able to detect individual cavitation events and provide real time data that can be useful in interpreting the results of biological experiments.

3. Acoustic Design Principles for Biological Sample Holder

The design of biological sample holders for ultrasound research has received very little attention in the past with most researchers making arbitrary choices of construction materials and sample holder geometries. Such holders as plastic test tubes, glass ampules, fingers of latex surgical gloves, metal cylinders with saran or mylar end windows, plastic petri dishes, and sealed polyethylene bags have been used. These holders have been placed in ultrasound fields of known intensity (previously measured without the sample holder in the field) with the claim that the biological sample was exposed to the measured intensity in that field. The assumption that the intensity inside the sample holder is the same as that in the field outside the holder is totally incorrect. The actual intensity can, in fact, be several orders of magnitude higher or lower than that in the outside field.

The reasons for the potentially large differences in intensity between the inside and outside of the sample holder can be seen from a

theoretical analysis of a basic biological sample holder design. All holders have a common basic design which consists of four interfaces and three sonation mediums (Figure 31). The differences in the characteristic impedances, the absorption coefficients and the thicknesses of the materials involved cause variations in ultrasound reflection and transmission within the sample holder. This, in turn, causes the formation of standing waves in the different medium with amplitudes determined by the magnitude of differences between the media.

The theoretical analysis of this effect can be quite complex but with the aid of the computer, the analysis can be simplified. Using the computer method of Beranek and Work (1949) (see appendix for a copy of the computer program) a theoretical analysis of the transmission properties of any sample holder design can be accomplished. An analysis of the intensity transmission coefficient (ratio of the intensity incident upon the first interface to the intensity exiting the last interface) gives important information about the acoustic characteristics of the sample holder design. If the intensity transmission coefficient is close to 1.0 then there has been little loss of transmitted energy due to interactions with the interfaces and consequently the intensity inside the sample holder will be close to that of the intensity outside the holder. If the intensity transmission coefficient, however, is much less than 1.0 then some of the transmitted energy has been reflected at one or more of the interfaces and the resulting intensity inside the sample may be greater or less than the intensity inside the sample holder depending on which interface is responsible for the reflections.

Applying the theoretical analysis to the basic sample holder design of Figure 31 (assuming walls made of plastic, biological medium

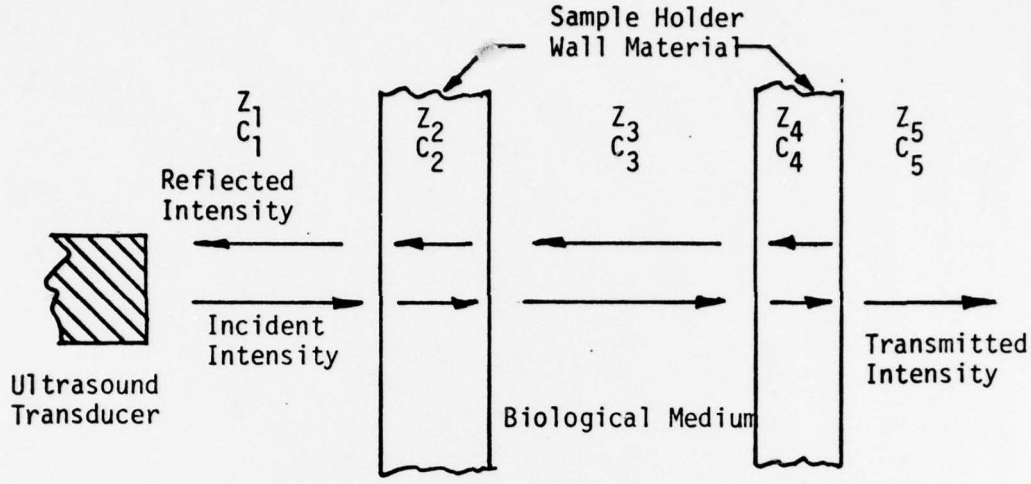

$Z_1 = Z_5 = 1.43 \times 10^5$ g/cm^2-sec (Castor Oil)

$Z_2 = Z_4 = 3.00 \times 10^5$ g/cm^2-sec (Plastic)

$Z_3 = 1.61 \times 10^5$ g/cm^2-sec (Blood)

$C_1 = C_5 = 1.51 \times 10^5$ cm/sec (Castor Oil)

$C_2 = C_4 = 2.30 \times 10^5$ cm/sec (Plastic)

$C_3 = 1.57 \times 10^5$ cm/sec (Blood)

Figure 31. Basic Biological Sample Holder Design

of blood and a sonation medium of castor oil) shows the effect of variations in the ultrasound frequency and dimensions of the sample holder. Figure 32 shows the effect on the transmission coefficient for changes in the ultrasound frequency, Figure 33 shows the effect on the transmission coefficient for changes in the thickness of the sample holder walls and Figure 34 shows the effect on the transmission coefficient for changes in the thickness of the blood. These figures show that drifting of the ultrasound frequency for the same sample or between exposed samples and small differences in the thicknesses between sample holders can cause significant differences in the transmission coefficient and consequently the intensity distribution inside of the sample holder. Just for this simple case, the differences in intensity could be as high as 50% for slight changes in frequency or dimensions.

Not all biological sample holder designs are as susceptible to changes in frequency and dimensions as the above design. A sample holder design which is almost totally void of this susceptibility can be made with the proper application of the acoustic design principles. Two key factors, when used in conjunction with each other, can provide this proper design: (1) the materials which are used in the design of the sample holder must be as closely matched for characteristic impedance as possible and (2) the thickness of the sample holder windows must be as thin as possible (see Introduction, Physics of Ultrasound), preferably much less than one-quarter of the ultrasound wavelength in that medium. These factors improve the transmission of the ultrasound by reducing the reflections at the interfaces and effectively eliminating the window material as a medium.

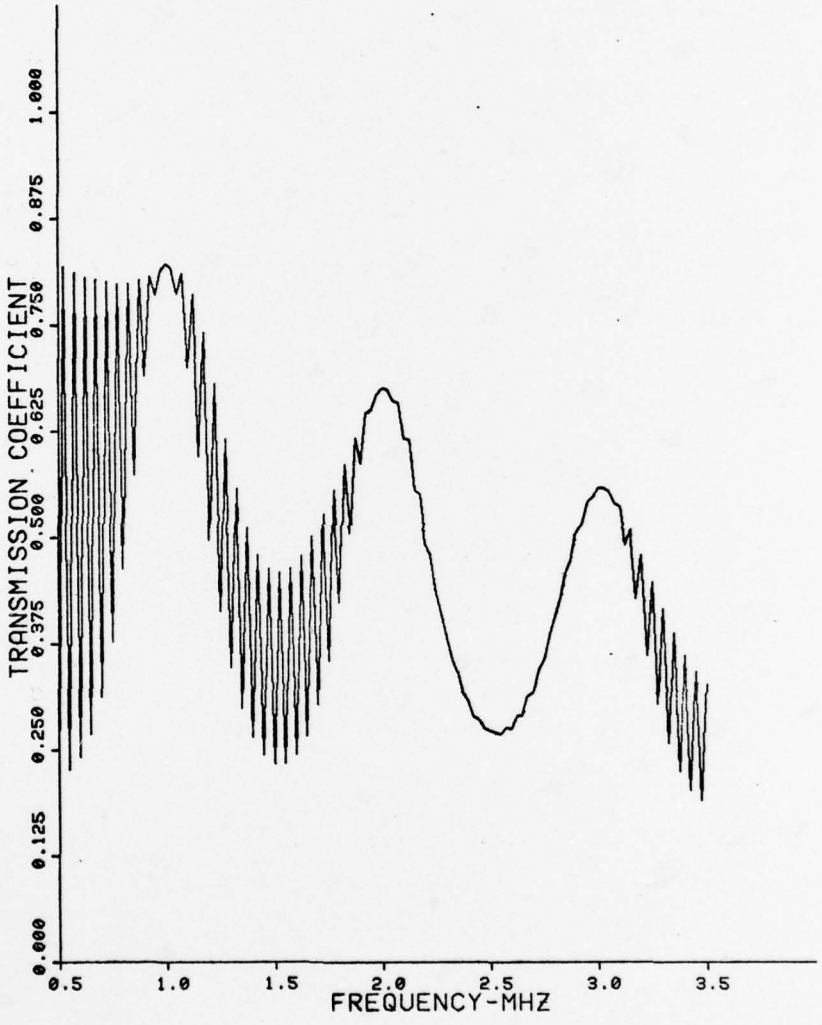

Figure 32. The Effect of Varying the Frequency of the Ultrasound on the Transmission Coefficient. The Major Resonance Peaks are Due to the Dimensions of the Blood Thickness in the Sample Holder and the Minor Resonance Peaks are Due to the Dimensions of the Lucite Windows

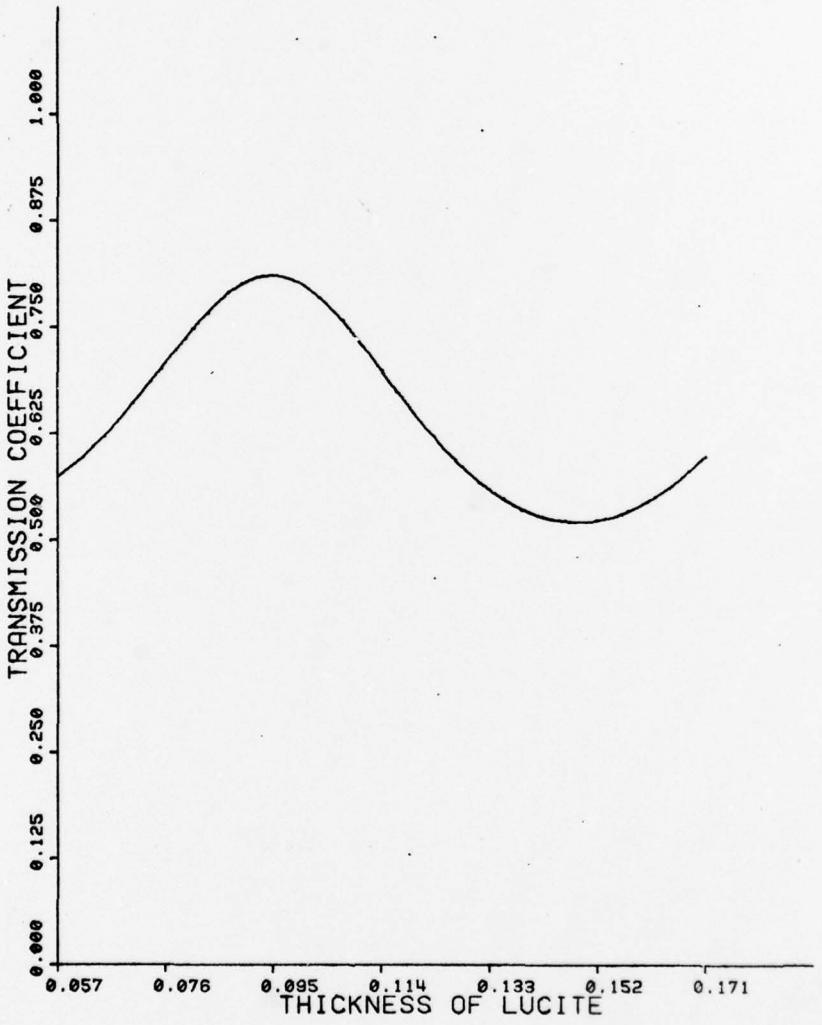

Figure 33. The Effect of Varying the Dimensions of the Lucite (Plastic) Windows of the Sample Holder on the Transmission Coefficient

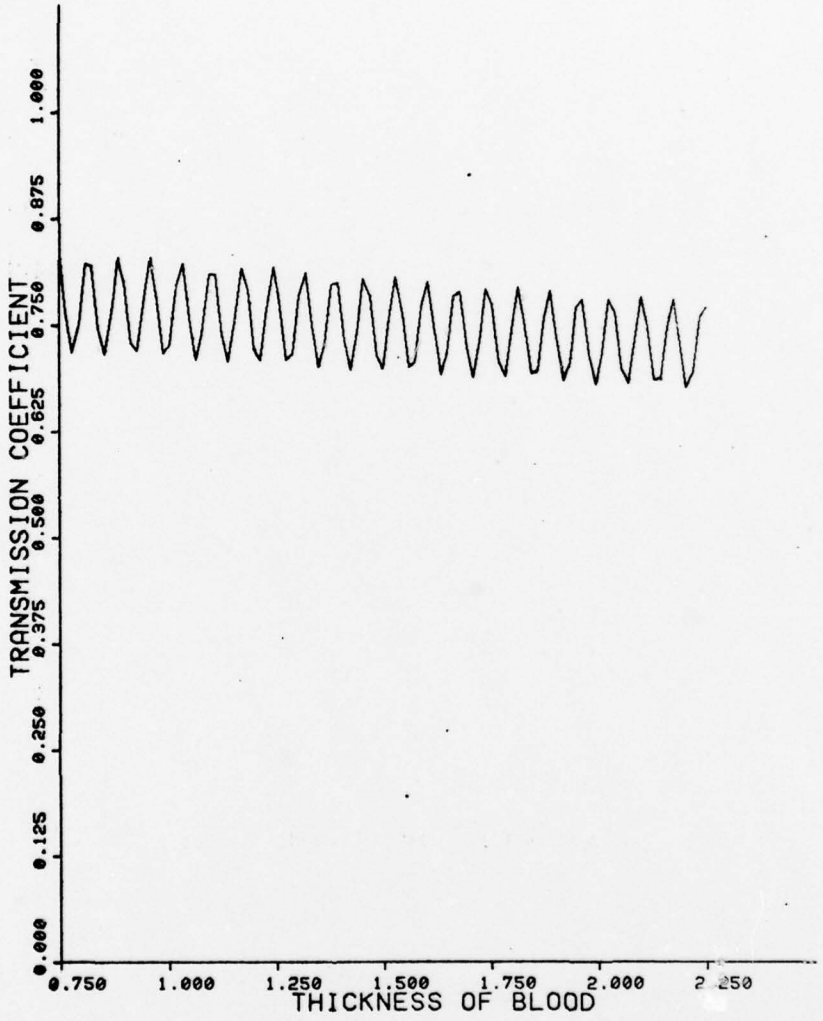

Figure 34. The Effect of Varying the Dimensions of the Blood in the Sample Holder on the Transmission Coefficient

The above design principles were utilized in the design of the biological sample holder used in these studies. Sample holders were constructed with 0.00127 cm thick mylar windows which allow almost complete transmission. The theoretical analysis for this sample holder design was shown previously in Figures 23, 24 and 25. They show a very low susceptibility to changes in frequency or dimensions of the sample holder and consequently the design is much more acceptable than the design shown in Figure 31.

D. Conclusions

1. The ultrasound and ionizing radiation exposure system described in detail in this chapter has been shown to provide known reproduceable exposures of blood samples to ultrasound, ionizing radiation and heat. The exposure parameters for this system are:

   a. Ultrasound - 1.1 MHz, CW, 0.0 to 4.0 W/cm^2 in the far field of the transducer.

   b. Ionizing Radiation - Co-60, 117.5 to 131 rads/min, (1.33 and 1.17 MeV photons).

   c. Heat - 24°C to 50°C.

2. Several limitations of the ultrasound and ionizing radiation exposure system were noted and proposed corrective action recommended. Limitations of the system included; sonation tank temperature variation of $\pm$ 0.5°C, maximum ultrasound intensity of only 4.0 W/cm^2, slight variation of ultrasound intensity distribution between different sample holders, and no real time cavitation detection method.

3. The design of biological sample holders can not be taken for granted as has been done in the past. Each sample holder design provides a unique set of acoustic characteristics which determine its ability or non-ability to perform its desired function of exposing the biological material to a known quantity of ultrasonic energy. A poorly designed sample holder can provide exposures which are far from the desired value and provide large variations in exposure within experiments and between experiments. This fact may help to explain the lack of consistency in the literature concerning the biological effects of ultrasound.

III. BIOLOGICAL STUDIES

A. Materials and Methods

Human lymphocytes in whole peripheral blood were exposed to various sequences of heat, ultrasound, ionizing radiation or combinations thereof using the ultrasound and ionizing radiation exposure system discussed in Chapter II. The exposed blood was then cultured, lymphocytes harvested and mitotic figures scored for gross chromosome aberrations. Blood from the same healthy male donor was used throughout the experiments and all biological experiments followed a standardized procedure.

1. Biological Sample Handing Procedures

a. Blood samples were drawn no earlier than 2 hours before any experiment in sterile 10 cc Vacutainers containing 143 U.S.P. units of sodium heparin. Samples were well mixed and held in a water bath at 37 $\pm$ 0.1°C until used in the experiments.

b. Chromosome Medium 1A, Cat. #167L, Grand Island Biological Company, Grand Island, N.Y., 14072, was reconstituted with 5 ml of Special Diluent for lyophilized chromosome medium 1A, Cat. #167D, same company using sterile technique and place in the incubator at 37 $\pm$ 0.1°C until ready for innoculation with the blood sample.

c. Blood was withdrawn from the Vacutainers using sterile 3 cc Plastipac syringes and placed in sterile (gas autoclaved) biological sample holders. Various exposure sequences were conducted and blood removed from the sample holders with a fresh sterile syringe. Reconstituted chromosome medium at 37°C was innoculated with 0.2 cc of

this blood.

d. Samples were incubated for 48 hours at 37 ± 0.1°C. Colcemid, Cat. #521L, same company, was added to the medium 1.5 hours before harvesting in a final concentration of 0.1 μg/ml.

e. During harvesting the cells were suspended in 0.075 M KCl for 10 minutes, washed with fixative (3 parts methanol to 1 part glacial acetic acid) until clear, dropped on clean glass slides, air dried, stained with 1 to 20 dilution Giemsa for 15 minutes, and covered.

f. Scoring of mitotic figures for chromosome aberrations was performed under oil objective at 1000X. All samples were scored blind for gross chromosomal aberrations and mitotic index (mitotic cells/1000 non-mitotic cells). Only those metaphase figures containing 46 centromeres were included in the analysis.

2. Biological Experiments Performed

a. Control Series

(1) A series of cultures were processed to determine the background aberration frequency levels for the blood donor who was to be used throughout the experiments. Cultures were made directly from Vacutainers.

(2) Blood was placed in biological sample holders for periods of 30 minutes, 2 hours, and 6 hours at 37 ± 0.1°C with the thermocouple inserted for the first 30 minutes of each exposure. Samples were incubated immediately after the hold period. These exposures were conducted to determine the possible toxicity of the biological sample holder and thermocouple.

b. Ionizing Radiation Alone Series

(1) Blood samples were exposed at 37 ± 0.5°C in the sonation tank to 100, 300, 500 rads Co-60 at a dose rate of 122.0 ± 7.0 rads/min. Samples were incubated immediately after the exposure. These exposures were conducted to determine the ionizing radiation dose response of the biological system.

(2) Blood samples were exposed to 300 rads Co-60 at a dose rate of 131.0 ± 7.5 rads/min and then held for periods of 30 minutes, 2 hours, and 6 hours at 37 ± 0.1°C in the biological sample holders. Samples were incubated immediately after the hold period. These exposures were conducted to determine if a delay in incubation had an effect on the aberration frequencies.

c. Ultrasound Alone Series

(1) Blood samples were exposed to 0.5, 1.0, 2.0, 4.0 W/cm^2, 1.1 MHz, CW, ultrasound for 30 minutes with an initial sonation tank temperature of 37°C. Samples were incubated immediately after the ultrasound exposures. Temperature profiles were recorded. These exposures were conducted to determine the ultrasound dose response.

(2) Blood samples were exposed to 3 W/cm^2, 1.1 MHz, CW, ultrasound for periods of 30, 45, 60 and 90 minutes from an initial sonation tank temperature of 37°C. Samples were incubated immediately after the exposure. Temperature profiles were recorded. Exposures were conducted to determine the effect of ultrasound exposure time.

d. Heat Alone Series

(1) Blood samples were exposed to 37 ± 0.1, 39 ± 0.1, 41 ± 0.1, 43 ± 0.1, 46 ± 0.1 and 50 ± 0.1°C for a period of 30 minutes

to determine the effect of temperature for a set exposure time.

(2) Blood samples were exposed to 43 $\pm$ 0.1°C for periods of 30, 45, 60, and 90 minutes to determine the effect of exposure time.

e. Combined Ultrasound and Ionizing Radiation Series

(1) Blood samples were exposed to sequences of ultrasound and ionizing radiation shown in Figure 35. All ionizing radiation exposures were 300 rads at 122.0 to 117.5 rads/min (dose rate different due to exposures at different times) and the ultrasound was 3 W/cm^2, 1.1 MHz, CW. These exposures were conducted to determine the response of the biological system to various sequences of application of the ultrasound and ionizing radiation.

(2) Blood samples were exposed to sequences no. 1, 2, 4 and 7 of ultrasound and ionizing radiation as shown in Figure 35. All radiation exposures were 100 rads at 117.5 $\pm$ 11.7 rads/min and the ultrasound exposures were at 3 W/cm^2, 1.1 MHz, CW. These exposures were performed to determine the effect of a change in the magnitude of the radiation dose.

(3) Blood samples were exposed to 30 minutes of ultrasound at .01, 1.5, 3.0 W/cm^2 with 300 rads at 117.5 $\pm$ 11.7 rads/min given at the midpoint of the 30 minute ultrasound exposure. The starting sonation tank temperature was 24°C for this series instead of the 37°C temperature of the previous experiments. These exposures were conducted to determine the effect of ultrasound intensity on the aberration frequency for combined ultrasound and ionizing radiation. The ultrasound intensity levels were chosen so as to give an equilibrium temperature in the sample holder of 24°, 30° and 37°C respectively.

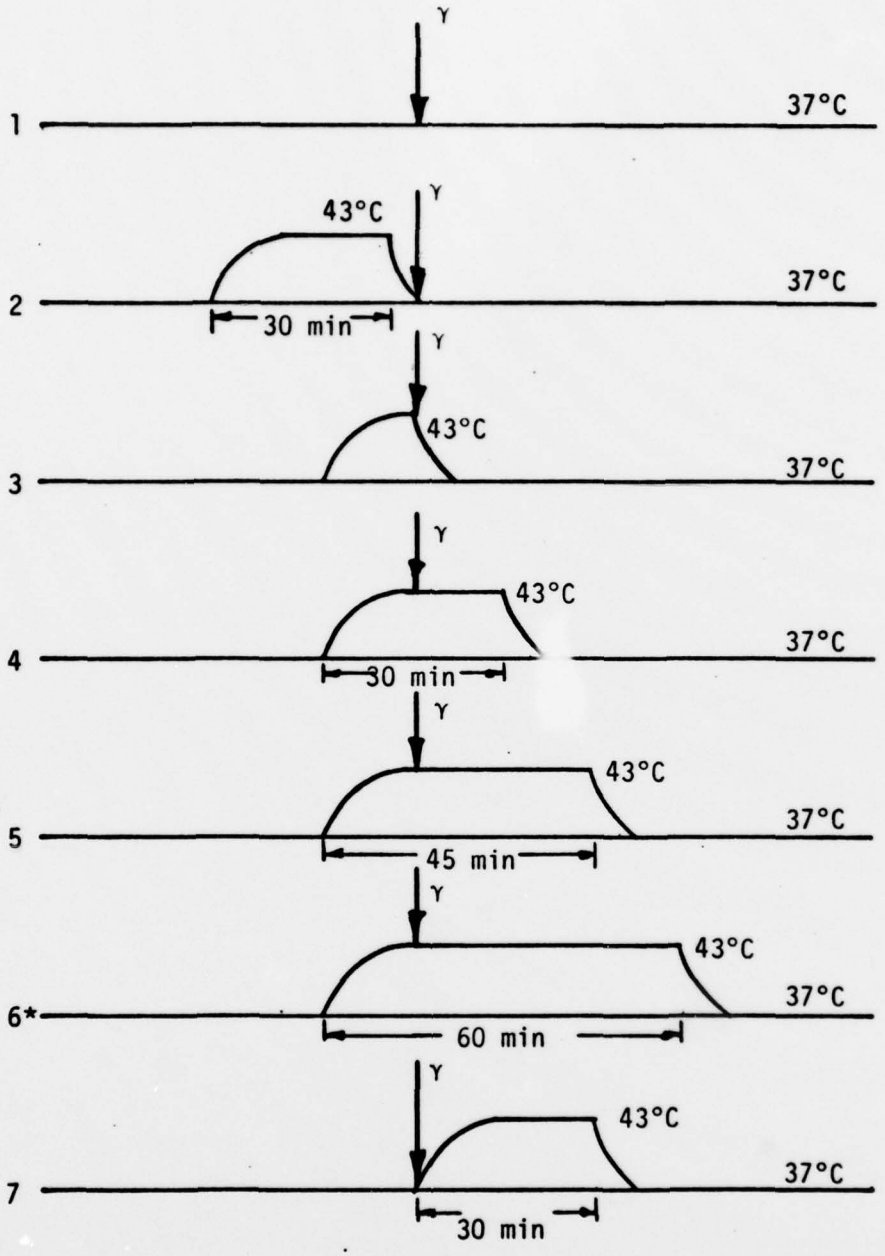

Rise and Decay Time of the Temperature in Sample Holder are Approximately 5 Minutes Each

*Note: Sequence No. 6 Not Run For Heat Plus Ionizing Radiation

Figure 35. Exposure Sequences for Heat or Ultrasound Plus Ionizing Radiation. Temperatures Shown are Either the Conductively Heat Produced Temperature or the Temperature Induced by 3.0 W/cm^2, CW, 1.1 MHz Ultrasound

f. Combined Heat Plus Ionizing Radiation Series

(1) Blood samples were exposed to the sequences of heat and ionizing radiation shown in Figure 35. All radiation exposures were 300 rads at 122.0 to 117.5 rads/min (dose rates different due to exposure at different time). These sequences duplicate the temperature profiles induced by 3 W/cm^2 ultrasound at 1.1 MHz, CW and serve as an environmental control for the combined ultrasound and ionizing radiation series no. 1.

(2) Blood samples were exposed to sequences no. 1, 2, 4 and 7 of heat and ionizing radiation shown in Figure 35. All radiation exposures were at 100 rads at 117.5 $\pm$ 11.7 rads/min. These exposures duplicate the temperature profiles induced by 3 W/cm^2 ultrasound and serve as an environmental control for the combined ultrasound and ionizing radiation series no. 2.

(3) Blood samples were exposed to 30 minutes of heat at 24 $\pm$ 0.5°, 30 $\pm$ 0.5°, 37 $\pm$ 0.5°, 43 $\pm$ 0.5°C with 300 rads at 122.7 $\pm$ 7.0 rads/min given at the midpoint of the 30 minute heat exposure. This experiment was designed to determine the effect of temperature during irradiation and to provide environmental controls for the combined ultrasound and ionizing radiation series no. 3.

3. Analysis of the Data

a. Raw Data

For each experiment noted above the following data were gathered; mitotic index, number of aberrant cells, number of mitotic figures scored, and number of chromosomal acentric fragments, minutes, dicentrics, and centric rings.

b. Summary Data

The raw data were processed by computer to give the following information: deletions, total exchanges (dicentrics plus centric rings), aberration frequencies (aberrations/metaphase scored) and standard errors (assumes poisson distribution of aberrations [Lloyd et al (1975)]) for all aberrations. Mitotic index values are included in the summary data, also.

c. Statistical Analysis of Data

Selected summary data for each exposure sequence were analyzed using the computer to determine if there was a statistically significant difference between the various exposures and their control values. Only the deletions, exchanges and aberrant cells were chosen for the statistical analysis. Deletions provide an indication of the non-repaired chromosome damage, exchanges provide an indication of the repaired or mis-repaired chromosome damage, and the aberrant cells provide an indication of the total amount of chromosome damage. No statistical analysis was performed on the mitotic index because of its great variability. It is included in the summary data for completeness and to provide information on gross cellular effects. The ionizing radiation alone exposures (100 or 300 rads at 37°C) were used as control values to determine if the combined sequences of heat or ultrasound plus ionizing radiation were significantly different from radiation alone. The heat plus ionizing radiation sequences were then used as control values to determine if there was a statistically significant difference between combined heat plus ionizing radiation and combined ultrasound plus ionizing radiation. The two sided students t-test [Armitage (1974)] was utilized for the analysis with the probabilities reported. A probability of < 0.05 was chosen as the

level of statistical significance.

d. Determination of the Sensitivity of the Statistical Analysis

An analysis was performed to determine the sensitivity of the method used in the statistical analysis shown above using the method of Armitage (1974). The purpose of this analysis was to determine the appropriate number of metaphase figures that must be scored to achieve sufficient sensitivity in the statistical analysis and to provide assistance in the interpretation of the results. The statistical criteria chosen for this analysis were an Alpha Error of 0.05 and Beta Error of 0.1 for a two sided probability test.

B. Results

1. Determination of the Sensitivity of the Statistical Analysis

The results of the analysis to determine the sensitivity of the statistical analysis are shown in Figures 36 and 37. Figure 36 shows the number of mitotic figures which must be scored vs the difference from the aberration frequency (selected as 0.5 for this example but could be calculated for any value of aberration frequency). This figure shows that the sensitivity (the smallest statistically significant difference between exposures) of the analysis improves with increase in the number of metaphases scored but above 200 metaphases scored very little sensitivity is gained by larger sample size. A total of 200 metaphase figures was chosen as the sample size for these experiments because it is considered large enough to provide good sensitivity but small enough to provide data collection in a reasonable length of time.

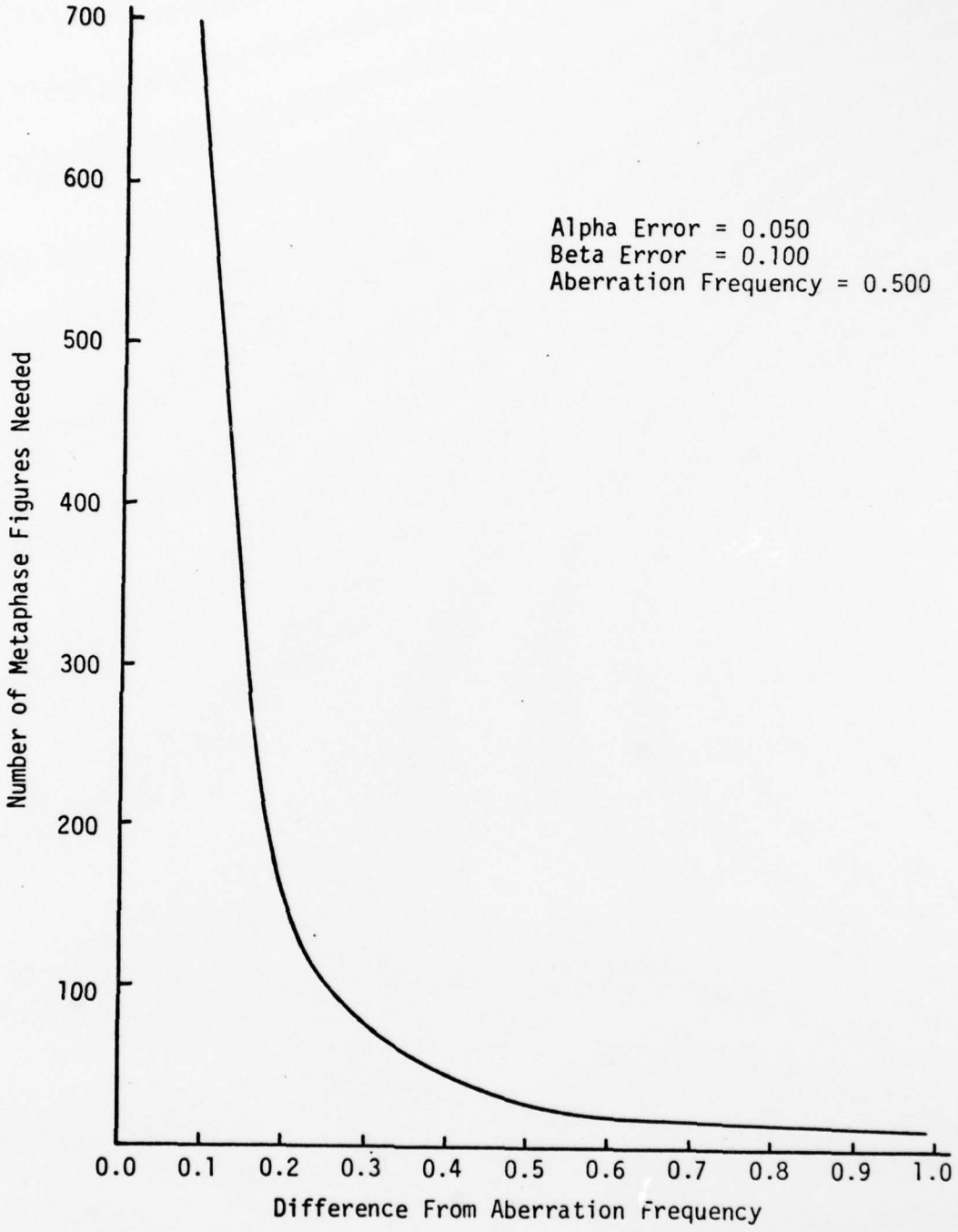

Figure 36. Number of Metaphase Figures that Must be Scored to Achieve the Smallest Significant Difference From the Aberration Frequency for Fixed Alpha, Beta and Aberration Frequency.

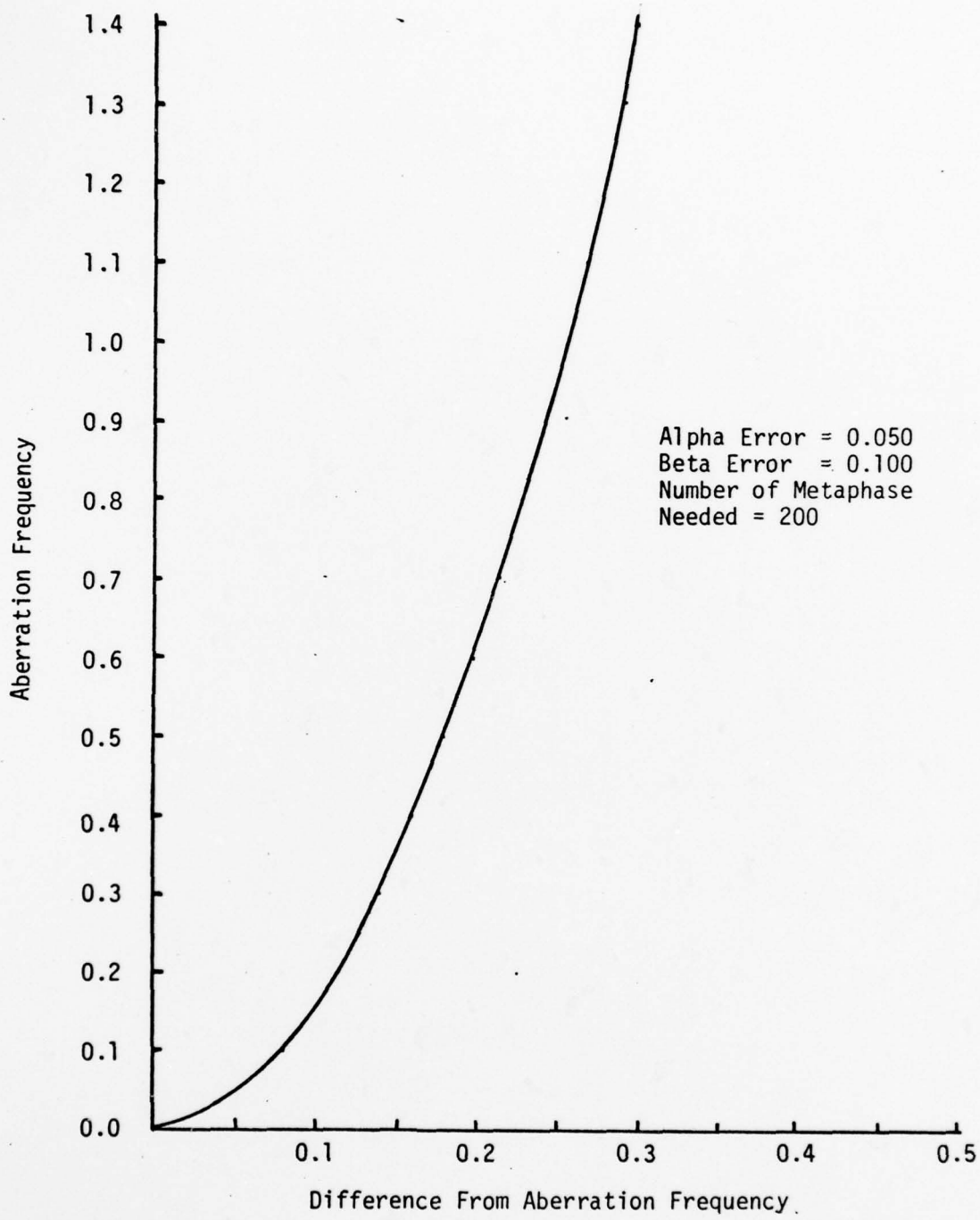

Figure 37. Aberration Frequency vs the Difference from the Aberration Frequency for Fixed Alpha, Beta and Sample Size

Figure 37 shows the sensitivity of the analysis for the chosen sample size of 200 metaphase figures. This figure shows that the smallest difference between exposures that one can expect to resolve statistically is not constant with respect to the aberration frequency. At lower aberration frequencies (< 0.2 aberrations per cell) the sensitivity of the statistical method is not as good as it is at higher levels on a percentage basis. For example, the smallest percentage difference that can be seen at 0.1 aberration frequency is 80% whereas the difference for 0.5 aberration frequency is 36%.

An attempt was made in all experiments, where a statistical analysis was to be performed, to score 200 metaphase figures. However, in several experiments 200 scoreable metaphase figures were not found and the analysis had to be made using a smaller sample size.

2. Control Series

Control Series No. 1 showed that the background level of aberrations in 200 metaphases scored in the blood donor was effectively zero. The results of Control Series No. 2 are shown in Table 5. There were no aberrations noted in any of the blood samples held for various time periods in the sample holders. There appears to be no cell toxicity from the materials in the biological sample holder. The slightly elevated mitotic index for the 6 hour hold period can not be explained but it appeared to have no effect on the aberration frequency.

3. Ionizing Radiation Alone Series

a. The results of the Ionizing Radiation Alone Series No. 1 are shown in Table A1 (summary data) and Figure 38 (graphical representation of summary data). The dose response of this biological exposure

Table 5

Test for Biological Sample Holder Toxicity

Time in Sample Holder	Mitotic Index Metaphase Cells/1000 Cells	Metaphases Scored	Aberrations
No Hold	4.5	100	0
30 Min	5.5	100	0
2 hrs	4.6	100	0
6 hrs	15.2	100	0

All Samples Held At 37 $\pm$ 0.1°C At All Times.

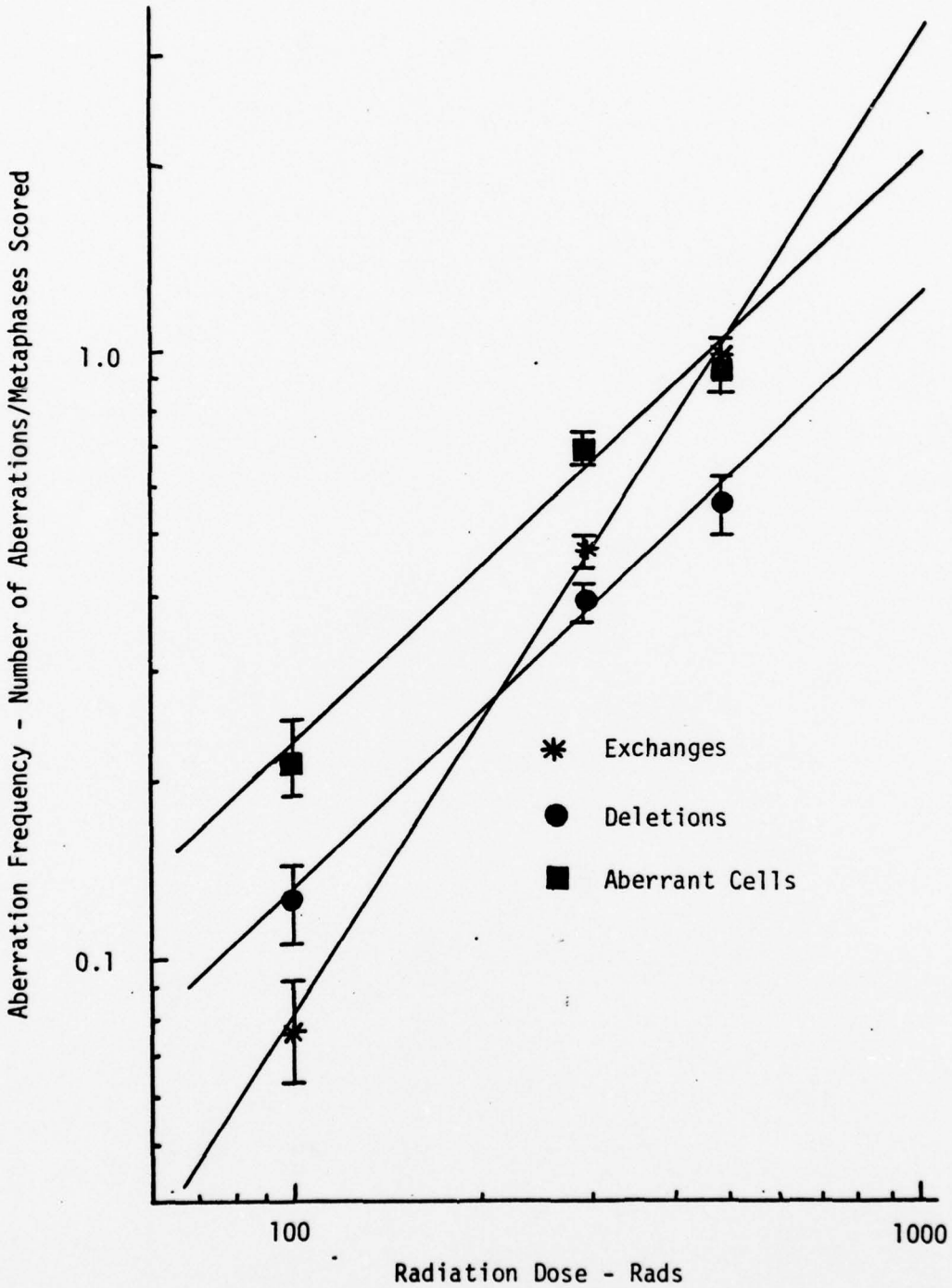

Figure 38. Chromosome Aberration Dose Response (Co-60 Radiation at 37°C and 122.0 rads/min Incubated Immediately at 37°C for 48 hours)

system appears to be consistent with the literature (see Chapter I, Chromosome Aberrations from Ionizing Radiation).

b. The results of the Ionizing Radiation Alone Series No. 2 are shown in Table A2 (summary data) and Table 6 (statistical analysis). There appears to be no statistically significant difference between the samples and consequently no apparent effect of delaying the incubation of irradiated blood samples for periods up to 6 hours provided the samples are held at 37 $\pm$ 0.1°C. This result is consistent with the literature (Vekemans and Leonard (1977)).

4. Ultrasound Alone Series

a. The results of the Ultrasound Alone Series No. 1 are shown in Table 7. There were no chromosome aberrations found in any of these 30 minute ultrasound exposures at intensities up to 4 W/cm^2. The lack of chromosome aberrations at the ultrasound intensities used is consistent with the literature (see Chapter I, Chromosome Aberrations Due to Ultrasound Alone). The mitotic index was depressed slightly at the higher intensities but was not greatly different. The peak temperatures (equilibrium temperatures) which resulted in the samples due to the ultrasound exposure are shown. In no case did the temperature exceed 45°C.

b. The results of the Ultrasound Alone Series No. 2 are shown in Table 8. All exposures at 3 W/cm^2, CW, 1.1 MHz, for various time periods, showed no aberrations and the mitotic index was only slightly depressed at the longer exposure periods. All equilibrium temperatures were 43 $\pm$ 0.5°C.

Table 6

STATISTICAL ANALYSIS FOR RADIATION ALONE SERIES NO. 2

EXPOSURE SEQUENCE	DIFFERENCE FROM CONTROL VALUES		
	DELETIONS	EXCHANGES	ABERRANT CELLS
300 RADS INCUBATE AFTER 30 MINUTES DELAY AT 37C	-0.026	-0.029	-0.042
	P=0.682	P=0.771	P=0.700
300 RADS INCUBATE AFTER 2 HOURS DELAY AT 37C	0.090	-0.027	0.033
	P=0.197	P=0.774	P=0.748
300 RADS INCUBATE AFTER 6 HOURS DELAY AT 37C	0.039	-0.019	0.011
	P=0.576	P=0.851	P=0.923

CONTROL VALUE IS 300 RADS INCUBATE IMMEDIATELY

Table 7

Effect of Ultrasound Intensity

Exposure W/cm^2	Mitotic Index	Metaphases Scored	Aberrations	Equilibrium Temperature in Sample Holder °C
4.0 (Max. Intensity)	8.0	100	0	44.5
2.0	5.3	100	0	41
1.0	11.5	100	0	39
0.5	10.3	100	0	38
Control	13.6	100	0	37

All Exposures for 30 Minutes

Tank Temperature was 37°C At Start of Each Exposure

Table 8

Effect of Ultrasound Exposure Time

Time Exposed to Ultrasound	Mitotic Index	Metaphases Scored	Aberrations
0 (no exposure)	6.0	50	0
30	5.0	50	0
45	1.0	50	0
60	3.0	50	0

Equilibrium Temperatures in Samples was 43 $\pm$ 0.5°C.

Ultrasound Exposures were 3.0 W/cm^2, CW, 1.1 MHz.

5. Heat Alone Series

a. The results of the Heat Alone Series No. 1 are shown in Table 9. There appears to be no chromosome aberration induction due to the heating but the mitotic index and the number of cells remaining in the culture drop to zero somewhere between 43 and 46°C. There was no difference between the cultures at the beginning or end of the experiment, also.

b. The results of the Heat Alone Series No. 2 are shown in Table 10. No chromosome aberrations were noted for any of the exposure times at 43 $\pm$ 0.5°C and the mitotic index was not significantly altered for exposures up to 60 minutes.

6. Combined Ultrasound and Ionizing Radiation

a. The results of the Combined Ultrasound and Ionizing Radiation Series No. 1 are shown in Table A3 (summary data) and Table 11 (statistical analysis). Table A3 shows no consistent trend in the mitotic index with exposure sequence. Table 11 shows that there is no statistically significant difference between the control (sequence 1) and sequences 2 or 7 for any aberrations but there is a difference for exchange aberrations in sequences 3-6. There is no consistent difference for deletions or aberrant cells for any sequences. Further statistical analysis of sequences 3-6 was performed to determine if there is an increasing or decreasing trend in the aberration frequencies with increasing ultrasound duration after irradiation. (Zero time for sequence 3, 13.5 minutes for sequence 4, 28.5 minutes for sequence 5, 43.5 minutes for sequence 6). This analysis is shown in Table 12 with a linear regression performed on the data and a statistical test

Table 9

Effect of Heat Alone

Temperature °C	Mitotic Index	Metaphases Scored	Aberrations
37 (start)	5.6	50	0
39	5.0	50	0
41	9.0	50	0
43	3.3	50	0
46	0.0	0	N/A
50	0.0	0	N/A
37 (end)	8.0	50	0

All Samples Exposed for 30 Minutes

Table 10

Effect of Heat Exposure Time

Time at 43°C Temperature-Min	Mitotic Index	Metaphases Scored	Aberrations
0	15.0	50	0
30	3.3	50	0
45	11.3	50	0
60	13.6	50	0

Table 11

STATISTICAL ANALYSIS FOR ULTRASOUND AND IONIZING RADIATION FOR 300 RADS

EXPOSURE SEQUENCE	DIFFERENCE FROM CONTROL VALUES: DELETIONS	EXCHANGES	ABERRANT CELLS
300 RADS IMMEDIATELY AFTER 30 MINUTES ULTRASOUND (SEQUENCE 2)	-0.024 P=0.640	-0.021 P=0.709	0.026 P=0.709
300 RADS SIMULTANEOUS WITH ULTRASOUND (SEQUENCE 3)	0.105 P=0.045	0.139 P=0.016	0.124 P=0.072
300 RADS SIMULTANEOUS WITH 30 MINUTES ULTRASOUND (SEQUENCE 4)	-0.067 P=0.061	0.220 P<0.001	0.070 P=0.168
300 RADS SIMULTANEOUS WITH 45 MINUTES ULTRASOUND (SEQUENCE 5)	0.016 P=0.772	0.165 P=0.009	-0.057 P=0.436
300 RADS SIMULTANEOUS WITH 60 MINUTES ULTRASOUND (SEQUENCE 6)	0.063 P=0.308	0.230 P<0.001	0.143 P=0.083
300 RADS IMMEDIATELY BEFORE 30 MINUTES ULTRASOUND (SEQUENCE 7)	0.109 P=0.052	-0.002 P=0.971	0.036 P=0.623

CONTROL VALUE IS 300 RADS INCUBATE IMMEDIATELY CONSOLIDATED VALUE (SEQUENCE 1)

Table 12

Effect of Increasing the Duration of Ultrasound After Irradiation

Total Time of Exposure After Radiation-Min	Aberration Frequencies		
	Aberrant Cells	Deletions	Exchanges
0 (Sequence 3)	0.850	0.490	0.605
13.5 (Sequence 4)	0.751	0.318	0.686
28.5 (Sequence 5)	0.624	0.401	0.631
43.5 (Sequence 6)	0.824	0.448	0.696
Intercept	0.760	0.418	0.623
Slope	-0.000419	-0.000197	+0.00147
t-statistic	0.124	0.071	1.160
Probability	0.912	0.949	0.366
Correlation Coefficient	-0.087	-0.050	0.634

to determine if the slope of the regression line is significantly different from zero. Table 12 shows that none of the aberration frequencies has a slope significantly different from zero but the slopes of the regression lines are shown to be slightly positive for the exchange aberrations and slightly negative for the deletions and aberrant cells. The correlation coefficients are shown to be quite low for all aberrations indicating the lack of linearity in the data.

b. The results of the Combined Ultrasound and Ionizing Radiation Series No. 2 (100 rads) are shown in Table A4 (summary data) and Table 13 (statistical analysis). Table A4 shows no apparent trend in mitotic index for the exposure sequences. Table 13 shows that there is no statistically significant difference between the control (sequence 1) and sequences 2 or 7 for any aberrations but there is a difference for exchanges and aberrant cells in sequence 4.

c. The results of the Combined Ultrasound and Ionizing Radiation Series No. 3 are shown in Table A5 (summary data) and Figure 39. Table A5 shows a slight downward trend in mitotic index with increasing intensity. Figure 39 shows the effect of ultrasound intensity on the aberration frequencies. Further statistical analysis of these data was performed to determine if there is an increasing or decreasing trend in the aberration frequencies with increasing ultrasound intensity. This analysis is shown in Table 14 with a linear regression performed and a statistical test to determine if the slope of the regression line is significantly different from zero. Table 14 shows that the deletions and exchanges approximate a linear function with correlation coefficients greater than 0.88 but none of the slopes are significantly different from zero. Although not significant the slopes of the regression lines for deletions are

Table 13

STATISTICAL ANALYSIS FOR ULTRASOUND AND IONIZING RADIATION FOR 100 RADS

EXPOSURE SEQUENCE	DIFFERENCE FROM CONTROL VALUES		
	DELETIONS	EXCHANGES	ABERRANT CELLS
100 RADS IMMEDIATELY AFTER 30 MINUTES ULTRASOUND (SEQUENCE 2)	0.030 P=0.346	-0.033 P=0.147	-0.015 P=0.702
100 RADS SIMULTANEOUS WITH ULTRASOUND (SEQUENCE 4)	0.035 P=0.275	0.067 P=0.014	0.090 P=0.034
100 RADS IMMEDIATELY BEFORE 30 MINUTES ULTRASOUND (SEQUENCE 7)	0.045 P=0.165	0.032 P=0.207	0.045 P=0.274

CONTROL VALUE IS 100 RADS INCUBATE IMMEDIATELY CONSOLIDATED VALUE (SEQUENCE 1)

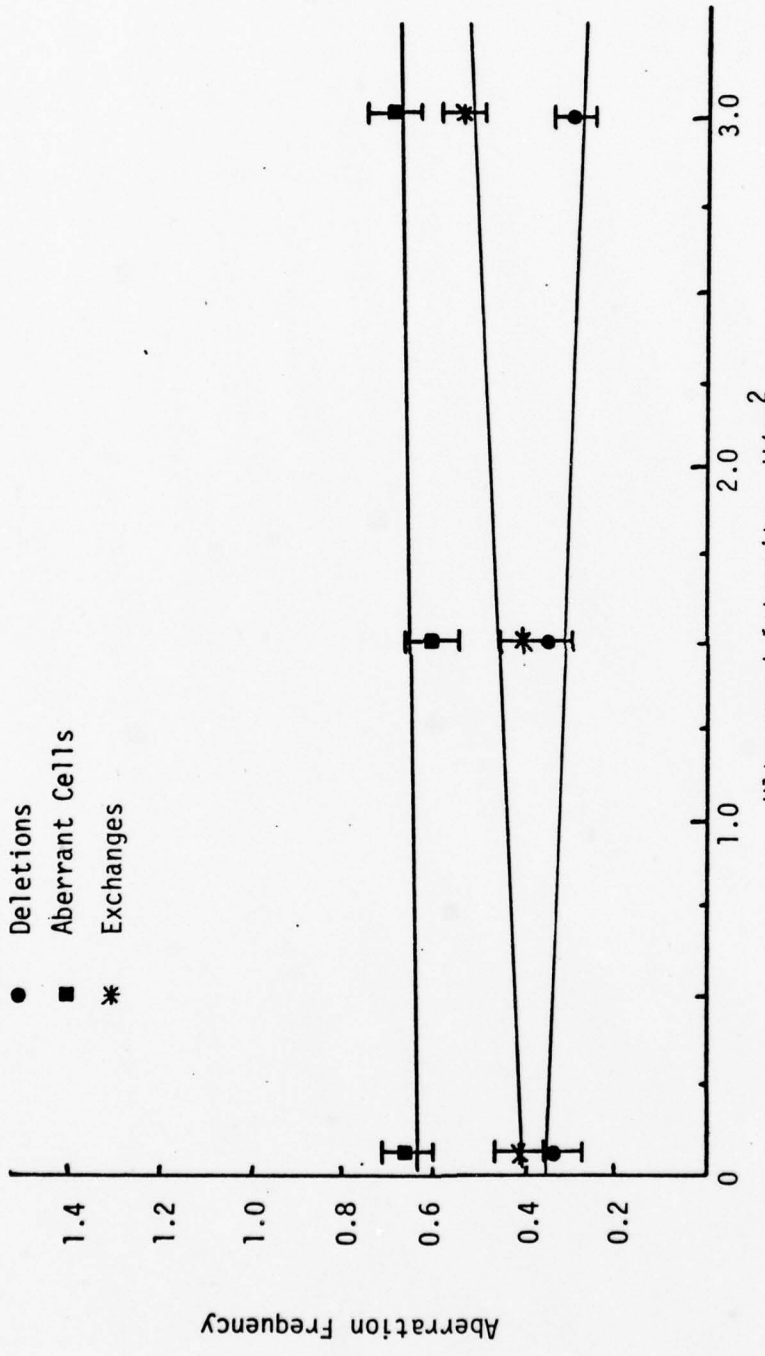

Figure 39. Effect of Ultrasound Intensity When Used Simultaneous with 300 rads Ionizing Radiation (30 Minutes Ultrasound with Radiation Given at Mid-point of Ultrasound exposure).

Table 14

Regression Analysis and Statistical Analysis of Combined Ultrasound and Ionizing Radiation Series No. 3 (300 rads)

Type of Aberrations	Regression Coefficients		Statistical Analysis		
	A	B	$t = \frac{B}{SE(B)}$	Probability	Correlation Coefficient
Deletions	0.35	-0.018	2.127	0.123	-0.905
Aberrant Cells	0.635	0.015	0.540	0.627	0.475
Exchanges	0.394	0.043	1.885	0.156	0.883

Regression Coefficients for General Equation $Y = A + BX$ Where Y = Aberration Yield and X = Ultrasound Intensity.

slightly negative and for exchanges and aberrant cells is slightly positive.

d. A statistical comparison was performed between sequence 4 of Table A3 and the 3.0 W/cm^2 ultrasound exposure of Table A5. This comparison is between identical intensity ultrasound and ionizing radiation exposures but different equilibrium sonation tank temperatures. Sequence 4 of Table A3 was for an equilibrium temperature of 43°C and the 3.0 W/cm^2 ultrasound exposure of Table A5 is for a sonation tank equilibrium temperature of 37°C. The results of the comparison, Table 15, show a statistically significant difference between the exchange aberration frequencies but not the aberrant cells or deletions.

7. Combined Heat and Ionizing Radiation Series

a. The results of the Combined Heat and Ionizing Radiation Series No. 1 (300 rads) are shown in Table A6 (summary data) and Table 16 (statistical analysis). Table A6 shows that the mitotic index is not affected for sequences 2 or 7 but is affected for sequences 3-5. (Note that sequence 6 was not performed for this series due to the pronounced depression of the mitotic index at the longer duration exposure of sequence 6). The effect becomes quite pronounced as the duration of the heat is increased (sequence 3-5). Table 16 shows that there is no statistically significant difference between the control (sequence 1) and sequences 2 or 7 for any aberration but there is a difference for exchange aberrations for sequences 3-5. There is no consistent difference for aberrant cells or deletions for any of the sequences. Further statistical analysis was performed to determine if there is an increasing or decreasing

Table 15

STATISTICAL ANALYSIS FOR COMPARISON OF 3.0W/CM**2 ULTRASOUND AND IONIZING RADIATION EXPOSURES

EXPOSURE SEQUENCE	DIFFERENCE FROM CONTROL VALUES		
	DELETIONS	EXCHANGES	ABERRANT CELLS
300 RADS SIMULTANEOUS WITH 30 MINUTES 3.0W/CM**2 ULTRASOUND 43C	0.023 P=0.619	0.141 P=0.036	0.046 P=0.522

CONTROL VALUE IS 300 RADS SIMULTANEOUS WITH 30 MINUTES 3.0W/CM**2 ULTRASOUND 37C

Table 16

STATISTICAL ANALYSIS FOR HEAT AND IONIZING RADIATION FOR 300 RADS

EXPOSURE SEQUENCE	DIFFERENCE FROM CONTROL VALUES DELETIONS	EXCHANGES	ABERRANT CELLS
300 RADS IMMEDIATELY AFTER 30 MINUTES AT 43C (SEQUENCE 2)	0.065 P=0.208	-0.021 P=0.704	0.029 P=0.670
300 RADS AT 43C INCUBATE IMMEDIATELY (SEQUENCE 3)	-0.029 P=0.601	0.165 P=0.011	0.057 P=0.453
300 RADS SIMULTANEOUS WITH 30 MINUTES AT 43C (SEQUENCE 4)	0.087 P=0.031	0.147 P=0.001	0.048 P=0.355
300 RADS SIMULTANEOUS WITH 45 MINUTES AT 43C (SEQUENCE 5)	0.064 P=0.491	0.248 P=0.016	0.156 P=0.208
300 RADS SIMULTANEOUS WITH 60 MINUTES AT 43C (SEQUENCE 6)	Sequence Not Performed		
300 RADS IMMEDIATELY BEFORE 30 MINUTES AT 43C (SEQUENCE 7)	-0.035 P=0.482	0.004 P=0.943	0.004 P=0.955

CONTROL VALUE IS 300 RADS INCUBATE IMMEDIATELY CONSOLIDATED VALUE (SEQUENCE 1)

trend in the aberration frequencies with increasing heat duration after radiation (zero time for sequence 3, 13.5 minutes for sequence 4, and 28.5 minutes for sequence 5). This analysis is shown in Table 17 with a linear regression performed and a statistical test to determine if the slopes of the regression lines are significantly different from zero. Table 17 shows that none of the aberration frequencies has a slope significantly different from zero but the slopes of the regression lines are slightly positive for all aberration types. The correlation coefficients of the regression lines show that the aberration data is marginally linear.

b. The results of the Combined Heat and Ionizing Radiation Series No. 2 (100 rads) are shown in Table A7 (summary data) and Table 18 (statistical analysis). Only exposure sequences 1, 2, 4 and 7 were conducted for these 100 rad exposures. Table A7 shows that there is no major effect on the mitotic index for any sequence of exposure. Table 18 shows that there is no statistical significant difference between the control (sequence 1) and any of the exposure sequences.

c. The results of the Combined Heat and Ionizing Radiation Series No. 3 are shown in Table A8 (summary data) and Figure 40. Table A8 shows that the mitotic index is reduced as the temperature increases but is not drastically altered over the range of temperatures used. Figure 40 shows the effect of temperature on the aberration frequencies. Further statistical analysis of these data was performed to determine if there is an increasing or decreasing trend in the aberration frequencies with increasing temperature. This analysis is shown in Table 19 with a linear regression performed and a statistical test to determine if the slope of the regression

Table 17

Effect of Increasing Heat Exposure After Irradiation

Time Exposed After Radiation (min)	Aberration Frequencies		
	Deletions	Aberrant Cells	Exchanges
0 (Sequence 3)	0.356	0.738	0.631
13.5 (Sequence 4)	0.472	0.729	0.613
28.5 (Sequence 5)	0.449	0.837	0.714
Intercept - Y	0.381	0.718	0.610
Slope - B	+0.00317	+0.0035	0.00298
t - statistic	1.090	1.565	1.285
Probability	0.473	0.362	0.421
Correlation Coefficient - r	0.736	0.842	0.789

Radiation Exposure 300 Rads Simultaneous with 43°C Heat.

Table 18

STATISTICAL ANALYSIS FOR HEAT AND IONIZING RADIATION FOR 100 RADS

EXPOSURE SEQUENCE	DIFFERENCE FROM CONTROL VALUES		
	DELETIONS	EXCHANGES	ABERRANT CELLS
100 RADS IMMEDIATELY AFTER 30 MINUTES AT 43C (SEQUENCE 2)	0.025 P=0.429	0.002 P=0.918	0.018 P=0.303
100 RADS SIMULTANEOUS WITH 30 MINUTES AT 43C (SEQUENCE 4)	0.030 P=0.346	-0.002 P=0.917	0.005 P=0.900
100 RADS IMMEDIATELY BEFORE 30 MINUTES AT 43C (SEQUENCE 7)	0.005 P=0.871	0.022 P=0.373	0.020 P=0.620

CONTROL VALUE IS 100 RADS INCUBATE IMMEDIATELY CONSOLIDATED VALUE (SEQUENCE 1)

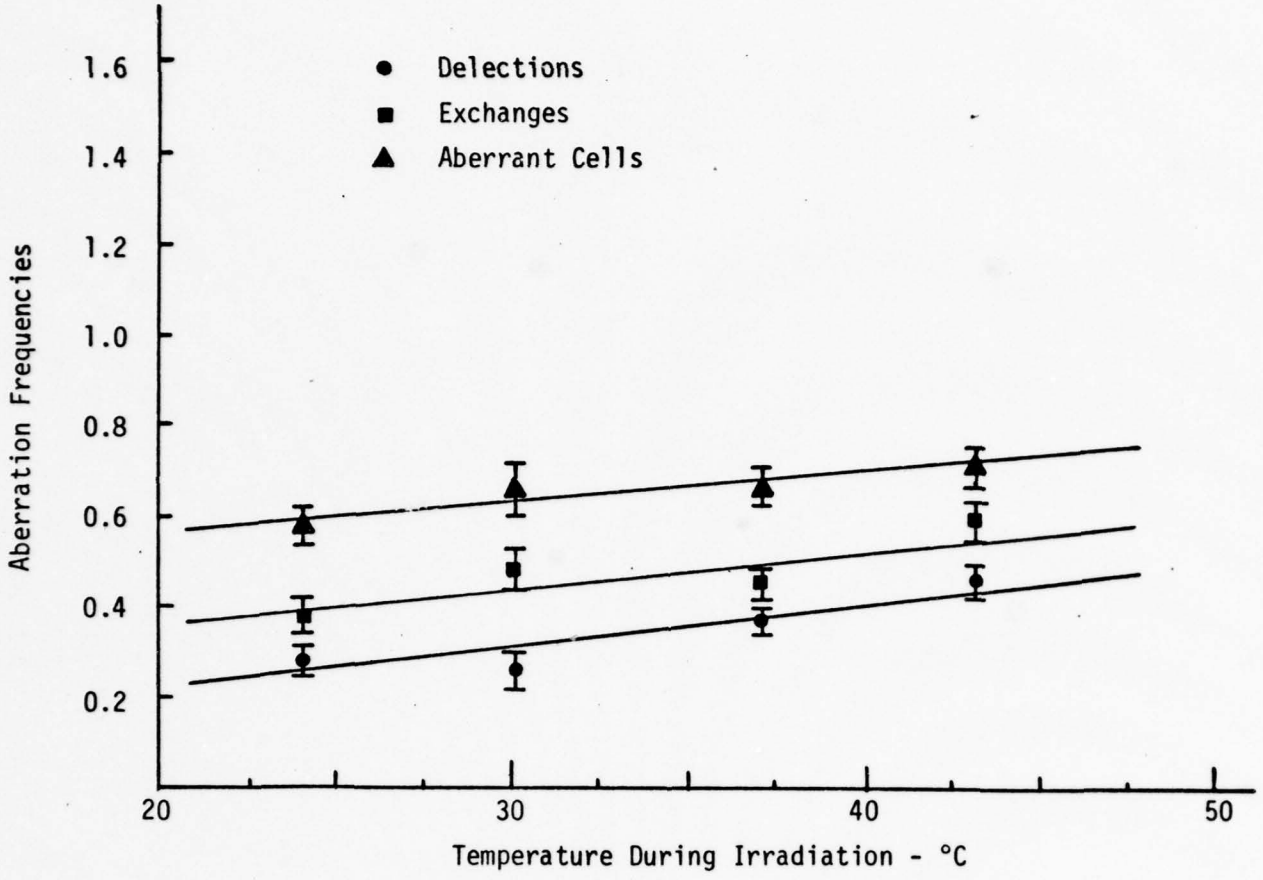

Figure 40. Effect of Temperature During Irradiation (30 Minutes of Heat with Radiation Given at the Mid-point of 300 rads, Co-60 at 122.7 rads/min)

Table 19

Regression Analysis and Statistical Analysis of Combined Heat and Ionizing Radiation Series No. 3 (300 rads)

Type of Aberrations	Regression Coefficients		Statistical Analysis		
	A	B	$t = \frac{B}{SE(B)}$	Probability	Correlation Coefficient
Deletions	0.008	0.01	3.373	0.028	0.922
Aberrant Cells	0.441	0.007	4.681	0.009	0.957
Exchanges	0.163	0.009	2.589	0.061	0.877

Regression Coefficients for Equation of the Form $Y = A + BX$ Where Y = Aberration Yield and X = Temperature

line is significantly different from zero. Table 19 shows that all aberrations approximate linear functions with correlation coefficients in excess of 0.877 and that the slopes of the regression lines for deletions and aberrant cells are significantly different from zero. The slope of the regression line for exchanges is marginally significant at $p = 0.061$.

8. Comparison of Heat plus Ionizing Radiation and Ultrasound plus Ionizing Radiation

a. A comparison of the heat or ultrasound and ionizing radiation Series No. 1 exposures was made using the data in Tables A3 and A6 to determine if there were statistically significant differences between aberration frequencies caused by heat or ultrasound. The heat plus ionizing radiation sequences were used as control values and the results are shown in Table 20. It can be seen that the only significant differences exist for deletion aberrations for sequences 4 and 7.

b. A similar comparison of the heat or ultrasound and ionizing radiation Series No. 2 exposures was made using Table A4 and A7. The results in Table 21 show that there is a statistically significant difference between heat and ultrasound for exchange aberrations in sequence 4.

c. A comparison of the heat or ultrasound and ionizing radiation Series No. 3 exposures was made using the data in Tables A5 and A8. The results in Table 22 show that there are no statistically significant differences between the heat and ultrasound exposures. It should be noted that only the 24°, 30°, and 37°C exposures were compared.

Table 20

STATISTICAL ANALYSIS FOR COMPARISON OF HEAT OR ULTRASOUND AND IONIZING RADIATION

EXPOSURE SEQUENCE	DIFFERENCE FROM CONTROL VALUES		
	DELETIONS	EXCHANGES	ABERRANT CELLS
300 RADS IMMEDIATELY AFTER HEAT OR ULTRASOUND (SEQUENCE 2)	-0.089 P=0.170	0.000 P=1.000	-0.003 P=0.970
300 RADS SIMULTANEOUS WITH HEAT OR US (SEQUENCE 3)	0.134 P=0.060	-0.026 P=0.761	0.067 P=0.484
300 RADS SIMULTANEOUS WITH 30 MIN. HEAT OR ULTRASOUND (SEQUENCE 4)	-0.154 P<0.001	0.073 P=0.165	0.022 P=0.693
300 RADS SIMULTANEOUS WITH 45 MIN. HEAT OR ULTRASOUND (SEQUENCE 5)	-0.048 P=0.650	-0.084 P=0.527	-0.213 P=0.115
300 RADS SIMULTANEOUS WITH 60 MIN. HEAT OR ULTRASOUND (SEQUENCE 6)	Comparison can not be made		
300 RADS IMMEDIATELY BEFORE HEAT OR ULTRASOUND (SEQUENCE 7)	0.144 P=0.034	-0.006 P=0.932	0.032 P=0.717

CONTROL VALUE IS 300 RADS INCUBATE IMMEDIATELY CONSOLIDATED VALUE (SEQUENCE 1)

Table 21

STATISTICAL ANALYSIS FOR COMPARISON OF HEAT OR ULTRASOUND AND IONIZING RADIATION FOR 100 RADS

EXPOSURE SEQUENCE	DIFFERENCE FROM CONTROL VALUES DELETIONS	EXCHANGES	ABERRANT CELLS
100 RADS IMMEDIATELY AFTER 30 MIN. HEAT OR ULTRASOUND (SEQUENCE 2)	0.005 P=0.898	-0.035 P=0.162	-0.025 P=0.583
100 RADS SIMULTANEOUS WITH 30 MIN. HEAT OR ULTRASOUND (SEQUENCE 4)	0.005 P=0.900	0.070 P=0.035	0.085 P=0.095
100 RADS IMMEDIATELY BEFORE 30 MIN. HEAT OR ULTRASOUND (SEQUENCE 7)	0.040 P=0.302	0.010 P=0.758	0.025 P=0.612

CONTROL VALUE IS 100 RADS INCUBATE IMMEDIATELY CONSOLIDATED VALUE (SEQUENCE 1)

Table 22

STATISTICAL ANALYSIS FOR COMPARISON OF HEAT OR ULTRASOUND AND IONIZING RADIATION

EXPOSURE SEQUENCE	DIFFERENCE FROM CONTROL VALUES		
	DELETIONS	EXCHANGES	ABERRANT CELLS
300 RADS SIMULTANEOUS WITH HEAT OR ULTRASOUND 24C	0.059 P=0.238	0.024 P=0.674	0.071 P=0.304
300 RADS SIMULTANEOUS WITH HEAT OR ULTRASOUND 30C	0.074 P=0.187	-0.075 P=0.274	-0.057 P=0.483
300 RADS SIMULTANEOUS WITH HEAT OR ULTRASOUND 37C	-0.090 P=0.066	0.079 P=0.164	0.024 P=0.725

CONTROL VALUE IS 300 RADS WITH 30 MINUTES AT 24C

Table 23

STATISTICAL ANALYSIS FOR COMPARISON OF ALL 300 RADS AT 37C INCUBATE IMMEDIATELY

EXPOSURE SEQUENCE	DIFFERENCE FROM CONTROL VALUES DELETIONS	EXCHANGES	ABERRANT CELLS
CONTROL VALUE NO. 1	0.015	-0.016	-0.006
	P=0.769	P=0.772	P=0.926
CONTROL VALUE NO. 2	-0.034	-0.102	-0.110
	P=0.644	P=0.209	P=0.267
CONTROL VALUE NO. 3	0.005	0.080	0.071
	P=0.932	P=0.216	P=0.365
CONTROL VALUE NO. 4	-0.005	-0.001	-0.001
	P=0.919	P=0.985	P=0.985

CONTROL VALUE IS CONSOLIDATED VALUE

9. Comparison of All Ionizing Radiation Alone Exposures

A comparison of all 300 rad 37°C exposures with immediate incubation was conducted to determine if reproduceable numbers of aberrations were being found for radiation exposures that were conducted at different times. Four separate 300 rad at 37°C incubate immediately exposures were made at different times throughout the conduct of the experiments which served as radiation controls for individual experiments. The summary data for the four exposures and a consolidated control (sum of all individual series) is shown in Table A9. The statistical analysis (Table 23) shows that there is no statistically significant difference between the consolidated value and any of the other control series for any type of aberration frequency.

C. Discussion

The discussion of the biological experiments include a discussion of the significant results of these experiments, the limitations of the biological system used in these experiments, and the potential impact of these results on the population in general, as well as cancer therapy patients and the fetal population in particular.

1. Discussion of the Significant Results of the Biological Experiments

The discussion of the significant results includes a brief summary of the significant results to add clarity to the further discussion, an analysis of the baseline experiments (control series, ultrasound alone, heat alone, ionizing radiation alone), a discussion

of the effects of combined applications of heat or ultrasound and ionizing radiation and finally, a comparison between the effects of heat plus ionizing radiation and ultrasound plus ionizing radiation.

a. Summary of Significant Results

(1) Control Experiments

(a) No aberrations were found in the donor's blood.

(b) Storage of blood in biological sample holders at 37°C for periods up to 6 hours did not produce any aberrations.

(2) Ionizing Radiation Alone

(a) The dose-response relationships for the chromosome aberration endpoint used in this biological system followed that found in the literature.

(b) Holding ionizing radiation exposed blood samples in the biological sample holders at 37°C for periods up to 6 hours had no effect on the aberration frequencies.

(3) Ultrasound Alone

(a) No aberrations were caused by 30 minute exposures of up to 4.0 W/cm^2 ultrasound.

(b) No aberrations were caused by 3.0 W/cm^2 ultrasound for exposure periods of up to 60 minutes.

(4) Heat Alone

(a) No aberrations were caused by 30 minute exposures to heat up to 50°C. Lymphocytes disappeared from the culture at temperatures above 46°C and the mitotic index dropped rapidly between 43°C and 46°C.

(b) No aberrations were caused by 43°C heat for exposure periods up to 60 minutes.

(5) Combined Ultrasound and Ionizing Radiation

(a) Ultrasound (3 W/cm^2) given immediately before or after ionizing radiation resulted in no significant increase in aberration frequencies for both 100 and 300 rad exposures.

(b) Ultrasound (3 W/cm^2) given simultaneously with ionizing radiation resulted in a significant increase in exchange aberrations for 100 and 300 rad exposures. Increasing the duration of ultrasound exposure after ionizing radiation slightly increased the exchange frequency and decreased the deletion frequency and number of aberrant cells. None of the changes, however, were statistically significant.

(c) Increasing the utrasound intensity (0.01-3.0 W/cm^2) during simultaneous ultrasound and ionizing radiation exposure slightly increased exchange aberrations and slightly decreased the deletions and number of aberrant cells. None of the changes were statistically significant, however.

(d) Exposure to 30 minutes ultrasound (3 W/cm^2) plus ionizing radiation (300 rads) produced a significant difference in exchange aberrations when the effects of two different equilibrium tank temperature, 37° and 43°C, were compared.

(6) Combined Heat and Ionizing Radiation

(a) Increased Heat (43°C) immediately before or after ionizing radiation resulted in no significant increase in aberration frequencies for both 100 and 300 rad exposures.

(b) Increased heat (43°C) simultaneous with the ionizing radiation resulted in a significant increase in exchange aberrations for the 300 rad exposures but not for the 100 rad exposure. Increasing the duration of elevated heat exposure after ionizing radiation had little effect for 300 rad exposures.

(c) The frequency of deletions, of exchanges and of aberrant cells increased linearly with increases in temperature during ionizing radiation, when 30 minutes heat exposures were made at 24-43°C with ionizing radiation (300 rads) given at mid-point of heat exposure.

(7) Comparison of Heat plus Ionizing Radiation and Ultrasound plus Ionizing Radiation

(a) There was no significant difference in aberration frequencies between identical sequences of heat (43°C) plus ionizing radiation at 300 rads and ultrasound (3 W/cm^2) plus ionizing radiation at 300 rads.

(b) There was a significant difference in exchange aberrations when the heat (43°C) plus ionizing radiation (100 rads) sequence No. 4 and the ultrasound (3 W/cm^2) plus ionizing radiation (100 rads) sequence No. 4 results are compared.

(c) Comparison of the combined heat (24-43°C) and ionizing radiation Series No. 3 and the combined ultrasound (0.01 W/cm^2-3 W/cm^2) and ionizing radiation Series No. 3 showed no significant differences in aberration frequencies for the same equilibrium temperatures. .

(8) Comparison of All Ionizing Radiation Alone Control Values

No significant difference in aberration frequencies was seen between the consolidated value (sum of all series) and each individual

series.

b. Analysis of Baseline Experiments

The baseline experiments show that there were no chromosome aberrations in the routinely processed cells of the blood donor, nor did the biological sample holder, ultrasound used alone, and increased heat used alone produce an effect. These results are consistent with scientific literature already discussed in the Introduction for the exposure levels and parameters used. The experiments using ionizing radiation alone show a chromosome aberration dose-response relationship which is consistent with the literature (see Introduction). Holding the exposed blood samples at 37 $\pm$ 0.1°C for up to 6 hours after ionizing radiation exposure has no effect on the aberration frequencies which is, also, consistent with the literature (Vekemans and Leonard (1977)).

The comparison of all the ionizing radiation alone control values (Table 23) shows that there were no statistically significant differences among the control series performed during the research. This indicates that the radiation exposure system could deliver a reproduceable dose, scoring of chromosome aberrations was consistent, the small decrease in radiation dose rate due to ^{60}Co source decay between the first and last experiments had an insignificant effect on chromosome aberration yields, and the comparison of all 300 rad exposure sequences was possible even though they were performed at different times.

These baseline experiments lay the foundation for the discussion of the combined sequences of heat or ultrasound plus ionizing radiation by showing that the heat, ultrasound, sample holder and donor contribute nothing to the aberration yield and the radiation

alone contributes known reproduceable aberration yields. Any statistically significant increase or decrease in aberration frequencies above that produced by radiation alone can then be attributed to some combined or synergistic effect.

c. Combined Ultrasound and Ionizing Radiation

(1) Series No. 1

There results show a significant effect of ultrasound on the aberration yields of human lymphocytes exposed in vitro when used simultaneously with ionizing radiation. The temporal sequence in which the ultrasound and ionizing radiation exposures are made appears to make a significant difference in the results (see Figure 35 for presentation of sequences). Exposure of the blood to ultrasound immediately before ionizing radiation or immediately after ionizing radiation appears to have no effect on the aberration yield but ultrasound used simultaneous with ionizing radiation has a significant effect. All four exposures (sequences 3-6) to 300 rads in which the ultrasound was given simultaneously with the radiation produced a significant increase in exchange aberrations. Sequences 3-6, also, show that there is a slight, but not statistically significant, increase in exchanges for an increase in duration of ultrasound exposure after radiation.

The mitotic index values for the ultrasound and ionizing radiation sequences do not appear to be a good indicator of the combined effects. The only apparent trend in mitotic index changes is a decrease in the index with increasing time of ultrasound exposure for sequences 3-6. This same trend is apparent in the series of experiments with ultrasound alone so it appears that the combined ultrasound and radiation sequences do not significantly affect the mitotic index.

(2) Series No. 2

The total radiation dose (100 rads or 300 rads) appears to have little effect on the results noted above. Exposure sequences 2, 4, and 7 for ultrasound plus ionizing radiation at 100 rads show identical results to the 300 rad exposures except that the aberration frequencies are proportionally lower due to the lower total dose. The same sequence effects are seen and the type of aberrations affected are the same.

(3) Series No. 3

The intensity of the ultrasound used during the simultaneous application of ultrasound and ionizing radiation (300 rads given at mid-point of 30 minutes ultrasound exposure) appears to have little effect on the aberration frequencies. Figure 39 and the statistical analysis of Table 14 appear to show that there is no statistically significant increase in the aberration frequencies (slope not statistically greater than zero) with increasing ultrasound intensity. It should be noted, however, that the regression lines do have positive slopes for most aberration frequencies and that this analysis has only three data points which make it extremely difficult to determine trends. Additional data could not be gathered at higher intensities due to the power limitations of the ultrasound generation system.

(4) Comparison of Identical Ultrasound and Ionizing Radiation Exposures with Different Tank Equilibrium Temperatures

The comparison between the two 30 minute, 3 W/cm^2 ultrasound plus ionizing radiation (300 rads) exposures which differed only in that one had a tank equilibrium temperature of 37°C (tank initially at room temperature) and the other with a 43°C equilibrium tank

temperature (tank initially at 37°C) revealed that there is a statistically significant increase in exchanges at the higher tank temperature. The significant increase at the higher temperature suggests that the mechanical (physical) properties of the ultrasound may not be responsible for the effects seen in the previous exposure sequences. If the combined effect was due to some ultrasound mechanical mechanism then we would expect to see little difference between these exposures because the ultrasound intensities were identical. Since the only difference between the exposures was the temperature during exposure it is suggested that heat or temperature during the exposure may be the mechanism responsible for the increase in aberration frequency. This suggestion was tested experimentally in the heat plus ionizing radiation exposure sequences which will be discussed later.

(5) Comparison of These Results with that Found in the Literature

The ultrasound plus ionizing radiation experiments appear to show that a synergistic effect occurs only when ultrasound is used simultaneously with ionizing radiation and that the primary effect is an increase in exchange aberrations. There was little or no effect on the aberration frequencies when ultrasound was used before or after ionizing radiation, when the duration of ultrasound exposure was increased after ionizing radiation, and when the total ionizing radiation dose was changed. The lack of an increase in the number of cells which contain aberrations, the increase in exchange aberrations only, and the absence of a statistically significant increase in all aberration frequencies with increasing ultrasound intensity suggests that ultrasound produced an enhancement in the chromosome repair and exchange formation process. This interpretation is based on the fact

that an increase in final number of detectable chromosome aberrations can result from several causes: (1) an increase in the initial or primary number of chromosome breaks or lesions, (2) an inhibition of the repair of the chromosome breaks, (3) an enhancement in the repair of the chromosome breaks. Each cause influences differently the frequency of the deletions, exchanges and aberrant cells. More primary breaks would result in more of all types of aberrations, an inhibition of repair would be reflected by more deletion aberrations and an enhancement in repair would be reflected by more exchange aberrations.

The increase in exchange aberrations at elevated sonation tank temperature for the same ultrasonic intensity suggests that the enhancement noted above is due to an increase in temperature and not due to ultrasound mechanical effects. Because only exchanges, which indicate the misrepaired fraction of aberrations, were increased significantly, it is suggested that there is an enhancement in repair of chromosome damage due to elevated temperature.

The above results appear to be consistent with the previous work performed by Harkanyi et al. (1978), Burr et al. (1977), Kunze-Muhl (1975), and Conger (1948) in that there is an increase in chromosome aberrations when ultrasound is used simultaneously with ionizing radiation and there is no effect when ultrasound is applied immediately before radiation.

There is an apparent inconsistency, however, with the findings of Burr et al. (1977) which showed a significant increase in aberrations for ultrasound given immediately after ionizing radiation. A possible explanation for this is that the temperature in the two systems was very much different. Burr et al. (1977) irradiated blood at 23°C and raised the temperature to approximately 37-40°C (not

measured) during sonation, whereas in the present study blood was irradiated at 37°C and the temperature increased to 43°C during sonation The large differential in temperature for the Burr et al. (1977) study may have caused a larger aberration difference which would be easier to detect as a significant increase. This temperature effect has only been suggested by one of the experiments performed (comparison of identical ultrasound and ionizing radiation exposures with different tank equilibrium temperatures). A more detailed discussion of this temperature effect is contained in the next section.

d. Combined Heat and Ionizing Radiation

(1) Series No. 1

The results of the heat plus ionizing radiation series show that temperature has a significant effect on the aberration yields of human lymphocytes exposed in vitro to ionizing radiation. The sequence of application of the heating and ionizing radiation appears to make a significant difference in the results. Exposure of the blood to heat immediately before or after ionizing radiation appears to have no effect on the aberration yield but heat used simultaneous with ionizing radiation has a significant effect. All three heat exposures (sequences 3-5), which were made simultaneously with the ionizing radiation, produced significant increases in exchange aberrations. Sequences 3-5, also, show that there is a slight, but not statistically significant, increase in all aberration types for an increase in duration of heat exposure after radiation.

The mitotic index values for the heat and ionizing radiation sequences appear to indicate the magnitude of the combined effect. The heat used alone or the ionizing radiation alone does not depress the mitotic index in the same manner as the combined sequences. The

effect appears to correspond to that of the simultaneous heat and ionizing radiation sequences (3-5) with a rapid drop in mitotic index as the duration of exposure to heat is increased after the irradiation.

(2) Series No. 2

The total radiation dose (100 rads or 300 rads) appears to have a slight effect on the aberration frequencies. Exposure sequences 2 and 7 show similar results for the 100 and 300 rad exposures but sequence 4 at 100 rads shows no significant increase in exchange aberration frequency whereas sequence 4 at 300 rads did.

(3) Series No. 3

The combined heat and ionizing radiation Series No. 3 (Figure 40) showed a significant increase in all aberration frequencies with increasing temperature (exchanges were marginally significant). An increase in all aberration types with increase in temperature suggests that more primary chromosome breaks occur at elevated temperatures.

(4) Comparison of These Results with that Found in the Literature

The combined heat and ionizing radiation Series No. 1 appears to show that a synergistic effect occurs only when heat is elevated simultaneously with ionizing radiation and that the effect is an increase in exchange aberrations. Heat used before or after ionizing radiation, and increasing the duration of heat exposure after ionizing radiation, appear to have little or no effect on the aberration frequencies. The magnitude of the ionizing radiation dose appears to have an effect on the aberration frequencies when heat is used simultaneously with ionizing radiation. No synergistic effect was seen at the lower total dose of 100 rads. The lack of an increase in the number of cells with aberrations and the increase in exchange

aberrations only, suggests that heat produced an enhancement in chromosome repair and exchange formation. However, the increase in all aberration frequencies with increasing temperature (24-43°C) for combined heat and ionizing radiation Series No. 3 suggests that the number of primary chromosome breaks is increased by increasing temperature. The results described above present two apparent inconsistencies: (1) the lack of a significant effect of temperature after radiation is not consistent with some of the literature and (2) the results of Series No. 1 suggest an improvement in repair due to heat but the results of Series No. 3 suggest an increase in the number of primary chromosome breaks due to heat. These apparent inconsistencies can possibly be explained by a closer review of the literature and the data.

The results of the combined heat and ionizing radiation Series No. 3 appear to be consistent with the previous work of Bajerska and Liniecki (1969) and Liniecki et al. (1973) who found that the frequencies of lymphocyte chromosomal dicentrics and fragments increased significantly with increasing temperature during irradiation at 300 rads (15.7 rads/min x-rays) in the temperature range of 10 to 37°C. Dicentrics showed an increase with temperature which was much larger than that of fragments. These results are, also, consistent with the findings of Bora and Soper (1971) who found that human lymphocytes exposed to x-rays at 300 rads (120 rads/min) in vitro at 5°C had fewer deletions and exchanges than exposure at 37°C. It must be noted, however, that in both of these studies the temperature was elevated to a maximum of only 37°C. No other studies were found which investigated these types of aberrations at temperatures above 37°C so it is not possible to compare the 43°C exposure data. The mechanism for the induction of the primary chromosome breaks is not

known, so a specific reason can not be given for the observed effect. Since the result at 43°C are unique and the results below 37°C are consistent with others, it would be reasonable to suggest that elevated temperature during radiation results in more primary chromosome breaks, resulting in an increase in all types of aberrations.

The results of the combined heat and ionizing radiation Series No. 1 do not appear to be consistent with the literature because they show that the temperature after radiation has very little effect. Heat (43°C) commencing immediately after radiation at 37°C and taking 5 minutes to reach the higher temperature produces no increase in any aberration frequencies. Extending the heat exposure duration from zero to 28.5 minutes after irradiation results in a slight but not statistically significant increase in all aberration frequencies. Numerous authors show a much more significant effect of temperature after irradiation.

For example, Bora and Soper (1971) showed that exposing human lymphocytes at 37°C, and immediately reducing the temperature after irradiation to 5°C for 65 minutes, results in a decrease in exchanges and no change in deletions. Reversing the order of the exposures (x-ray at 5°C, then raise to 37°C) gave an increase in exchanges and no change in deletions.

Schmid et al. (1976) used split dose experiments to demonstrate that the mean time in which primary breaks induced by both dose-fractions can interact to form dicentric chromosomes in human lymphocytes is 110 minutes. Primary chromosome breaks induced by radiation were found to exist for an exponentially decaying period after radiation. Timerlake et al. (1976), using alkaline sucrose gradients, found that single strand DNA breaks induced by ionizing radiation in human

lymphocytes are not completely repaired for periods of up to 2 hours or more after radiation.

Further evidence of the effect of temperature on the repair of chromosome radiation damage can be seen in the data of Spiegler and Norman (1969) and (1970). They measured the rate of unscheduled DNA synthesis (repair) in human lymphocytes after irradiation and found that there were two distinct rates of synthesis following radiation; a fast rate occurring during the first 30 minutes following radiation and a slow rate occurring for up to 7 hours after radiation. In addition, they found that the fast rate was significantly affected by temperature with the rate increasing by a factor of 5 from 22°C up to 42°C. Above 42°C the rate dropped and above 45°C total degradation of the system occurred. The increase in the rate of repair of DNA breaks in human lymphocytes with increasing temperature is in keeping with the other references which show an increase in exchange formation when the temperature is elevated after radiation. The importance of this increasing rate, however, lies in the fact that it continues above 37°C up to 42°C before it starts to decrease. Previous cellular studies (Li et al. (1976)) have shown that the ability to repair radiation induced damage is enhanced as temperatures increase up to 37°C and is inhibited at temperatures above 37°C. The data from Spiegler and Norman (1970) and the results of the present study suggest that a different mechanism is responsible for the noted effects in human lymphocytes.

The above referenced studies suggest that chromosomal and DNA breaks are available for interaction for an exponentially decreasing period after ionizing radiation exposure. If increased temperature

during this period enhances the interaction by improving the repair processes then an increase in exchange aberrations would be expected. The primary effect of an increase in temperature after irradiation would, therefore, be an increase in repair and, often, an increase in exchange aberration frequency.

The two apparent inconsistencies noted above in the results of the combined heat and ionizing radiation exposures can now be explained on the basis of the conclusions of the above references and experimental data. Aberration yields from radiation exposure depend on the temperature, both during and after radiation, with the primary effects being an increase or decrease in the number of primary chromosome breaks and an increase or decrease in repair, respectively. Since all of the exposures in the present experiments, where elevated temperatures were maintained both during and after radiation exposure, we would expect to see an increase in all aberrations as a result of the temperature during radiation and a larger increase in exchanges due to the temperature after radiation.

The results of these experiments appear to be consistent with the above statement if one considers the magnitude of the temperature increases, the sensitivity of the statistical analysis and the potential variability of the data are considered. The statistically significant increase in all aberrations after the combined heat and ionizing radiation Series No. 3 followed a temperature change of 19°C (24-43°) and the statistically significant increase in exchanges only, after the combined heat and ionizing radiation Series No. 1, followed a temperature increase of 6°C (37-43°C). The larger temperature differential would be more likely to produce a significant increase in all aberrations. The raw data for the combined heat and ionizing

radiation Series No. 1 (Table 16) does show a small increase in aberrant cells and deletions (not statistically significant) and a larger increase in exchanges (statistically significant). A larger temperature differential in this experiment might have made it easier to see a significant increase in aberrant cells and deletions, resulting in data that would be consistent with all other experiments. Likewise, a larger increase in temperature in the combined heat and ionizing radiation Series No. 1 might have produced larger changes in exchange aberrations, making the detection of a significant change with increasing duration of heat exposure easier. Additional experiments using larger temperature differentials were not performed because it was felt that they would be out of the scope of these experiments, which was to investigate the potential synergistic effect of ultrasound and ionizing radiation for exposure parameters approximating actual in vivo conditions (37°C).

e. Comparison of the Combined Heat and Ionizing Radiation and Ultrasound and Ionizing Radiation Series

A comparison of the results of the combined heat and ionizing radiation experiments and the combined ultrasound and ionizing radiation experiments reveals a number of similarities in the data. Statistical comparison of the Series No. 1 (300 rads) results for both experiments (Table 19) shows that thermal heating to the same temperature as that induced by ultrasound causes the same effect. The overall magnitude of the effect appears to be the same and the effect of exposure sequence appears to be the same. The effect is consistent for all simultaneous exposures (sequence 3-6). Comparison of Series No. 2 (100 rads) results for both experiments (Table 20) shows that heat and ultrasound act differently for sequence 4. The

ultrasound apparently causes a greater effect than heat for the simultaneous exposure. This result, although highly significant based on the statistical analysis, should be viewed with caution due to the small number of aberrations at 100 rads and the decreased sensitivity of the statistical analysis at low frequency. Comparison of Series No. 3 results for both experiments (Table 21) shows that ultrasound and heat act the same for different temperatures. The magnitude of the effect and the type of aberrations produced appear to be the same. It should be noted that this comparison only includes the exposures resulting in temperatures of 24, 30 and 37°C, with the 43°C exposure omitted. The omission is due to the lack of sufficient ultrasound intensity in our generating system to achieve 43°C induced heat.

There appears to be several slight, but not statistically significant, differences between the combined heat and ionizing radiation and combined ultrasound and ionizing radiation exposures that should be noted. The magnitude of the aberration increases for the combined heat and ionizing radiation Series No. 3 were larger than the increases for the combined ultrasound and ionizing radiation Series No. 3 even though the gross temperatures were the same. The mitotic index showed a larger decrease with increasing duration of heat exposure after radiation for the combined heat and ionizing radiation Series No. 1 than the combined ultrasound and ionizing radiation Series No. 1. Increasing the heat exposure duration after radiation produced a larger effect on aberration frequencies than increasing the ultrasound exposure duration after radiation. The types of aberrations were slightly different, also, with all aberrations increased by the heat exposure and only exchanges increased by the ultrasound. These differences between heat and ultrasound exposures

are slight and may be due to statistical error or temperature variation in the tank (± 0.5°C) but they can not be ruled out as minor effects due to the small sample sizes and marginal statistics.

It appears that the majority of the experiments performed support the conclusion that the simultaneous use of ultrasound and ionizing radiation results in a synergistic effect and that the effect is primarily due to the heating induced in the medium by the ultrasound. The primary effect noted is a small increase (not statistically significant) in deletions and aberrant cells and a larger increase (statistically significant) in exchange aberrations. The results of these experiments and the literature appear to support the conclusion that elevated temperature at the time of radiation causes an increase in the number of primary chromosome breaks, resulting in more of all aberration types, while elevated temperature after radiation causes an enhancement of the repair and exchange formation process, resulting in more exchange aberrations.

2. Limitations of the Biological System

The analysis of the chromosomes of human lymphocytes exposed in vitro is a useful tool in determining radiation effects on mammalian cell systems because of their synchronous cell population, well defined dose response characteristics, well established procedure, and correlation with cell death. However, there are significant limitations to this biological system that must be mentioned which affect the interpretation of the results of these studies. As mentioned previously in the Introduction there are numerous environmental factors which can affect the aberration yields significantly, i.e., stimulator capability of the insult used, temperature of exposure, incubation time,

oxygen tension, preparation of the samples, scoring technique, state of health of the blood donor, etc. Most of these items can be controlled during the experiments but some can not. As a result there can be significant variations in the gathered data over and above that of merely sample size statistics especially at low doses. This variability in the results makes it difficult to determine small differences produced by the different exposures. This fact is suggested as the cause of the inconsistency of several of the experiments performed. A greater ability to detect small changes in biological effect would have been helpful in many of these experiments.

An additional limitation of this biological procedure is its cost in money and time. Each experiment with heat, ultrasound and/or ionizing radiation requires multiple exposures and multiple cultures which rapidly increase the total work load involved. This limitation results in a low volume of studies that can be performed in a given time period, which in turn reduces the total number of variables that can be studied. Since the evaluation of heat, ultrasound and ionizing radiation involves large numbers of varied exposure conditions, it was necessary to restrict any study to only a limited number of selected exposure variables.

3. Potential Impact of This Study

The results of this study appear to show that ultrasound when used simultaneously with ionizing radiation can be a potential radiosensitizing agent. This effect has only been shown for specific exposure criteria and for effect on the human chromosome but assuming that other exposure parameters and cell systems would act in a similar manner, what would be the potential impact on the population in general

and cancer therapy patients and the fetal population in particular?

The radiosensitizing ability of ultrasound appears to stem from its ability to generate heat in the target tissue with the heat causing the increase in radiosensitivity. If this is true, then low intensity ultrasound exposures where the temperature of the tissue is not raised by more than several degrees will not significantly increase the risk of radiation damage. In addition, those ultrasound exposures which occur before or after radiation exposures will not significantly increase the risk because the temperature will not be raised during the radiation exposure. This means that most diagnostic ultrasound procedures including those to the fetal population should not produce a significant radiosensitizing effect due to the low average ultrasound intensity with consequent lack of heating, as well as the non-simultaneous administration of other diagnostic procedures such as diagnostic x-ray and nuclear medicine tests.

Radiation therapy, on the other hand, may benefit by the potential application of the combined effect of ultrasound and ionizing radiation. Since the purpose of radiation therapy is to deliver a tumorcidal dose of radiation while sparing the surrounding non-cancerous tissue, the use of focused ultrasound to provide increased radiosensitivity in the tumor may be possible. Ultrasound of sufficiently high intensity which is focused at the proper depth is tissue (see Figure 1) could deliver very rapid heating and consequently increase the radiosensitivity of the tissue. The magnitude of this effect is unknown for ultrasound but if we assume that the radiosensitivity produced by the ultrasound heating is the same as for pure conductive heating, then radiosensitivity can be increased significantly in some tumor systems (Bronk (1976)). The ultrasound

may also provide the additional benefits of increased vascularity (improved oxygenation of tumor) and increased membrane permeability (improved uptake of drugs) which could further enhance the radiosensitivity of the tumor. A note of caution should be considered, however, before using high intensity ultrasound for therapy purposes, because high intensity means high shear stresses and fluid streaming in the tissue, creating a need to study the potential for causing possible metastatis of the tumor.

D. Conclusions

Small lymphocytes in human peripheral blood were exposed in vitro to various sequences of ultrasound, heat and/or ionizing radiation using a specially designed and tested ultrasound and ionizing radiation exposure system. The results of these experiments justify several significant conclusions:

1. Ultrasound used alone causes no chromosome aberrations up to 4 W/cm^2 for 30 minutes exposures and up to 3 W/cm^2 for 60 minutes. Heat used alone causes no chromosome aberrations up to 50°C for 30 minutes exposures with rapid fall in mitotic index occurring in the range of 43-46°. In addition, no aberrations are caused by heat exposures of 43°C for up to 60 minutes.

2. There is a synergistic effect between ultrasound (3 W/cm^2) and ionizing radiation (300 and 100 rads) given simultaneously. The effect is primarily an increase in exchange aberrations. Ultrasound given before or after irradiation does not produce cytogenetic damage. Extending the exposure duration of ultrasound after simultaneous ultrasound and radiation does not increase chromosome aberration

frequencies significantly above that of ultrasound given only during the irradiation. Increasing the ultrasound intensity during simultaneous ultrasound and ionizing radiation slightly increases the exchange frequency but not significantly.

3. There is a synergistic effect between (43°C) heat and ionizing radiation (300 rads) for the simultaneous exposures. The major effect appears to be an increase in exchange aberrations. Increasing the temperature immediately before or after irradiation has little effect on the chromosome aberration frequencies. Extending the duration of the elevated temperature after irradiation has little effect over that of the elevated temperature alone during the radiation exposure. The temperature during ionizing radiation exposure has a significant effect on the chromosome aberration yield. Increasing the temperature during irradiation in the range of 24°C to 43°C causes an increase in all types of aberrations, suggesting that temperature during irradiation increases the number of primary chromosome breaks.

4. Comparison of the effects of the combined heat and ionizing radiation exposures and the combined ultrasound and ionizing radiation exposures shows no significant difference. It appears that the synergistic effect between ultrasound and ionizing radiation is caused by the heat induced in the biological medium by the ultrasound energy.

5. It is concluded from these experiments and the literature that heat or ultrasound given simultaneously with ionizing radiation cause an increase in primary chromosomal breaks and that heat or ultrasound given after irradiation cause an increase in exchange aberrations.

IV. REFERENCES

Abdulla, U., Dewhurst, C.J., Campbell, S., Talbert, D., Lucas, M. and Mullarkey, M. "Effect of Diagnostic Ultrasound on Maternal and Fetal Chromosomes," Lancet 2, 829-831 (1971).

Abdulla, U., Talbert, D., Lucas, M. and Mullarkey, M. "Effects of Ultrasound on Chromosomes of Lymphocyte Cultures," Brit. Med. J. 3, 797-799 (1972).

Angulo-Carpio, M.D. and Orellans, E. "Aportaciones para el estudio de las variaciones cromosomica inducidas por ultrasonidos," Genet. Iberica 3, 3-22 (1951).

Armitage, P. "Statistical Methods in Medical Research," John Wiley & Sons, New York, 1971.

Asche, G. "Kernaberrationen durch Ultraschall," Strahlentherapie 85, 215 (1951).

Bajerska, A. and Liniecki, J. "The Influence of Temperature at Irradiation in vitro on the Yield of Chromosomal Aberrations in Pheripheral Blood Lymphocytes," Int. J. Radiat. Biol. 16, 483-493 (1969).

Baum, G. "Diagnostic Ultrasound," Plenum Press, 1966.

Beranek, L.L. and Work, G.A. "Sound Transmission through Multiple Structures Containing Flexible Blankets," J. Acoust. Soc. Amer. 21, 419-428 (1949).

Bernstine, R.L. "Safety Studies with Ultrasonic Doppler Technic," Obstet. Gynecol. 34, 707-709 (1969).

Bessler, W. "Ultraschall wirkungen an Embryonen von Triton alpestris," Strahlentherapie 89, 292-307 (1952).

Blitz, J. "Fundamentals of Ultrasound," Butterworths, London, 1967.

Bobrow, M., Blackwell, N., Unrau, A.E. and Bleaney, B. "Absence of any Observed Effect of Ultrasonic Irradiation of Human Chromosomes," J. Obstet. and Gyn. Brit. Comm. 78, 730-736 (1971).

Bora, K.C. and Soper, L. "Influence of Temperature on the Induction and Repair of Radiation Induced Aberrations in Human Chromosome," Can. J. Genet. Cytol. 13, 364-368 (1971).

Boyd, E., Abdulla, U., Donald, I., Fleming, J.E.E., Hall, A.J. and Ferguson-Smith, M.A. "Chromosome Breakage and Ultrasound," Brit. Med. J. 2, 501-502 (1971).

Braeman, J., Coakley, W.T., and Gould, R.K. "Human Lymphocyte, Chromosome and Ultrasonic Cavitation," Brit. J. of Radiol. 47, 158-161 (1974).

Brewen, J.G., Preston, R.J. and Littlefield, L.G. "Radiation-Induced Human Chromosome Aberration Yields Following an Accidental Whole-Body Exposure to ^{60}Co γ-rays," Radiat. Res. 49, 647-656 (1972).

Brock, R.D., Peacock, W.J., Kossoff, G. and Robinson, D. "Chromosome Aberrations Induced by Ultrasonic Irradiation," Workshop Proceedings, Interaction of Ultrasound and Biological Tissues, Battelle Memorial Institute, National Science Foundation, Bureau of Radiological Health, USPHS, FDA, HEW Pub. 73-8008, Sep. 72, pp. 83-86.

Bronk, B.V. "Thermal Potentiation of Mammalian Cell Killing: Clues for Understanding and Potential for Tumor Therapy," Adv. in Radiat. Biol. 6, 267-323 (1976).

Brown, B. and Gordon, D. "Ultrasonic Techniques in Biology and Medicine," Iliffe Books, Ltd., 1967.

Buckton, K.E. and Baker, N.V. "An Investigation into the Possible Chromosome Damaging Effects of Ultrasound on Human Blood Cells," Brit. J. of Radiol. 45, 340-342 (1972).

Buckton, K.E. and Evans, H.J. "Methods for the Analysis of Human Chromosome Aberrations," World Health Organization, Geneva, Switzerland, 1973.

Burr, J.G. "A Study of the Synergistic Effects of Ultrasound and Ionizing Radiation," M.S. Thesis, University of Pittsburgh (1976).

Burr, J.G., Wald, N., Pan, S. and Preston, K. "The Synergistic Effect of Ultrasound and Ionizing Radiation on Human Lymphocytes," Symposium on "Action of Physical and Chemical Mutagens on the Somatic Chromosomes of Man," Medical Research Council Clinical and Population Cytogenetics Unit, Edinburgh, Scotland, 7-8 July 1977.

Clark, P.R., Hill, C.R. and Adams, K. "Synergism Between Ultrasound and X-Rays in Tumour Therapy," Brit. J. of Radiol. 43, 97-99 (1970).

Coakley, W.T. "Acoustical Detection of Single Cavitation Events in a Focused Field in Water at 1 MHz," J. Acoust. Soc. Amer. 49, 792-801 (1971).

Coakley, W.T., Hughes, D.E., Slade, J.S. and Laurence, K.M. "Chromosome Aberrations After Exposure to Ultrasound," Brit. Med. J. 1, 109-110 (1971).

Coakley, W.T., Slade, J.S., Braeman, J. and Moore, J.L. "Examination of Lymphocytes for Chromosome Aberrations after Ultrasonic Irradiation," Brit. J. of Radiol. 45, 328-332 (1972).

Conger, A.D. "The Cytogenetic Effect of Sonic Energy Applied Simultaneously with X-Rays," Proc. Nat. Acad. Sci. U.S. 34, 470-474 (1948).

Craig, A.G. and Tyler, J.M.R. "Synergism between Gamma and Ultrasonic Irradiation of the Bacterium E. Coli B," Proceedings of the IVth International Congress of IRPA, Paris, France, 24-30 Apr 1977, pg. 229-232.

DeRobertis, E.D.P., Francisco, A.S. and DeRobertis, E.M.F. "Cell Biology," W.B. Saunders Company, Philadelphia, 1975.

Dewey, W.C., Miller, H.H. and Leeper, D.B. "Chromosomal Aberrations and Mortality of X-irradiated Mammalian Cells: Emphasis on Repair," Proc. Nat. Acad. Sci. U.S. 68, 667-671 (1971).

Dharkar, S.P. "Sensitization of Microorganisms to Radiation by Previous Ultrasonic Treatment," J. Food Sci. 29, 641-643 (1964).

Dubrow, R.J. "Mutagenic Effect of Ultrasonic Vibration on Drosophila melanogaster," M.S. Thesis, University of Conn. (1949).

Dunn, F. and Fry, F.J. "Ultrasonic Field Measurement using the Suspended Ball Radiometer and Thermocouple Probe," in Interaction of Ultrasound and Biological Tissues, Workshop Proceedings, Nov. 8-11, 1971, DHEW Publication 73-8008, pg. 173-176.

Dyer, H.J. "Changes in the Behavior of Mosses Treated with Ultrasound," J. Acoust. Soc. Amer. 37, 1195 (Abstr. 1965).

Elkind, M.M. and Sinclair, W.K. in Current Topics in Radiation Research, Vol. I, p. 165, M. Ebert and A. Howard, Editors, North-Holland, Amsterdam, 1965.

El'piner, I.E. "Ultrasound--Physical, Chemical and Biological Effects," Consultants Bureau, N.Y., 1964.

Evans, H.J. "Action of Radiations on Chromosomes," The Scientific Bases of Medicine Annual Reviews, Athlone Press, London, Chapter XVIII, pg. 321-339, 1967.

Evans, H.J. "Repair and Recovery at Chromosome and Cellular Levels: Similarities and Differences," In Recovery and Repair Mechanisms in Radiobiology. Brookhaven Symp. Biol. 20, 111-133 (1967).

Fischman, H.K., Coleman, D.J. and Lizzi, F.L. "Effects of Ultrasound on Human Chromosomes," J. of Cell Biol. 55, 74a (1972).

Fischer, P., Golob, E. Kratochwil, A. and Kunze-Muhl, E. "Chromosomenuntersuchung nach ultraschallein wirkung," Wien. Klin. Wochschrift 23, 436-437 (1967).

Fox, B.W. and Lajtha, L.G. "Radiation Damage and Repair Phenomena," Br. Med. Bull. 29, 16-21 (1973).

Fry, W.J. and Dunn, F. "Ultrasound; Analysis and Experimental Methods in Biological Research," Physical Techniques in Biological Research, Vol. 4. Ed. W.L. Nastuk, pp. 261-394 (Academic Press, N.Y.) 1962.

Fujita, S. and Sakuma, S. "The Influence of Ultrasound on Ionizing Radiation Effects," Radiat. Res. 59, 311 (1974).

Galpern-Lemaitre, H., Gustot, P. and Levi, S. "Ultrasound and Marrow-Cell Chromosomes," Lancet 2, 505-506 (1973).

Garber, E.D. "Cytogenetics: An Introduction," McGraw-Hill Book Company, New York, 1972.

Harkanyi, Z., Szollar, J. and Vigvari, Z. "A Search for an Effect of Ultrasound Alone and in Combination with X-rays on Chromosomes in vivo," Br. J. Radiol. 51, 46-49 (1978).

Hering, E.R. and B.J. Shepstone. "Observations on the Combined Effects of Ultrasound and X-Rays on the Growth of the Roots of Zea mays," Phys. Med. Biol. 21, 2, 263-271 (1976).

Hill, C.R. "The Possibility of Hazard in Medical and Industrial Applications of Ultrasound," Brit. J. of Radiol. 41, 561 (1968).

Hill, C.R., Joshi, G.P. and Revell, S.H. "A Search for Chromosome Damage Following Exposure of Chinese Hamster Cells to High Intensity, Pulsed Ultrasound," Brit. J. Radiol. 45, 333-334 (1972).

Hussey, Matthew. "Diagnostic Ultrasound," John Wiley & Sons, New York, 1975.

Ikeuchi, T., Sasaki, M., Oshimura, M., Azumi, J, Tsuji, K. and Shimizu, T. "Ultrasound and Embryonic Chromosomes," Brit. Med. J. 1:112 (1973).

"Interaction of Ultrasound and Biol gical Tissue," Workshop Proceedings, Battelle Seattle Research Center, Seattle, Wash., Nov. 8-11, 1971.

Javish, J. "Distribution of Chromosome Damage in Irradiated Chinese Hamster Cell Cultures, " (Abst.), Radiat. Res. 27, 493 (1966).

Khokhar, M.T. and Oliver, R. "An Investigation of Chromosome Damage in Vicia-faba Root Tips after Exposure to 1.5 MHz Ultrasonic Radiation," Int. J. Radiat. Biol. 28, 373-383 (1975).

Kim, Albert Mu-Yon. "Chromosomenalysen nach Behandlung von menschlichem Veneblut mit Rontgenstrahlen und ultraschall," Ph.D. Dissertation, Univ. of Vienna (1968).

Kinsler, L.E. and Frey, P. "Fundamentals of Acoustics," 2nd edn. John Wiley & Sons Inc., New York (1962).

Kunze-Muhl, E. "Chromosome Damage in Human Lymphocytes After Different Combinations of X-Ray and Ultrasonic Treatment," Proceedings of the Second European Congress on Ultrasonics in Medicine, Munich, 12-16, May 1975, Excerpta Medica, Amsterdam, Oxford (ISBN 90 219 02974) pg. 1-9 (1975).

Kunze-Muhl, E. and Golob, E. "Chromosomen analysen nach Ultraschallein wirkung," Humangenetik 14, 237-246 (1972).

Lehmann, J.F., Herrick, J.F. and Krusen, F.H. "The Effects of Ultrasound on Chromosomes, Nuclei, and Other Structures of the Cells in Plant Tissues," Arch. Phys. Med. Rehabil. 35, 141-148 (1954).

Lehmann, J.F., Krusen, F.H. "Biophysical Effects of Ultrasonic Energy on Carcinoma and their Possible Significance," Arch. of Phy. Med. and Rehabil. 36, 452-459 (1955).

Levi, S., Gustot, P. and Galperin-Lemaitre, H. "In vivo Effect of Ultrasound at Human Therapeutic Doses on Marrow Cell Chromosomes of Golden Hamster, Humangenetik 25(2) 133-41 (1974).

Li, G.C., Evans, R.G. and Hahn, G.M. "Modification and Inhibition of Potentially Lethal X-Ray Damage by Hyperthermia," Radiat. Res. 67, 491-501 (1976).

Liniecki, J., Bajerska, A. and Karniewicz, W. "The Influence of Blood Oxygenation During in vitro Irradiation Upon the Yield of Dicentric Chromosomal Aberrations in Lymphocytes," Bull. Acad. Polon. Sci., Ser. Sci. Biol. 21, 69-75 (1973).

Lloyd, D.C., Purrott, R.J., Dolphin, G.W., Bolton, D. and Edwards, A.A. "The Relationship between Chromosome Aberrations and Low LET Radiation Dose to Human Lymphocytes," Int. J. Radiat. Biol. 28, 75-90 (1975).

Loewy, A.G. and Siekevitz, P. "Cell Structure and Function," Holt, Rinehart and Winston, Inc., New York, 1969.

Lucas, M., Mullarkey, M. and Abdulla, U. "Study of Chromosomes in Newborn After Ultrasonic Fetal Heart Monitoring in Labour," Brit. Med. J. 3, 795-796 (1972).

Macintosh, I.J.C., Brown, R.C., and Coakley, W.T. "Ultrasound and "In Vitro" Chromosome Aberrations," Brit. J. of Radiol. 48, 230-2 (1975).

Macintosh, I.J.C. and Davey, D.A. "Chromosome Aberrations Induced by an Ultrasonic Foetal Pulse Detector," Brit. Med. J. 4, 92-93 (1970).

Macintosh, I.J.C. and Davey, D.A. "Relationship Between Intensity of Ultrasound and Induction of Chromosome Aberrations," Brit. J. of Radiol. 45, 320-327 (1972).

Martins, B.I. "A Study of the Effects of Ultrasonic Waves on the Reproductive Integrity of Mammalian Cells Cultured In Vitro," Ph.D. Dissertation, Lawrence Berkeley Laboratory, Univ. of California, Donner Lab, Berkeley, Cal., LBL-37, 1971.

Mermut, S., Katayama, K.P., Castillo, R.D. and Jones, H.W. "The Effect of Ultrasound on Human Chromosomes in vitro," Obstet. Gynecol. 41, 4-6 (1973).

Newcomer, E.H. "Observation on Dosage, the Mechanisms of Action and the Recovery of Cells Exposed to Ultrasonic Vibrations," Am. J. Botany 41, 384-389 (1954).

Newcomer, E.H. and Wallace, R.H. "Chromosomal and Nuclear Aberrations Induced by Ultrasonic Vibration," Am. J. Botany 36, 230 (1949).

Peacocke, A.R. and Prichard, N.J. "Some Biophysical Aspects of Ultrasound," in Progress in Biophysics and Molecular Biology, Vol. 18 (Eds. J.A.V. Butler and D. Noble) Pergamon Press, 1968, 185-209.

Pourhardi, P., Bonhomme, D.E. and Turchini, J.P. "Action des ultrasons sur la spermatogenese (souris). Etude Histologique," Arch. Anat. Microscop. Morphol. Exp. 54, 847 (1965).

Prempree, T., Michelsen, A. and Merz, T. "The Repair of Chromosome Breaks Induced by Pulsed X-Rays of Ultra-High Dose-Rate," Int. J. Radiat. Biol. 15, 571-574 (1969).

Purrott, R.J. and Reeder, E. "The Effect of Changes in Dose Rate on the Yield of Chromosome Aberrations in Human Lymphocytes Exposed to Gamma Radiation," Mutation Res. 35, 437-444 (1976).

Pydorich, M.S. "Complex Treatment of Eyelid Epithelioma," Oftal. Zurmal 21, 281 (1966).

Rapacholi, M.H. "Electrophoretic Mobility of Tumor Cells Exposed to Ultrasound and Ionizing Radiation," Nature (London) 227, 166-167 (1970).

Rott, H.D. and Soldner, R. "The Effect of Ultrasound on Human Chromosomes in Vitro," Humangenetik 20, 103-12 (1973).

Schmid, E., Bauchinger, M. and Mergenthaler, W. "Analysis of the Time Relationship for the Interaction of X-ray-Induced Primary Breaks in the Formation of Dicentric Chromosomes," Int. J. Radiat. Biol. 30, 339-346 (1976).

Selman, G.G. "The Effect of Ultrasonics on Mitosis," Exp. Cell Res. 3, 656-674 (1952).

Serr, D.M., Padeh, B., Zakut, H., Shaki, R., Mannor, S.M. and Kalner, B. "Studies on the Effects of Ultrasonic Waves on the Fetus," European Congress of Perinatal Medicine, London (1970).

Slotova, J., Karpfel, Z. and Hrazdira, I. "Chromosome Aberrations Caused by the Effect of Ultrasound in the Meristematic Cells of Vicia faba," Biol. Plant (Praha) 9, 49-55 (1967).

Spencer, J.I. "Effects of Intense Ultrasonic Vibrations on Pisum. I. on Root Meristems," Growth 16, 243-272 (1952).

Spiegler, P. and Norman, A. "Kinetics of Unscheduled DNA Synthesis Induced by Ionizing Radiation in Human Lymphocytes," Radiat. Res. 39, 400-412 (1969).

Spiegler, P. and Norman, A. "Temperature Dependence of Unscheduled DNA Synthesis in Human Lymphocytes," Radiat. Res. 43, 187-195 (1970).

Spring, E. "Increased Radiosensitivity Following Simultaneous Ultrasonic and Gamma Ray Irradiation," Radiology 93, 175-176 (1969).

Spring, E., Rytila, A. and Blomquist, K. "The Effect of Simultaneous Gamma and Ultrasonic Radiation Upon the Growth of He-La Cells," Helsinki: Finnish Society for Medical and Biological Engineering, Proceedings of 1st Nordic Meeting on Medical and Biological Engineering, pp. 95-97 (1970).

Stockdale, H.R. and Hall, C.R. "Use of a Sphere Radiometer to Measure Ultrasonic Beam Power," Ultrasound Med. Biol. 2:219 (1976).

Takaki, H. and Yosioka, K. "Acoustic-Radiation Force on a Solid Elastic Sphere," J. Acoust. Soc. Amer. 46, 1139-1143 (1969).

Timberlake, N., Hellman, S. and Belli, J.A. "Phytohemagglutinin-Stimulated Human Lymphocytes: DNA Sedimentation Behavior," Int. J. Radiat. Oncology Biol. Phys. 1, 455-464 (1976).

Todd, P. and Schroy, C.B. "X-Ray Inactivation of Cultured Mammalian Cells: Enhancement by Ultrasound," Radiology 113, 445-447 (1974).

Vekemans, M. and Leonard, A. "Influence of Blood Storage After in vitro Exposure to Ionizing Radiations on the Yield of Chromosome Aberrations Observed in Human Lymphocytes," Int. J. Radiat. Biol. 31, 493-498 (1977).

Wallace, R.H. and Bushnell, R.J. "Production of Phenotypic and Genotypic Variations in Seedlings by Ultrasonic Vibrations," Am. J. Botany 35, 813 (1948) (Abstract).

Wallace, R.H., Bushnell, R.J. and Newcomer, E.H. "The Induction of Cytogenic Variations by Ultrasonic Waves," Science 107, 577-578 (1948).

Watts, P.L., Hall, A.J. and Fleming, J.E.E. "Ultrasound and Chromosome Damage," Brit. J. of Radiol. 45, 335-339 (1972).

Wells, P.N.T. "Physical Principles of Ultrasonic Diagnosis," Academic Press, New York, 1969.

Woeber, K. "Histologische Untersuchungen uber die Sofortreaktion des Zellkerns beim Walker-Karzinom der Ratte nach Ultraschall ein wirkung," Strahlentherapie 85, 207-214 (1951).

Woeber, K. "Combination of Ultrasound and X-Ray Radiation in the Treatment of Cancer," Int. J. Phys. Med. 4, 10 (1969).

Yamaha, G. and Ueda, R. "Uber den Einfloss der Ultraschallwellen auf die Wurzelspitzenzellen von Vicia faba L," Cytologia Tokyo 9, 524-529 (1939).

APPENDIX I

```
**************************
*     LENGTH.FTN          20-MAR-78     11:07:08          PAGE    1
**************************

$BATCH
C ***********************************************************
C *    PROGRAM TO CALCULATE TRANSMISSION COEFFICIENT        *
C *    VS. THE CHANGE IN THICKNESS OF A MEDIUM              *
C *          COPYRIGHT JOHN C. BURR 5 JULY 1977             *
C *            RUN ON INTERDATA 7/32  FORTRAN V             *
C ***********************************************************
C
C THIS PROGRAM ACCEPTS SPECIFIC DATA CONCERNING THE PROPERTIES
C OF THE MEDIUM AND INTERFACES. CALCULATES THE IMPEDANCES AND
C PRESSURES AT THE INTERFACES. DETERMINES THE RATIO OF THE
C PRESSURES AT THE EXTREMES. CONVERTS TO INTENSITY, AND
C CALCULATES THE INTENSITY TRANSMISSION COEFFICIENT DUE TO
C THE IMPEDANCE MISMATCH. THE TRANSMISSION LOSS DUE TO
C ABSORPTION AND REFLECTION ARE CALCULATED TOGETHER.
C THE TRANSMISSION COEFFICIENT VS. THE CHANGE IN LENGTH IS
C PRINTED AND PLOTTED IN GRAPH FORM.
C
C VARIABLES USED:
C        NINTER = NUMBER OF INTERFACES
C        INTER = NINTER + 1 (AN INDEX VALUE)
C        LINTER = NINTER - 1(AN INDEX VALUE)
C        CHRIMP(I) = ARRAY OF CHARACTERISTIC IMPEDANCES
C        SPEED(I) = ARRAY OF SPEED OF SOUND IN MEDIA
C        LENGTH(I) = ARRAY OF LENGTH OF THE MEDIA
C        DBLOSS(I) = DECIBEL/CM LOSS IN MEDIUM
C        LOSFAC(I) = LOSS FACTOR FOR EACH MEDIA
C        FREQ = FREQUENCY OF THE ULTRASOUND
C        ACTIMP(I) = ACTUAL IMPEDANCE OF THE INTERFACE
C        IMPED(I) = COMPLEX IMPEDANCE OF MEDIUMS
C        PRESUR(I) = PRESSURE AT THE INTERFACE
C        PHI(I) = TEMPORARY VARIABLE
C        TEMP,XTEMP,ZTEMP = TEMPORARY VARIABLES
C        WAVNUM = WAVE NUMBER
C        GAMMA(I) = TEMPORARY VARIABLE
C        PROD = PRODUCT OF THE PRESSURE RATIOS
C        TRNSPR = TEMPORARY VALUE OF TRANSCOEF.
C        INTENS(I) = INTENSITY TRANSMISSION COEFFICIENT
C        NAME(I) = NAME OF THE DATA FILE TO BE READ
C        TITLE(I) = TITLE OF THE GRAPH TO BE PLOTTED.
C        NOTES(I) = NOTES TO BE MADE ON THE GRAPH(STRING)
C        NCHART = NUMBER OF CHARACTERS IN TITLE
C        NCHARN = NUMBER OF CHARACTERS IN NOTE
C        XNOTE,YNOTE = COORDINATES OF THE NOTE
C        X = X-COORDINATE FOR CENTERING TITLE
C        LEN(I) = LENGTH OF MEDIUM THAT IS VARIED
C        TLEN = TEMPORARY VALUE OF LEN(I)
C        DX = SCALING FACTOR FOR PLOTTING X AXIS
C        XLENTH = STARTING VALUE FOR INDEXING VARIED MEDIUM
C        XAXIS(I) = ANNOTATION FOR THE X AXIS
C        XSPEC = X AXIS SPECIFICATION
C
C LOGICAL DEVICES USED:
C       5 - CONSOLE
C       6 - LINE PRINTER
C       VERSATEC USED TO PLOT DATA - REQUIRES F5RTLVII
```

```
C        7 = DATA FILE
C
C FUNCTIONS USED;
C        ARCOTH(X) = ARC HYPERBOLIC COTANGENT OF A COMPLEX NUMBER
C        COTH(X) = HYPERBOLIC COTANGENT OF A COMPLEX NUMBER
C        COSH(X) = HYPERBOLIC COSINE
C
C
      DIMENSION SPEED(25),DBLOSS(25),CHRIMP(25),LOSFAC(25),
     *NAME(3),NOTES(12)
      COMPLEX GAMMA(10),ACTIMP(10),TEMP,PHI(10),PRESUR(10)
     *    ,PROD,COTH,COSH,ARCOTH,TRNSFR,ZTEMP,IMPED(10)
      REAL INTENS(101),LOSS,LENGTH(10),LEN(101)
      INTEGER TITLE(12),XAXIS(12)
      DATA PI/3.141592654/
C
C READ IN THE NAME OF THE DATA FILE AND OPEN THE FILE.
C
      WRITE(5,900)
900   FORMAT('ENTER THE DATA FILE NAME(3A4)')
      READ(5,905) (NAME(I),I=1,3)
905    FORMAT(3A4)
C
      CALL OPENW(7,NAME,1,0,0,STATUS)
C
C READ IN THE VARIABLES TO BE USED
C
      READ(7,910) NINTER
910   FORMAT(I2)
      INTER = NINTER + 1
      READ(7,915) (CHRIMP(I),I=1,INTER)
915   FORMAT(10E8.2)
      READ(7,915) (SPEED(I),I=1,INTER)
      READ(7,920) (LENGTH(I),I=2,NINTER)
920   FORMAT(10F5.3)
      READ(7,920) (DBLOSS(I),I=1,INTER)
      READ(7,925) (LOSFAC(I),I=1,INTER)
925   FORMAT(10I2)
      READ(7,930) FREQ
930   FORMAT(E8.2)
C
C SELECT THE MEDIUM WHICH IS TO BE VARIED
C
      READ(7,935) MEDIUM
935   FORMAT(I2)
C
C START OUTER LOOP TO CALCULATE TRANSMISSION COEFFICIENT FOR
C A SPECIFIC LENGTH.
C
      XLENTH = LENGTH(MEDIUM)
      DO 10 I=1,101
      LENGTH(MEDIUM) = (0.49 + 0.01 * I) * XLENTH
      LEN(I) = LENGTH(MEDIUM)
C
C CALCULATE THE COMPLEX IMPEDANCES OF THE MEDIUMS
C
```

```
      DO 15 J=1,INTER
         WAVNUM = 2.0 * PI * FREQ/SPEED(J)
         IF(LOSFAC(J).EQ.2) GO TO 50
         DB = DBLOSS(J) * FREQ/1.0E+06
         GO TO 60
50       CONTINUE
         DB = DBLOSS(J) * (FREQ/1.0E+06)**2
60       CONTINUE
         ALPHA = DB/8.68
         GAMMA(J) = CMPLX(-ALPHA,WAVNUM)
         XTEMP = 2 * PI * FREQ * CHRIMP(J)/SPEED(J)
         IMPED(J) = CMPLX(0.0,XTEMP)/GAMMA(J)
15     CONTINUE
C
C INITIALIZE THE IMPEDANCE AT THE FIRST INTERFACE
C
      ACTIMP(1) = IMPED(1)
C
C CALCULATE THE PRESSURE RATIOS AND IMPEDANCES AT INTERFACES
C
      DO 20 J=2,NINTER
        ZTEMP = ACTIMP(J-1)/IMPED(J)
        PHI(J) = ARCOTH(ZTEMP)
        TEMP = PHI(J) -(GAMMA(J) * LENGTH(J))
        ACTIMP(J) = COTH(TEMP) * IMPED(J)
        PRESUR(J-1) = COSH(PHI(J))/COSH(TEMP)
20    CONTINUE
C
C CALCULATE THE PRODUCT OF THE PRESSURE RATIOS TO GET THE
C RATIO OF THE PRESSURES FOR THE EXTREMES.
C
      LINTER = NINTER - 1
      PROD = PRESUR(1)
      IF(LINTER.EQ.1) GO TO 40
      DO 30 J=2,LINTER
        PROD = PROD * PRESUR(J)
30    CONTINUE
C
40    CONTINUE
C
C
C CALCULATE THE TRANSMISSION COEFFICIENT FOR IMPEDANCE MISMATCH
C
      TRNSPR = PROD * (2.0 * ACTIMP(NINTER))/(ACTIMP(NINTER) +
     *      IMPED(INTER))
      INTENS(I) = CABS(TRNSPR)**2 * REAL(IMPED(INTER))/
     *       REAL(IMPED(1))
10    CONTINUE
C
      WRITE(5,970)
970   FORMAT('WANT DATA PRINTED (Y,N)')
      READ(5,975) NDATA
975   FORMAT(A1)
      IF(NDATA.EQ.'N') GO TO 2000
C
C PRINT OUT THE DATA TO CHECK
```

```
C
      WRITE(6,1030) NINTER
1030  FORMAT(1X,'NUMBER OF INTERFACES = ',I4)
      WRITE(6,1040) (CHRIMP(I),I=1,INTER)
1040  FORMAT(1X,'CHARACTERISTIC IMPEDANCE =',10E10.2)
      WRITE(6,1050) (SPEED(I),I=1,INTER)
1050  FORMAT(1X,'SPEED OF SOUND =',10E10.2)
      WRITE(6,1060) (LENGTH(I),I=2,NINTER)
1060  FORMAT(1X,'LENGTH OF INTERFACE =',10F7.3)
      WRITE(6,1070) (DBLOSS(I),I=1,INTER)
1070  FORMAT(1X,'DECIBEL LOSS = ',10F7.3)
      WRITE(6,1080) (LOSFAC(I),I=1,INTER)
1080  FORMAT(1X,'LOSS FACTOR = ',10I4)
      WRITE(6,1090) FREQ
1090  FORMAT(1X,'FREQUENCY =',E10.2)
C
      WRITE(6,940)
940   FORMAT('1','LENGTH',11X,'TRANSMISSION COEFFICIENT',//)
C
      DO 70 I=1,101
        WRITE(6,945) LEN(I),INTENS(I)
945     FORMAT(1X,F6.3,14X,F8.4)
70    CONTINUE
C
2000   CONTINUE
C
C
C PLOT THE DATA ON VERSATEC
C
      READ(7,965) SCALE
965   FORMAT(F5.2)
      CALL MODE(1,9999.,SCALE,9999.)
      READ(7,960) XOFFST,YOFFST
      CALL MODE(2,9999.,9999.,XOFFST)
      CALL MODE(3,9999.,9999.,YOFFST)
      DX = (LEN(101) - LEN(1))/6.0
      TLEN = LEN(1)
      CALL MODE(8,TLEN,DX,9999.)
      CALL MODE(9,0.0,0.125,9999.)
      CALL DRAW(LEN,INTENS,101,441)
       READ(7,980) XSPEC,(XAXIS(I),I=1,12)
980    FORMAT(F4.1,12A4)
       CALL AXES(XSPEC,XAXIS,24.3,'TRANSMISSION COEFFICIENT')
      CALL MODE(4,0.15,0.1,9999.)
C
C PLOT THE TITLE IF WANTED
C
      READ(7,950) (TITLE(I),I=1,12)
950   FORMAT(12A4)
      IF(TITLE(1).EQ.'    ') GO TO 100
      READ(7,955) NCHART
955   FORMAT(I2)
      X = 3.5 - (NCHART * 0.15)/2.0
      CALL NOTE(X,8.5,TITLE,NCHART)
C
100    CONTINUE
```

```
C
C PLOT NOTES IF WANTED
C
      READ(7,950) (NOTES(I),I=1,12)
      IF(NOTES(1).EQ.'            ') GO TO 90
      READ(7,955) NCHARN
      READ(7,960) XNOTE,YNOTE
960   FORMAT(2F5.2)
      CALL MODE(4,0.10,0.075,9999.)
      CALL NOTE(XNOTE,YNOTE,NOTES,NCHARN)
      GO TO 100
C
90    CONTINUE
C
C CLOSE THE PLOTS
C
      CALL DRAW(0.,0.,1,9000)
      CALL DRAW(0,0,0,9999)
C
      STOP
      END
C
C LIST OF THE FUNCTIONS
C
      COMPLEX FUNCTION ARCOTH(X)
      COMPLEX ARCOTH,X
      ARCOTH = CLOG((X+1.0)/(X-1.0))/2
      RETURN
      END
C
      COMPLEX FUNCTION COTH(X)
      COMPLEX COTH,X,CEXP
      COTH = (CEXP(X) + CEXP(-X))/(CEXP(X) - CEXP(-X))
      RETURN
      END
C
      COMPLEX FUNCTION COSH(Y)
      COMPLEX COSH,Y,CEXP
      COSH = (CEXP(Y) + CEXP(-Y))/2
      RETURN
      END
$BEND
```

```
**************************
*     GBR25.FTN          20-MAR-78     11:08:43          PAGE    1
**************************

$BATCH
C ********************************************************
C *     PROGRAM TO CALCULATE TRANSMISSION COEFFICIENTS   *
C *         COPYRIGHT JOHN G. BURR   1 JULY 1977         *
C *           RUN ON INTERDATA 7/32  FORTRAN V           *
C ********************************************************
C
C THIS PROGRAM ACCEPTS SPECIFIC DATA CONCERNING THE PROPERTIES
C OF THE MEDIUM AND INTERFACES, CALCULATES THE IMPEDANCES AND
C PRESSURES AT THE INTERFACES, DETERMINES THE RATIO OF THE
C PRESSURES AT THE EXTREMES, CONVERTS TO INTENSITY, AND
C CALCULATES THE INTENSITY TRANSMISSION COEFFICIENT DUE TO
C THE INPEDANCE MISMATCH. THE TRANSMISSION LOSS DUE TO BOTH
C THE ABSORPTION AND THE REFLECTION ARE CALCULATED TOGETHER.
C THE FREQUENCY VS. THE TRANSMISSION COEFFICIENT IS PRINTED
C AND PLOTTED IN GRAPH FORM.
C
C VARIABLES USED:
C         NINTER = NUMBER OF INTERFACES
C         INTER = NINTER + 1 (AN INDEX VALUE)
C         LINTER = NINTER - 1(AN INDEX VALUE)
C         CHRIMP(I) = ARRAY OF CHARACTERISTIC IMPEDANCES
C         SPEED(I) = ARRAY OF SPEED OF SOUND IN MEDIA
C         LENGTH(I) = ARRAY OF LENGTH OF THE MEDIA
C         DBLOSS(I) = DECIBEL/CM LOSS IN MEDIUM
C         LOSFAC(I) = LOSS FACTOR FOR EAC MEDIA
C         F(I) = FREQUENCY OF THE ULTRASOUND
C         ACTIMP(I) = ACTUAL IMPEDANCE OF THE INTERFACE
C         IMPED(I) = COMPLEX IMPEDANCE OF THE MEDIUMS
C         PRESUR(I) = PRESSURE AT THE INTERFACE
C         PHI(I) = TEMPORARY VARIABLE
C         XTEMP,ZTEMP,TEMP = TEMPORARY VARIABLES
C         WAVNUM = WAVE NUMBER
C         GAMMA(I) = TEMPORARY VARIABLE
C         PROD = PRODUCT OF THE PRESSURE RATIOS
C         TRNSPR = TEMPORARY VALUE OF TRANSCOEF.
C         INTENS(I) = INTENSITY TRANSMISSION COEFFICIENT
C         NAME(I) = NAME OF THE DATA FILE TO BE READ
C         TITLE(I) = TITLE OF THE GRAPH TO BE PLOTTED.
C         NOTES(I) = NOTES TO BE MADE ON THE GRAPH(STRING)
C         NCHART = NUMBER OF CHARACTERS IN TITLE
C         NCHARN = NUMBER OF CHARACTERS IN NOTE
C         XNOTE,YNOTE = COORDINATES OF THE NOTE
C         X = X-COORDINATE FOR CENTERING TITLE
C
C LOGICAL DEVICES USED:
C       5 - CONSOLE
C       6 - LINE PRINTER
C       VERSATEC USED TO PLOT DATA - REQUIRES F5RTLVII
C       7 = DATA FILE
C
C FUNCTIONS USED;
C       ARCOTH(X) = ARC HYPERBOLIC COTANGENT OF A COMPLEX NUMBER
C       COTH(X) = HYPERBOLIC COTANGENT OF A COMPLEX NUMBER
C       COSH(X) = HYPERBOLIC COSINE
C
```

```
      DIMENSION SPEED(25),DBLOSS(25),CHRIMP(25),LOSFAC(25),
     *NAME(3),NOTES(12)
      COMPLEX GAMMA(10),ACTIMP(10),TEMP,PHI(10),PRESUR(10)
     *    ,PROD,COTH,COSH,ARCOTH,TRNSPR,ZTEMP,IMPED(10)
      REAL INTENS(125),LOSS,LENGTH(10),F(125)
      INTEGER TITLE(12)
      DATA PI/3.141592654/
C
C READ IN THE NAME OF THE DATA FILE AND OPEN THE FILE.
C
      WRITE(5,900)
900   FORMAT('ENTER THE DATA FILE NAME(3A4)')
      READ(5,905) (NAME(I),I=1,3)
905    FORMAT(3A4)
C
      CALL OPENW(7,NAME,1,0,0,STATUS)
C
C READ IN THE VARIABLES TO BE USED
C
      READ(7,910) NINTER
910   FORMAT(I2)
      INTER = NINTER + 1
      READ(7,915) (CHRIMP(I),I=1,INTER)
915   FORMAT(10E8.2)
      READ(7,915) (SPEED(I),I=1,INTER)
      READ(7,920) (LENGTH(I),I=2,NINTER)
920   FORMAT(10F5.3)
      READ(7,920) (DBLOSS(I),I=1,INTER)
      READ(7,925) (LOSFAC(I),I=1,INTER)
925   FORMAT(10I2)
C
C START OUTER LOOP TO CALCULATE TRANSMISSION COEFFICIENT FOR
C A SPECIFIC FREQUENCY.
C
      DO 10 I=1,121
        F(I) = 0.475E6 + I * 0.025E6
C
C CALCULATE THE COMPLEX IMPEDANCES OF THE MEDIUMS.
C
      DO 15 J=1,INTER
        WAVNUM = 2.0 * PI * F(I)/SPEED(J)
        IF(LOSFAC(J).EQ.2) GO TO 40
        DB = DBLOSS(J) * F(I)/1.0E+06
        GO TO 50
40      DB = DBLOSS(J) * (F(I)/1.0E+06)**2
50      CONTINUE
        ALPHA = DB/8.68
        GAMMA(J) = CMPLX(-ALPHA,WAVNUM)
        XTEMP = 2 * PI * F(I) * CHRIMP(J)/SPEED(J)
        IMPED(J) = CMPLX(0.0,XTEMP)/GAMMA(J)
15      CONTINUE
C
C INITIALIZE THE FIRST IMPEDANCE AT INTERFACE.
C
      ACTIMP(1) = IMPED(1)
C
```

```
C CALCULATE THE PRESSURE RATIOS AND IMPEDANCES AT INTERFACES
C
      DO 20 J=2,NINTER
        ZTEMP = ACTIMP(J-1)/IMPED(J)
        PHI(J) = ARCOTH(ZTEMP)
        TEMP = PHI(J) - (GAMMA(J) * LENGTH(J))
        ACTIMP(J) = COTH(TEMP) * IMPED(J)
        PRESUR(J-1) = COSH(PHI(J))/COSH(TEMP)
20    CONTINUE
C
C CALCULATE THE PRODUCT OF THE PRESSURE RATIOS TO
C GET THE RATIO AT THE EXTREMES.
C
      LINTER = NINTER - 1
      PROD = PRESUR(1)
      IF(LINTER.EQ.1) GO TO 130
      DO 30 J=2,LINTER
        PROD = PROD * PRESUR(J)
30    CONTINUE
C
130   CONTINUE
C
C CALCULATE THE TOTAL LOSS DUE TO ABSORPTION AND TRANS.
C
      TRNSPR = PROD * (2.0 * ACTIMP(NINTER))/(ACTIMP(NINTER) +
     *      IMPED(INTER))
      INTENS(I) = CABS(TRNSPR)**2 * REAL(IMPED(INTER))/
     *       REAL(IMPED(1))
10    CONTINUE
C
      WRITE(5,965)
965   FORMAT('WANT DATA PRINTED (Y,N)')
      READ(5,970) NDATA
970   FORMAT(A1)
      IF(NDATA.EQ.'N') GO TO 2000
C
C PRINT OUT THE DATA TO CHECK
C
      WRITE(6,1030) NINTER
1030  FORMAT(1X,'NUMBER OF INTERFACES = ',I4)
      WRITE(6,1040) (CHRIMP(I),I=1,INTER)
1040  FORMAT(1X,'CHARACTERISTIC IMPEDANCE =',10E10.2)
      WRITE(6,1050) (SPEED(I),I=1,INTER)
1050  FORMAT(1X,'SPEED OF SOUND =',10E10.2)
      WRITE(6,1060) (LENGTH(I),I=2,NINTER)
1060  FORMAT(1X,'LENGTH OF INTERFACE =',10F7.3)
      WRITE(6,1070) (DBLOSS(I),I=1,INTER)
1070  FORMAT(1X,'DECIBEL LOSS = ',10F7.3)
      WRITE(6,1080) (LOSFAC(I),I=1,INTER)
1080  FORMAT(1X,'LOSS FACTOR = ',10I4)
C
      WRITE(6,930)
930   FORMAT('1','FREQUENCY',11X,'TRANSMISSION COEFFICIENT',//)
C
      DO 70 I=1,121
        WRITE(6,935) F(I),INTENS(I)
```

```
935      FORMAT(1X,1PE10.2,11X,0PF8.4)
70     CONTINUE
C
2000     CONTINUE
C
C
C CONVERT THE FREQUENCIES TO MHZ FOR PLOTTING.
C
       DO 80 I=1,121
         F(I) = F(I)/1.0E+06
80     CONTINUE
C
C PLOT THE DATA ON VERSATEC
C
       READ(7,955) SCALE
955    FORMAT(F5.2)
       CALL MODE(1,9999.,SCALE,9999.)
       READ(7,960) XOFFST,YOFFST
960    FORMAT(2F5.2)
       CALL MODE(2,9999.,9999.,XOFFST)
       CALL MODE(3,9999.,9999.,YOFFST)
       CALL MODE(8,0.5,0.5,9999.)
       CALL MODE(9,0.0,0.125,9999.)
       CALL DRAW(F,INTENS,121,441)
       CALL AXES(13.1,'FREQUENCY-MHZ',24.3,'TRANSMISSION COEFFICIENT')
       CALL MODE(4,0.15,0.1,9999.)
C
C PLOT THE TITLE IF WANTED
C
       READ(7,940) (TITLE(I),I=1,12)
940    FORMAT(12A4)
       IF(TITLE(1).EQ.'    ') GO TO 100
       READ(7,945) NCHART
945    FORMAT(I2)
       X = 3.5 - (NCHART * 0.15)/2.0
       CALL NOTE(X,8.5,TITLE,NCHART)
C
100      CONTINUE
C
C PLOT NOTES IF WANTED
C
       READ(7,940) (NOTES(I),I=1,12)
       IF(NOTES(1).EQ.'    ') GO TO 90
       READ(7,945) NCHARN
       READ(7,950) XNOTE,YNOTE
950    FORMAT(2F5.2)
       CALL MODE(4,0.10,0.075,9999.)
       CALL NOTE(XNOTE,YNOTE,NOTES,NCHARN)
       GO TO 100
C
90     CONTINUE
C
C CLOSE THE PLOTS
C
       CALL DRAW(0.,0.,1,9000)
       CALL DRAW(0,0,0,9999)
```

AD-A061 537 AIR FORCE INST OF TECH WRIGHT-PATTERSON AFB OHIO F/G 6/18
THE SYNERGISTIC EFFECT OF ULTRASOUND AND IONIZING RADIATION ON --ETC(U)
1978 J G BURR
UNCLASSIFIED AFIT-CI-79-71D NL

3 OF 3
AD
A061537

END
DATE
FILMED
2-79
DDC

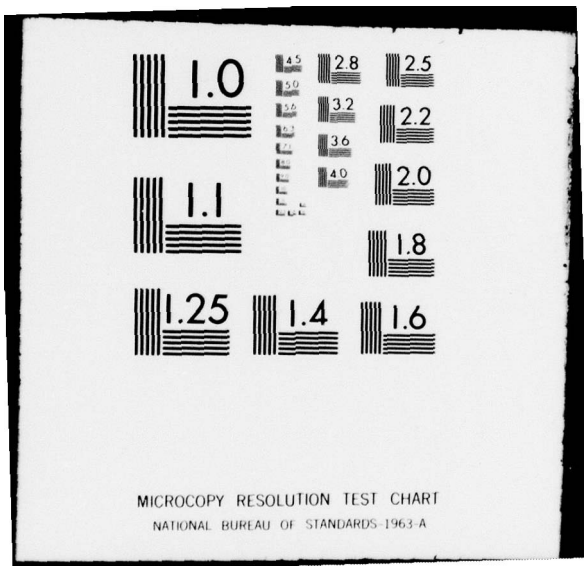
1.0
1.1
1.25
1.4
1.6
1.8
2.0
2.2
2.5
2.8
3.2
3.6
4.0
4.5
5.0
MICROCOPY RESOLUTION TEST CHART
NATIONAL BUREAU OF STANDARDS-1963-A

```
C
      STOP
      END
C
C LIST OF THE FUNCTIONS
C
      COMPLEX FUNCTION ARCOTH(X)
      COMPLEX ARCOTH,X
      ARCOTH = CLOG((X+1.0)/(X-1.0))/2
      RETURN
      END
C
      COMPLEX FUNCTION COTH(X)
      COMPLEX COTH,X,CEXP
      COTH = (CEXP(X) + CEXP(-X))/(CEXP(X) - CEXP(-X))
      RETURN
      END
C
      COMPLEX FUNCTION COSH(Y)
      COMPLEX COSH,Y,CEXP
      COSH = (CEXP(Y) + CEXP(-Y))/2
      RETURN
      END
$BEND
```

APPENDIX II

Table A1

SUMMARY DATA FOR RADIATION ALONE SERIES NO. 1

100 RADS AT 37C INCUBATE IMMEDIATELY

METAPHASES SCORED 400 MITOTIC INDEX 10.0

	NUMBER OF ABERRATIONS	ABERRATION FREQUENCY	ABERRATION STANDARD ERROR
FRAGMENTS	80	0.200	0.022
MINUTES	10	0.025	0.008
DICENTRICS	29	0.072	0.013
CENTRIC RINGS	2	0.005	0.004
DELETIONS	50	0.125	0.018
EXCHANGES	31	0.077	0.014
ABERRANT CELLS	84	0.210	0.023

300 RADS AT 37C INCUBATE IMMEDIATELY

METAPHASES SCORED 618 MITOTIC INDEX 6.8

	NUMBER OF ABERRATIONS	ABERRATION FREQUENCY	ABERRATION STANDARD ERROR
FRAGMENTS	618	1.000	0.040
MINUTES	93	0.150	0.016
DICENTRICS	267	0.432	0.026
CENTRIC RINGS	21	0.034	0.007
DELETIONS	238	0.385	0.025
EXCHANGES	288	0.466	0.027
ABERRANT CELLS	421	0.681	0.033

Table A1 (Contd.)

SUMMARY DATA FOR RADIATION ALONE SERIES NO. 1
(CONTINUED)

500 RADS AT 37C INCUBATE IMMEDIATELY

METAPHASES SCORED 155 MITOTIC INDEX 2.0

	NUMBER OF ABERRATIONS	ABERRATION FREQUENCY	ABERRATION STANDARD ERROR
FRAGMENTS	287	1.852	0.109
MINUTES	71	0.458	0.054
DICENTRICS	134	0.865	0.075
CENTRIC RINGS	12	0.077	0.022
DELETIONS	86	0.555	0.060
EXCHANGES	146	0.942	0.078
ABERRANT CELLS	142	0.916	0.077

Table A2

SUMMARY DATA FOR RADIATION ALONE SERIES NO. 2

300 RADS INCUBATE IMMEDIATELY

METAPHASES SCORED 106 MITOTIC INDEX 9.6

	NUMBER OF ABERRATIONS	ABERRATION FREQUENCY	ABERRATION STANDARD ERROR
FRAGMENTS	86	0.811	0.087
MINUTES	15	0.142	0.037
DICENTRICS	48	0.453	0.065
CENTRIC RINGS	7	0.066	0.025
DELETIONS	24	0.226	0.046
EXCHANGES	55	0.519	0.070
ABERRANT CELLS	67	0.632	0.077

300 RADS INCUBATE AFTER 30 MINUTES DELAY AT 37C

METAPHASES SCORED 100 MITOTIC INDEX 8.0

	NUMBER OF ABERRATIONS	ABERRATION FREQUENCY	ABERRATION STANDARD ERROR
FRAGMENTS	78	0.780	0.088
M NUTES	19	0.190	0.044
DICENTRICS	45	0.450	0.067
CENTRIC RINGS	4	0.040	0.020
DELETIONS	20	0.200	0.045
EXCHANGES	49	0.490	0.070
ABERRANT CELLS	59	0.590	0.077

Table A2 (Contd.)

SUMMARY DATA FOR RADIATION ALONE SERIES NO. 2
(CONTINUED)

300 RADS INCUBATE AFTER 2 HOURS DELAY AT 37C

METAPHASES SCORED 120 MITOTIC INDEX 10.2

	NUMBER OF ABERRATIONS	ABERRATION FREQUENCY	ABERRATION STANDARD ERROR
FRAGMENTS	101	0.842	0.084
MINUTES	17	0.142	0.034
DICENTRICS	58	0.483	0.063
CENTRIC RINGS	1	0.008	0.008
DELETIONS	38	0.317	0.051
EXCHANGES	59	0.492	0.064
ABERRANT CELLS	80	0.667	0.075

300 RADS INCUBATE AFTER 6 HOURS DELAY AT 37C

METAPHASES SCORED 98 MITOTIC INDEX 8.5

	NUMBER OF ABERRATIONS	ABERRATION FREQUENCY	ABERRATION STANDARD ERROR
FRAGMENTS	80	0.816	0.091
MINUTES	19	0.194	0.044
DICENTRICS	48	0.490	0.071
CENTRIC RINGS	1	0.010	0.010
DELETIONS	26	0.265	0.052
EXCHANGES	49	0.500	0.071
ABERRANT CELLS	63	0.643	0.081

Table A3

SUMMARY DATA FOR ULTRASOUND AND IONIZING RADIATION FOR 300 RADS

300 RADS INCUBATE IMMEDIATELY CONSOLIDATED VALUE (SEQUENCE 1)

METAPHASES SCORED 618 MITOTIC INDEX 6.8

	NUMBER OF ABERRATIONS	ABERRATION FREQUENCY	ABERRATION STANDARD ERROR
FRAGMENTS	618	1.000	0.040
MINUTES	93	0.150	0.016
DICENTRICS	267	0.432	0.026
CENTRIC RINGS	21	0.034	0.007
DELETIONS	238	0.385	0.025
EXCHANGES	288	0.466	0.027
ABERRANT CELLS	421	0.681	0.033

300 RADS IMMEDIATELY AFTER 30 MINUTES ULTRASOUND (SEQUENCE 2)

METAPHASES SCORED 191 MITOTIC INDEX 2.5

	NUMBER OF ABERRATIONS	ABERRATION FREQUENCY	ABERRATION STANDARD ERROR
FRAGMENTS	188	0.984	0.072
M NUTES	20	0.105	0.023
DICENTRICS	77	0.403	0.046
CENTRIC RINGS	8	0.042	0.015
DELETIONS	69	0.361	0.043
EXCHANGES	85	0.445	0.048
ABERRANT CELLS	133	0.707	0.061

Table A3 (Contd.)

SUMMARY DATA FOR ULTRASOUND AND IONIZING RADIATION FOR 300 RADS (CONTINUED)

300 RADS SIMULTANEOUS WITH ULTRASOUND (SEQUENCE 3)

METAPHASES SCORED 200 MITOTIC INDEX 9.0

	NUMBER OF ABERRATIONS	ABERRATION FREQUENCY	ABERRATION STANDARD ERROR
FRAGMENTS	266	1.330	0.082
MINUTES	29	0.145	0.027
DICENTRICS	115	0.575	0.054
CENTRIC RINGS	6	0.030	0.012
DELETIONS	98	0.490	0.049
EXCHANGES	121	0.605	0.055
ABERRANT CELLS	161	0.805	0.063

300 RADS SIMULTANEOUS WITH 30 MINUTES ULTRASOUND (SEQUENCE 4)

METAPHASES SCORED 506 MITOTIC INDEX 6.7

	NUMBER OF ABERRATIONS	ABERRATION FREQUENCY	ABERRATION STANDARD ERROR
FRAGMENTS	647	1.279	0.050
MINUTES	105	0.208	0.020
DICENTRICS	323	0.638	0.036
CENTRIC RINGS	24	0.047	0.010
DELETIONS	161	0.318	0.025
EXCHANGES	347	0.686	0.037
ABERRANT CELLS	380	0.751	0.039

Table A3 (Contd.)

SUMMARY DATA FOR ULTRASOUND AND IONIZING RADIATION FOR 300 RADS (CONTINUED)

300 RADS SIMULTANEOUS WITH 45 MINUTES ULTRASOUND (SEQUENCE 5)

METAPHASES SCORED 157 MITOTIC INDEX 1.0

	NUMBER OF ABERRATIONS	ABERRATION FREQUENCY	ABERRATION STANDARD ERROR
FRAGMENTS	195	1.242	0.089
MINUTES	20	0.127	0.028
DICENTRICS	93	0.592	0.061
CENTRIC RINGS	6	0.033	0.016
DELETIONS	63	0.401	0.051
EXCHANGES	99	0.631	0.063
ABERRANT CELLS	98	0.624	0.063

300 RADS SIMULTANEOUS WITH 60 MINUTES ULTRASOUND (SEQUENCE 6)

METAPHASES SCORED 125 MITOTIC INDEX 1.0

	NUMBER OF ABERRATIONS	ABERRATION FREQUENCY	ABERRATION STANDARD ERROR
FRAGMENTS	176	1.408	0.106
MINUTES	18	0.144	0.034
DICENTRICS	80	0.640	0.072
CENTRIC RINGS	7	0.056	0.021
DELETIONS	56	0.448	0.060
EXCHANGES	87	0.696	0.075
ABERRANT CELLS	103	0.824	0.081

Table A3 (Contd.)

SUMMARY DATA FOR ULTRASOUND AND IONIZING RADIATION FOR 300 RADS (CONTINUED)

300 RADS IMMEDIATELY BEFORE 30 MINUTES ULTRASOUND (SEQUENCE 7)

METAPHASES SCORED 166 MITOTIC INDEX 4.0

	NUMBER OF ABERRATIONS	ABERRATION FREQUENCY	ABERRATION STANDARD ERROR
FRAGMENTS	181	1.090	0.081
MINUTES	24	0.145	0.030
DICENTRICS	73	0.440	0.051
CENTRIC RINGS	4	0.024	0.012
DELETIONS	82	0.494	0.055
EXCHANGES	77	0.464	0.053
ABERRANT CELLS	119	0.717	0.066

Table A4

SUMMARY DATA FOR ULTRASOUND AND IONIZING RADIATION FOR 100 RADS

100 RADS INCUBATE IMMEDIATELY CONSOLIDATED VALUE (SEQUENCE 1)

METAPHASES SCORED 400 MITOTIC INDEX 10.0

	NUMBER OF ABERRATIONS	ABERRATION FREQUENCY	ABERRATION STANDARD ERROR
FRAGMENTS	80	0.200	0.022
MINUTES	10	0.025	0.008
DICENTRICS	29	0.072	0.013
CENTRIC RINGS	2	0.005	0.004
DELETIONS	50	0.125	0.018
EXCHANGES	31	0.077	0.014
ABERRANT CELLS	84	0.210	0.023

100 RADS IMMEDIATELY AFTER 30 MINUTES ULTRASOUND (SEQUENCE 2)

METAPHASES SCORED 200 MITOTIC INDEX 5.0

	NUMBER OF ABERRATIONS	ABERRATION FREQUENCY	ABERRATION STANDARD ERROR
FRAGMENTS	39	0.195	0.031
MINUTES	2	0.010	0.007
DICENTRICS	9	0.045	0.015
CENTRIC RINGS	0	0.000	0.000
DELETIONS	31	0.155	0.028
EXCHANGES	9	0.045	0.015
ABERRANT CELLS	39	0.195	0.031

Table A4 (Contd.)

SUMMARY DATA FOR ULTRASOUND AND IONIZING RADIATION FOR 100 RADS (CONTINUED)

100 RADS SIMULTANEOUS WITH ULTRASOUND (SEQUENCE 4)

METAPHASES SCORED 200 MITOTIC INDEX 7.5

	NUMBER OF ABERRATIONS	ABERRATION FREQUENCY	ABERRATION STANDARD ERROR
FRAGMENTS	61	0.305	0.039
MINUTES	5	0.025	0.011
DICENTRICS	26	0.130	0.025
CENTRIC RINGS	3	0.015	0.009
DELETIONS	32	0.160	0.028
EXCHANGES	29	0.145	0.027
ABERRANT CELLS	60	0.300	0.039

100 RADS IMMEDIATELY BEFORE 30 MINUTES ULTRASOUND (SEQUENCE 7)

METAPHASES SCORED 200 MITOTIC INDEX 4.5

	NUMBER OF ABERRATIONS	ABERRATION FREQUENCY	ABERRATION STANDARD ERROR
FRAGMENTS	53	0.265	0.036
MINUTES	2	0.010	0.007
DICENTRICS	22	0.110	0.023
CENTRIC RINGS	0	0.000	0.000
DELETIONS	34	0.170	0.029
EXCHANGES	22	0.110	0.023
ABERRANT CELLS	51	0.255	0.036

Table A5

SUMMARY DATA FOR ULTRASOUND AND IONIZING RADIATION FOR VARIOUS INTENSITIES

300 RADS WITH 30 MINUTES AT 24C

METAPHASES SCORED 350 MITOTIC INDEX 8.8

	NUMBER OF ABERRATIONS	ABERRATION FREQUENCY	ABERRATION STANDARD ERROR
FRAGMENTS	266	0.760	0.047
MINUTES	36	0.103	0.017
DICENTRICS	124	0.354	0.032
CENTRIC RINGS	13	0.037	0.010
DELETIONS	102	0.291	0.029
EXCHANGES	137	0.391	0.033
ABERRANT CELLS	206	0.589	0.041

300 RADS SIMULTANEOUS WITH 30 MINUTES 10MW/CM**2 ULTRASOUND

METAPHASES SCORED 200 MITOTIC INDEX 9.0

	NUMBER OF ABERRATIONS	ABERRATION FREQUENCY	ABERRATION STANDARD ERROR
FRAGMENTS	167	0.835	0.065
MINUTES	26	0.130	0.025
DICENTRICS	79	0.395	0.044
CENTRIC RINGS	4	0.020	0.010
DELETIONS	70	0.350	0.042
EXCHANGES	83	0.415	0.046
ABERRANT CELLS	132	0.660	0.057

Table A5 (Contd.)

SUMMARY DATA FOR ULTRASOUND AND IONIZING RADIATION FOR VARIOUS INTENSITIES (CONTINUED)

300 RADS SIMULTANEOUS WITH 30 MINUTES 1.5W/CM**2 ULTRASOUND

METAPHASES SCORED 200 MITOTIC INDEX 6.0

	NUMBER OF ABERRATIONS	ABERRATION FREQUENCY	ABERRATION STANDARD ERROR
FRAGMENTS	167	0.835	0.065
MINUTES	24	0.120	0.024
DICENTRICS	80	0.400	0.045
CENTRIC RINGS	4	0.020	0.010
DELETIONS	69	0.345	0.042
EXCHANGES	84	0.420	0.046
ABERRANT CELLS	122	0.610	0.055

300 RADS SIMULTANEOUS WITH 30 MINUTES 3.0W/CM**2 ULTRASOUND

METAPHASES SCORED 200 MITOTIC INDEX 5.0

	NUMBER OF ABERRATIONS	ABERRATION FREQUENCY	ABERRATION STANDARD ERROR
FRAGMENTS	195	0.975	0.070
MINUTES	42	0.210	0.032
DICENTRICS	100	0.500	0.050
CENTRIC RINGS	9	0.045	0.015
DELETIONS	59	0.295	0.038
EXCHANGES	109	0.545	0.052
ABERRANT CELLS	141	0.705	0.059

Table A6

SUMMARY DATA FOR HEAT AND IONIZING RADIATION FOR 300 RADS

300 RADS INCUBATE IMMEDIATELY CONSOLIDATED VALUE (SEQUENCE 1)

METAPHASES SCORED 618 MITOTIC INDEX 6.8

	NUMBER OF ABERRATIONS	ABERRATION FREQUENCY	ABERRATION STANDARD ERROR
FRAGMENTS	618	1.000	0.040
MINUTES	93	0.150	0.016
DICENTRICS	267	0.432	0.026
CENTRIC RINGS	21	0.034	0.007
DELETIONS	238	0.385	0.025
EXCHANGES	288	0.466	0.027
ABERRANT CELLS	421	0.681	0.033

300 RADS IMMEDIATELY AFTER 30 MINUTES AT 43C (SEQUENCE 2)

METAPHASES SCORED 200 MITOTIC INDEX 10.0

	NUMBER OF ABERRATIONS	ABERRATION FREQUENCY	ABERRATION STANDARD ERROR
FRAGMENTS	199	0.995	0.071
MINUTES	33	0.165	0.029
DICENTRICS	86	0.430	0.046
CENTRIC RINGS	3	0.015	0.009
DELETIONS	90	0.450	0.047
EXCHANGES	89	0.445	0.047
ABERRANT CELLS	142	0.710	0.060

Table A6 (Contd.)

SUMMARY DATA FOR HEAT AND IONIZING RADIATION FOR 300 RADS (CONTINUED)

300 RADS AT 43C INCUBATE IMMEDIATELY (SEQUENCE 3)

METAPHASES SCORED 149 MITOTIC INDEX 3.0

	NUMBER OF ABERRATIONS	ABERRATION FREQUENCY	ABERRATION STANDARD ERROR
FRAGMENTS	184	1.235	0.091
MINUTES	24	0.161	0.033
DICENTRICS	87	0.584	0.063
CENTRIC RINGS	7	0.047	0.018
DELETIONS	53	0.356	0.049
EXCHANGES	94	0.631	0.065
ABERRANT CELLS	110	0.738	0.070

300 RADS SIMULTANEOUS WITH 30 MINUTES AT 43C (SEQUENCE 4)

METAPHASES SCORED 447 MITOTIC INDEX 4.0

	NUMBER OF ABERRATIONS	ABERRATION FREQUENCY	ABERRATION STANDARD ERROR
FRAGMENTS	592	1.324	0.034
MINUTES	90	0.201	0.021
DICENTRICS	249	0.557	0.035
CENTRIC RINGS	25	0.056	0.011
DELETIONS	211	0.472	0.032
EXCHANGES	274	0.613	0.037
ABERRANT CELLS	326	0.729	0.040

Table A6 (Contd.)

SUMMARY DATA FOR HEAT AND IONIZING RADIATION FOR 300 RADS (CONTINUED)

300 RADS SIMULTANEOUS WITH 45 MINUTES AT 43C (SEQUENCE 5)

METAPHASES SCORED 49 MITOTIC INDEX 0.1

	NUMBER OF ABERRATIONS	ABERRATION FREQUENCY	ABERRATION STANDARD ERROR
FRAGMENTS	71	1.449	0.172
MINUTES	5	0.102	0.046
DICENTRICS	33	0.673	0.117
CENTRIC RINGS	2	0.041	0.029
DELETIONS	22	0.449	0.096
EXCHANGES	35	0.714	0.121
ABERRANT CELLS	41	0.837	0.131

300 RADS SIMULTANEOUS WITH 60 MINUTES AT 43C (SEQUENCE 6)

METAPHASES SCORED 0 MITOTIC INDEX 0.0

	NUMBER OF ABERRATIONS	ABERRATION FREQUENCY	ABERRATION STANDARD ERROR
FRAGMENTS	0	0.000	0.000
MINUTES	0	0.000	0.000
DICENTRICS	0	0.000	0.000
CENTRIC RINGS	0	0.000	0.000
DELETIONS	0	0.000	0.000
EXCHANGES	0	0.000	0.000
ABERRANT CELLS	0	0.000	0.000

Table A6 (Contd.)

SUMMARY DATA FOR HEAT AND IONIZING RADIATION FOR 300 RADS
(CONTINUED)

300 RADS IMMEDIATELY BEFORE 30 MINUTES AT 43C (SEQUENCE 7)

METAPHASES SCORED 200 MITOTIC INDEX 8.3

	NUMBER OF ABERRATIONS	ABERRATION FREQUENCY	ABERRATION STANDARD ERROR
FRAGMENTS	198	0.990	0.070
MINUTES	26	0.130	0.025
DICENTRICS	89	0.445	0.047
CENTRIC RINGS	5	0.025	0.011
DELETIONS	70	0.350	0.042
EXCHANGES	94	0.470	0.048
ABERRANT CELLS	137	0.685	0.059

Table A7

SUMMARY DATA FOR HEAT AND IONIZING RADIATION FOR 100 RADS

100 RADS INCUBATE IMMEDIATELY CONSOLIDATED VALUE (SEQUENCE 1)

METAPHASES SCORED 400 MITOTIC INDEX 10.0

	NUMBER OF ABERRATIONS	ABERRATION FREQUENCY	ABERRATION STANDARD ERROR
FRAGMENTS	80	0.200	0.022
MINUTES	10	0.025	0.008
DICENTRICS	29	0.072	0.013
CENTRIC RINGS	2	0.005	0.004
DELETIONS	50	0.125	0.018
EXCHANGES	31	0.077	0.014
ABERRANT CELLS	84	0.210	0.023

100 RADS IMMEDIATELY AFTER 30 MINUTES AT 43C (SEQUENCE 2)

METAPHASES SCORED 200 MITOTIC INDEX 11.0

	NUMBER OF ABERRATIONS	ABERRATION FREQUENCY	ABERRATION STANDARD ERROR
FRAGMENTS	44	0.220	0.033
MINUTES	4	0.020	0.010
DICENTRICS	14	0.070	0.019
CENTRIC RINGS	2	0.010	0.007
DELETIONS	30	0.150	0.027
EXCHANGES	16	0.080	0.020
ABERRANT CELLS	44	0.220	0.033

Table A7 (Contd.)

SUMMARY DATA FOR HEAT AND IONIZING RADIATION FOR 100 RADS (CONTINUED)

100 RADS SIMULTANEOUS WITH 30 MINUTES AT 43C (SEQUENCE 4)

METAPHASES SCORED 200 MITOTIC INDEX 5.5

	NUMBER OF ABERRATIONS	ABERRATION FREQUENCY	ABERRATION STANDARD ERROR
FRAGMENTS	43	0.215	0.033
MINUTES	2	0.010	0.007
DICENTRICS	15	0.075	0.019
CENTRIC RINGS	0	0.000	0.000
DELETIONS	31	0.155	0.028
EXCHANGES	15	0.075	0.019
ABERRANT CELLS	43	0.215	0.033

100 RADS IMMEDIATELY BEFORE 30 MINUTES AT 43C (SEQUENCE 7)

METAPHASES SCORED 200 MITOTIC INDEX 6.0

	NUMBER OF ABERRATIONS	ABERRATION FREQUENCY	ABERRATION STANDARD ERROR
FRAGMENTS	44	0.220	0.033
MINUTES	4	0.020	0.010
DICENTRICS	19	0.095	0.022
CENTRIC RINGS	1	0.005	0.005
DELETIONS	26	0.130	0.025
EXCHANGES	20	0.100	0.022
ABERRANT CELLS	46	0.230	0.034

Table A8

SUMMARY DATA FOR HEAT AND IONIZING RADIATION FOR VARIOUS TEMPERATURES

300 RADS WITH 30 MINUTES AT 24C

METAPHASES SCORED 350 MITOTIC INDEX 8.8

	NUMBER OF ABERRATIONS	ABERRATION FREQUENCY	ABERRATION STANDARD ERROR
FRAGMENTS	266	0.760	0.047
MINUTES	36	0.103	0.017
DICENTRICS	124	0.354	0.032
CENTRIC RINGS	13	0.037	0.010
DELETIONS	102	0.291	0.029
EXCHANGES	137	0.391	0.033
ABERRANT CELLS	206	0.589	0.041

300 RADS WITH 30 MINUTES AT 30C

METAPHASES SCORED 192 MITOTIC INDEX 8.6

	NUMBER OF ABERRATIONS	ABERRATION FREQUENCY	ABERRATION STANDARD ERROR
FRAGMENTS	168	0.875	0.068
MINUTES	27	0.141	0.027
DICENTRICS	87	0.453	0.049
CENTRIC RINGS	8	0.042	0.015
DELETIONS	52	0.271	0.038
EXCHANGES	95	0.495	0.051
ABERRANT CELLS	128	0.667	0.039

Table A8 (Contd.)

SUMMARY DATA FOR HEAT AND IONIZING RADIATION FOR VARIOUS TEMPERATURES (CONTINUED)

300 RADS WITH 30 MINUTES AT 37C

METAPHASES SCORED 618 MITOTIC INDEX 6.8

	NUMBER OF ABERRATIONS	ABERRATION FREQUENCY	ABERRATION STANDARD ERROR
FRAGMENTS	618	1.000	0.040
MINUTES	93	0.150	0.016
DICENTRICS	267	0.432	0.026
CENTRIC RINGS	21	0.034	0.007
DELETIONS	238	0.385	0.025
EXCHANGES	288	0.466	0.027
ABERRANT CELLS	421	0.681	0.033

300 RADS WITH 30 MINUTES AT 43C

METAPHASES SCORED 447 MITOTIC INDEX 4.0

	NUMBER OF ABERRATIONS	ABERRATION FREQUENCY	ABERRATION STANDARD ERROR
FRAGMENTS	592	1.324	0.054
MINUTES	90	0.201	0.021
DICENTRICS	249	0.557	0.035
CENTRIC RINGS	25	0.056	0.011
DELETIONS	211	0.472	0.032
EXCHANGES	274	0.613	0.037
ABERRANT CELLS	326	0.729	0.040

Table A9

SUMMARY DATA FOR COMPARISON OF ALL 300 RADS AT 37C INCUBATE IMMEDIATELY

CONSOLIDATED VALUE

METAPHASES SCORED 618 MITOTIC INDEX 6.8

	NUMBER OF ABERRATIONS	ABERRATION FREQUENCY	ABERRATION STANDARD ERROR
FRAGMENTS	618	1.000	0.040
MINUTES	93	0.150	0.016
DICENTRICS	267	0.432	0.026
CENTRIC RINGS	21	0.034	0.007
DELETIONS	238	0.385	0.025
EXCHANGES	288	0.466	0.027
ABERRANT CELLS	421	0.681	0.033

CONTROL VALUE NO. 1

METAPHASES SCORED 200 MITOTIC INDEX 6.5

	NUMBER OF ABERRATIONS	ABERRATION FREQUENCY	ABERRATION STANDARD ERROR
FRAGMENTS	201	1.005	0.071
MINUTES	31	0.155	0.028
DICENTRICS	83	0.415	0.046
CENTRIC RINGS	7	0.035	0.013
DELETIONS	80	0.400	0.045
EXCHANGES	90	0.450	0.047
ABERRANT CELLS	135	0.675	0.058

Table A9 (Contd.)

SUMMARY DATA FOR COMPARISON OF ALL 300 RADS AT 37C INCUBATE IMMEDIATELY (CONTINUED)

CONTROL VALUE NO. 2

METAPHASES SCORED 77 MITOTIC INDEX 4.0

	NUMBER OF ABERRATIONS	ABERRATION FREQUENCY	ABERRATION STANDARD ERROR
FRAGMENTS	60	0.779	0.101
MINUTES	10	0.130	0.041
DICENTRICS	27	0.351	0.067
CENTRIC RINGS	1	0.013	0.013
DELETIONS	27	0.351	0.067
EXCHANGES	28	0.364	0.069
ABERRANT CELLS	44	0.571	0.086

CONTROL VALUE NO. 3

METAPHASES SCORED 141 MITOTIC INDEX 5.0

	NUMBER OF ABERRATIONS	ABERRATION FREQUENCY	ABERRATION STANDARD ERROR
FRAGMENTS	146	1.035	0.086
MINUTES	32	0.227	0.040
DICENTRICS	67	0.475	0.058
CENTRIC RINGS	10	0.071	0.022
DELETIONS	55	0.390	0.053
EXCHANGES	77	0.546	0.062
ABERRANT CELLS	106	0.752	0.073

Table A9 (Contd.)

SUMMARY DATA FOR COMPARISON OF ALL 300 RADS AT 37C INCUBATE IMMEDIATELY (CONTINUED)

CONTROL VALUE NO. 4

METAPHASES SCORED 200 MITOTIC INDEX 12.0

	NUMBER OF ABERRATIONS	ABERRATION FREQUENCY	ABERRATION STANDARD ERROR
FRAGMENTS	211	1.055	0.073
MINUTES	20	0.100	0.022
DICENTRICS	90	0.450	0.047
CENTRIC RINGS	3	0.015	0.009
DELETIONS	76	0.380	0.044
EXCHANGES	93	0.465	0.048
ABERRANT CELLS	136	0.680	0.058